Delft University of Technology

Workability study for going-on-location of jack-up vessels

Gijs Holland

June 1, 2023

TU Delft

MO4 NEXT LEVEL FORECASTING

CALYPSO

Workability study for going-on-location of jack-up vessels

by

Gijs Frederik Holland

Master Thesis

to obtain the degree of Master of Science in Offshore and Dredging Engineering
at the Delft University of Technology.

Student number:	4590376	
Project duration:	September 1, 2022 – June 1, 2023	
Thesis committee:	Dr. ir. P. van der Male,	TU Delft, chairman
	Dr. ir. P. Naaijen,	TU Delft, supervisor
	Dr. ir. E. Kementzetzidis,	TU Delft, supervisor
	Ir. M. Hoogeveen,	Calypso
	Ir. M. Paalvast,	MO4 Motion Forecasting Service

Abstract

This thesis focuses on the going-on-location (GoL) operation of jack-up vessels in the offshore wind energy industry. The GoL process involves the transition of a jack-up vessel from a free-floating state to a state where it's elevated above the waterline and pinned to the seabed. The workability of these vessels is significantly affected by the impact loads experienced during the GoL process, particularly when interacting with stiff seabeds and non-negligible sea states. In current methodologies, certain parameters like wave height and wave period set the limitations to when GoL process can proceed. For safety reasons, the GoL process is halted if these conditions are exceeded. Instead of solely depending on external factors like wave height and wave period, the focus transitions towards how the vessel dynamics relate to the impact forces it encounters during the GoL. To address this limitation, a comprehensive framework has been developed that combines hydrodynamic, structural, and soil-spudcan interaction elements to evaluate impact forces during the GoL process.

The framework offers a flexible and case-specific configuration. It allows for easy modifications, integration, and replacement of components and input parameters. This case-specific arrangement is advantageous due to the wide range of jack-up vessels and environmental variations.

In model implementations adhering to the framework, the jack-up vessel is represented as a multi-body structure, in contrast to the conventional rigid-body representation often employed. Within the multibody approach the spudcans, the legs, and the vessel are described by separate bodies each with its own properties.
The primary focus of this research is on the dynamic soil-spudcan interaction process, which has not been extensively covered in existing standards. The soil-spudcan interaction model is to determine the instantaneous force acting on the spudcan as it contacts the seabed during GoL. By integrating elasto-plastic soil behavior into the soil-spudcan interaction element, the model encompasses descriptions of soil resistance to spudcan penetration and lateral displacement, taking into account memory and potentially stateful characteristics.

A simulation model, adhering to the framework, has been developed, integrating hydromechanical, structural, and soil-spudcan interaction submodels within the Orcaflex environment. Three distinct simulation scenarios are examined: an undisturbed vessel (free-floating), a disturbed vessel (full GoL), and a pinned vessel (elevated jack-up). The disturbed vessel scenario, which includes a full GoL process, has exhibited consistency in both undisturbed vessel simulations, where the vessel is the free-floating stage, and in pinned vessel simulations, where the vessel is in the pinned stage. The impact phase is situated between these two boundary cases, and the framework effectively represents simulation models within its scope.
In addition, simulations with varying sea states are performed for regular and irregular sea states. Simulations involving varying regular wave patterns suggest that the maximum downward spudcan velocity (DSV) is a critical parameter influencing the magnitude of impact forces on the spudcans. For irregular waves, the simulations indicate that the maximum impact forces are more closely related to the pinned vessel scenario, as the maximum impact occurs towards the end of the impact phase.

In conclusion, this thesis has effectively described the behavior of jack-up vessels during the impact phase of the GoL process. For any model utilizing the framework, the GoL process can be simulated, and the results can be analyzed to assess workability. Furthermore, the study proposes a potential correlation between vessel dynamics and maximal impact forces, a relationship that could potentially guide on-board decision-making processes. The enhanced understanding of the interaction between the spudcan and the seabed, along with the comprehensive framework, contributes to improving the decision-making process for executing the GoL operation of jack-up vessels in the offshore wind energy industry.

Preface

This master's thesis represents the final stage of my Offshore and Dredging Engineering master's program at Delft University of Technology. During the research process, I faced various challenges, but thanks to the constant support of my supervisors, family, and friends, I managed to overcome them and reach this important milestone. During the course of my thesis, I, unfortunately, suffered a broken ankle, which posed a significant drawback as I was unable to commute to the offices of MO4 and Calypso for several months. However, in retrospect, this situation provided an opportunity to work from home, enabling me to make significant progress in finalizing my literature review and improving my programming skills. Thus, in a somewhat counter-intuitive way, this personal setback may have actually benefited my work for this report. I am proud of my accomplishments and would like to express my appreciation to the following people in particular.

First of all, I would like to thank my supervisor, Maas, for his support and guidance throughout the entire process. The days at your office in Voorschoten were extremely helpful. Your skill in teaching me how to turn engineering ideas into working models has been super valuable. Maas consistently found the perfect balance between allowing me to explore independently and providing insights when needed.

Secondly, I would like to express my gratitude to Mark for giving me the opportunity to conduct my research with MO4 and for sharing insights into the offshore sector. His thorough understanding of physics greatly contributed to the identification and quick overview of crucial technical aspects of my research.

Thirdly, I want to thank all the other people at MO4 for sharing their knowledge, and enthusiasm, and making my time at the office enjoyable. I particularly appreciated the first Wednesdays of each month when the "game evenings" took place, which I truly enjoyed.

Furthermore, I would like to thank Vagelis, my university supervisor, for his guidance. He was able to answer all my soil-related questions, and more importantly, provided me with additional questions to ponder. I appreciate the time you dedicated to my project, especially during a significant period in your life. I am happy to call you Dr. Ir. E. Kementzetzidis. Additionally, I would like to express my gratitude to Peter for his expertise in the hydrodynamic aspects of my research and for his enthusiasm throughout the project.

Lastly, I cannot emphasize enough the invaluable support from my family and friends throughout this final phase of my academic journey.

Contents

List of Figures

List of Tables

Nomenclature

CEL Combined Eulerian-Lagrangian

CFD Computational Fluid Dynamics

COG Center Of Gravity

CPT Cone Penetration Test

DAF Dynamic Amplification Factor

DNV Det Norske Veritas

DOF Degree Of Freedom

DPS Dynamic Positioning System

DSV Downward Spudcan Velocity

EOM Equation Of Motion

Fd Frequency-Domain

FE Finite Element

GoL Going-on-location

Hs Significant wave height

ISO International Standard Organisation

$JONSWAP$ Joint North Sea Wave Project

KC Keulegan-Carpenter

LC Load Case

ODE Ordinary Differential Equations

RAO Response Amplitude Operator

SEU Self-Elevating Unit

$SNAME$ Society of Naval Architects and Marine Engineers

$SSA - I$ Site Specific Assessment for Installation

SSA Site Specific Assessment

Td Time-Domain

Tp Wave period

$WTIV$ Wind Turbine Installation Vessels

Chapter 1

Introduction

In recent decades, the escalating global energy demand has driven the oil and gas industry to expand its operations to remote offshore locations, abundant in hydrocarbon reserves. However, these challenging offshore environments present numerous operational and logistical obstacles. Consequently, self-elevating units (SEUs) have emerged as viable solutions for offshore drilling, production, and maintenance operations. SEUs are specialized offshore platforms capable of floating and elevating themselves above the water level using their own legs, providing mobility and flexibility in offshore exploration. In offshore exploration, it is essential to carry out drilling efforts at different locations to determine if there are usable oil and gas deposits.
Typically, SEUs employed in the oil and gas industry feature a three-legged structure to ensure stability on the ocean floor, see Figure 1.2. However, the increasing global emphasis on addressing climate change, primarily caused by the rise in greenhouse gas concentrations, has led to a growing interest in offshore renewable energy sources, such as wind energy. As the demand for green energy intensifies with the expanding global population, the offshore industry is shifting towards sustainable energy production.
The global shift towards renewable energy has led to a change in the use of SEUs which are becoming increasingly important. SEUs are often used as Wind Turbine Installation Vessels (WTIVs), see Figure 1.1. Instead of remaining stationary at a single location, WITVs need to relocate more often to perform installations at various sites. The ability of WITVs to self-elevate provides stability during offshore installations, making them versatile and cost-efficient in the offshore renewable energy industry.
This change in approach requires WITVs to demonstrate increased flexibility and adaptability to a variety of environmental conditions. They need to withstand severe weather and ocean conditions while having the ability to travel considerable distances to reach new sites. As a result, there is a growing need for inventive WITV designs and technologies that guarantee safe and efficient functioning across diverse settings. Continued research is crucial for developing the essential safety guidelines for deploying and retrieving WITVs in the ever-changing offshore energy sector.

Figure 1.1: Typical self-elevating unit used for oil and gas exploration (M. J. Cassidy, 2011).

Figure 1.2: Typical Wind Turbine Installation Vessel (DNV , 2021).

1.1 Jack-up vessels

Wind Turbine Installation Vessels (WTIVs) are purpose-built vessels engineered specifically for the assembly of offshore wind farms. Commonly known as jack-up vessels, these ships are equipped with heavy-lifting cranes, dynamic positioning systems, and a range of specialized equipment to facilitate the transportation and installation of wind turbine components, including tower sections, nacelles, and blades. Jack-up vessels have become a crucial part of the offshore wind industry, enabling the construction of large-scale wind farms in challenging marine environments.
Jack-up vessels are generally used in five primary modes: transit, installation, preloading, operation, and going-off-location. In transit mode, the vessel moves between locations using self-propulsion or assistance from tugboats. The legs are fully raised, and the vessel's weight is entirely supported by the hull's buoyancy. Upon arriving at the designated location, the legs are lowered to the seabed and jacked until the hull is elevated above the water, entering the installation mode. Spudcans at the end of each leg provide a stable foundation on the seabed by creating a large bearing area. At this stage, the soil's bearing capacity on the spudcan is sufficient to lift the hull, eliminating the need for buoyancy support. To ensure safe operations, the legs undergo preloading to increase bearing capacity. Preloading can be achieved by using preload tanks or by sequentially loading the legs with crosswise opposing leg pairs. After completing preload operations, the hull is jacked up to its operational air gap, which is the distance between the hull's lower end and the mean sea level. Once the air gap is reached, the unit is ready for operations. Upon completing the operations, the going-off-location is started and the legs are retrieved and removed from the seabed. After completion of the going-off-location the vessel is prepared for transit once again.
Before installing spudcans on the seabed, it is essential to assess all pertinent site-specific parameters to ensure the safe and effective operation of the jack-up vessel. Therefore, prior to each jack-up installation, it is essential to conduct a site-specific assessment (SSA). As jack-up vessels often undergo frequent movements between locations, efficient analysis of these parameters becomes increasingly critical.

1.2 Site-specific assessment

Wind farms typically require between 50 and 300 jack-up installations, with the number of jack-up installations being approximately twice the number of wind turbines (Ekici, 2018). To ensure safe operations, a site-specific assessment (SSA) must be performed before installing a jack-up vessel at a particular location (Olsson, 2014). The SSA evaluates the vessel's capability to operate safely at a specific site in the elevated mode by analyzing the vessel's, environmental, and soil data, which are then integrated into a report assessing the suitability of the jack-up vessel for the given location. The SSA process is regulated and standardized through technical guidelines and rules provided by the Society of Naval Architects and Marine Engineers (SNAME) and the International Standard Organisation (ISO). While these guidelines follow a similar technical methodology, they differ in terms of load and resistance factors. The SSA for WITV's can be categorized into four main sections (Hoyle et al., 2014):

- Geotechnical site assessment: This involves analyzing soil characteristics such as composition, density, and strength, as well as the geotechnical properties of the seabed, including a leg punch-through check. A

punch-through occurs when the legs of a jack-up barge unexpectedly penetrate the seabed after previously being supported (Skinner & Mote, 2015).

- Hydrodynamic site assessment: This entails examining wave, current, and wind conditions at the installation site and their impact on the jack-up vessel during various operation modes.
- Environmental site assessment: This comprises evaluating environmental factors such as marine life presence, water depth, and potential collisions with other vessels or objects.
- Structural site assessment: This consists of analyzing the structural integrity and stability of the jack-up vessel, along with the loads and forces it will experience during different operation modes.

The SSA is crucial for safe operations in elevated mode but does not directly focus on the going-on-location (GoL) process. During the installation process, the GoL phase takes place when the legs initially come into contact with the seabed. The initial contact and subsequent interactions between the spudcan and soil hold significant implications, as the impact forces generated during these interactions can be substantial. As the GoL process progresses, the vessel's weight is partially sustained by the hull's buoyancy and the leg reaction force exerted by the soil. However, the SSA used for jack-up vessels primarily concentrates on the vessel's performance during storms and ultimate limit states (Matter et al., 2005). For the GoL process, the Site Specific Assessment for Installation (SSA-I) should be used. The SSA-I is not as well-known or extensive as the SSA, but is becoming increasingly important. Understanding the GoL process and its potential effects on workability is essential for the successful installation and operation of a jack-up vessel. The jack-up industry is constantly pursuing innovative strategies and technologies to optimize insights in the GoL process and enhance workability. These advancements ultimately contribute to the overall performance and success of jack-up vessel operations, ensuring greater efficiency and cost-effectiveness in the rapidly evolving offshore energy sector.

1.3 Going-on-location and workability

The going-on-location (GoL) process is often the most challenging and critical aspect of deploying a jack-up vessel. During the GoL, the tip of the spudcan is the first part of the leg to come into contact with the seabed. The interaction between the spudcan and seabed is a complex, non-linear dynamic process that transpires within a short time frame (Olsson, 2014). The leg and spudcan must withstand the impact forces during this collision, which could potentially compromise the safety and stability of the vessel. These impact forces, characterized as the horizontal and vertical forces exerted on the spudcan by the seabed during touchdown, are absorbed through the collision between the spudcan and seabed, as illustrated in Figure 1.3. The successful completion

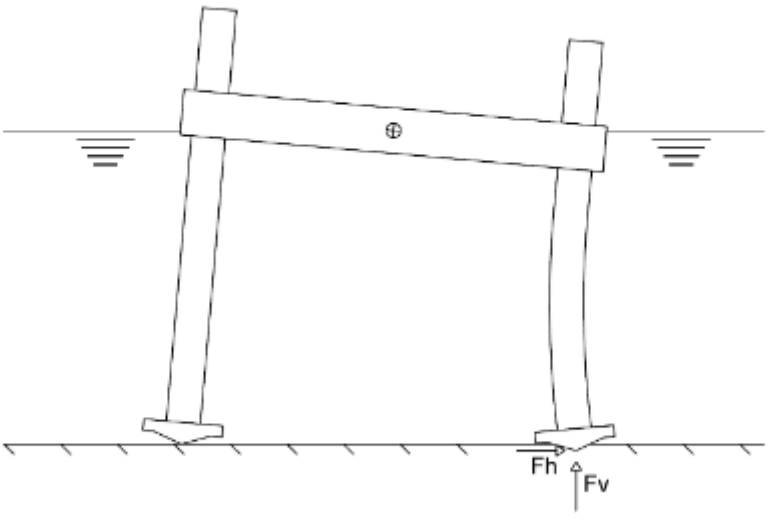

Figure 1.3: Horizontal and vertical forces acting on the spudcan, due to impact with the seabed (DNV , 2021)

of the GoL process relies on a combination of factors, such as sea state, water depth, and soil conditions. These factors significantly affect the stress magnitudes experienced by the legs and jacking systems, resulting from the interactions between the spudcan and the seabed (Ekici, 2018). Such impacts have the potential to cause structural damage to the legs and spudcans, ultimately posing a risk to the stability and safety of the jack-up

vessel (Chakrabarti, 2012).
To mitigate these risks, jack-up vessel manufacturers typically provide guidelines that outline the operational sea state limits for the GoL under various environmental conditions. Often referred to as the jack-up vessel manual, these guidelines serve as a critical resource for ensuring the safe and successful deployment of a jack-up vessel. The safe conditions for proceeding with the GoL are determined by a combination of vessel-specific parameters and environmental factors such as wave height (h_S), wave period (t_p), and heading (Ringsberg et al., 2017). These conditions help establish weather windows within which it is safe for the vessel to carry out the GoL. Generally, the most common limiting wave height for GoL is approximately $H_s = 2$ meters (Hoes, 2015) (Smith et al., 1994).
In addition to the jack-up vessel manual, the marine supervisor responsible for positioning the jack-up vessel may rely on in-house models, often based on guidelines from Det Norske Veritas (DNV), to support the decision-making process. Dynamic in-house models are employed to analyze the impact forces acting on the spudcan. These models use various inputs, such as wave and wind data, to simulate site-specific conditions and compute the forces the spudcan may encounter during the GoL process. By considering all available information and drawing from their experience, the marine supervisor makes informed decisions about proceeding with the GoL. Research conducted by Chakrabarti (2012), Ringsberg et al. (2017), Olsson (2014) and Smith et al. (1995) have revealed that in-house models may overestimate the impact loads due to assumptions made in the DNV guidelines (DNV GL, 2015). In-house models are frequently based on assumptions made in the DNV guidelines. It is important to note that the DNV guidelines do not take into account the seabed's composition, which can significantly affect the forces encountered by the vessel during the GoL. Consequently, in-house prediction models based on DNV guidelines may not accurately represent seabed conditions, as they assume an infinitely rigid surface regardless of the actual seabed composition. Furthermore, the in-house models lack an accurate description of the soil-spudcan interaction, see Section 3.3.3. The combination of the environmental conditions outlined in the jack-up manual and the assumptions made by DNV is considered to result in conservative decision-making, which prioritizes the safety of jack-up vessel operations (Chakrabarti, 2012) (Ringsberg et al., 2017). This conservative approach is adopted in the offshore industry due to the potentially severe consequences of a jack-up vessel failure. Utilizing advanced models can provide a more comprehensive understanding of the limiting factors during the GoL process. This increased accuracy can result in better-informed decision-making by the marine supervisor responsible for positioning the jack-up vessel, allowing for more efficient use of weather windows. Lower downtime will improve the efficiency and productivity of the jack-up vessel.

1.4 Objective and scope

The going-on-location (GoL) of a jack-up vessel installation is one of the key operating limiting factors, as critical impacts occur between the spudcan and the seabed. The workability of a jack-up vessel within offshore wind energy becomes therefore more strongly related to the GoL process. Hence there is a growing interest in understanding the limitations of impact analysis between the spudcan and the seabed and how the workability of jack-ups. For sites with stiff seabeds and with non-negligible sea states, the impact loads could damage the legs and/or jacking system. In the existing methodology, certain parameters like wave height can set limitations to when the GoL process can proceed. If these conditions are exceeded, operations would typically be halted for safety and operational integrity reasons. This approach results in conservative and imprecise decision-making for the GoL process. The focus shifts from solely relying on external conditions like wave height, to a better understanding of how the vessel's own dynamics can influence the impact forces on the spudcan. So, even in situations where the wave height exceeds traditional safety limits, if the vessel's dynamics are understood to be within safe bounds for withstanding the resulting impact forces, operations could continue.
An enhanced understanding of the interaction between the spudcan dynamics and the seabed can lead to improved installation limitations. This becomes particularly advantageous when it is possible to determine installation limits on-site, right before the initiation of the GoL process. A practical onboard decision-making approach would be to establish a correlation between vessel dynamics and the impact forces, thereby enabling more informed operational decisions.
Therefore, the main goal of this study is to enhance the decision-making process for executing the GoL operation through the development of a comprehensive framework. This framework combines hydrodynamic, structural, and soil-spudcan interaction elements to evaluate the GoL operation, with a particular focus on the leg impact phase.
This thesis is an interdisciplinary study that involves the fields of hydrodynamics, structural dynamics, and dynamic soil-spudcan interaction analysis. While the first two elements of the study are well-established areas of research, the soil-spudcan interaction is not extensively covered by the standards (SNAME, 2008) (ISO-19905-1). Therefore, the primary focus of this research is on the soil-spudcan interaction that occurs during the

GoL process of jack-up vessels, with emphasis on the description and modeling of the spudcan's impact on the seabed.

1.4.1 Research question

The main research question is presented below, along with three sub-questions that will help to answer the main question:

Main research question

The main research question to be investigated is:

How can the workability of a jack-up vessel be improved through decision-making support for the going-on-location?

Sub-questions

1. **How can a comprehensive framework for modeling the going-on-location process contribute to decision-support for jack-up vessels during this operation?**
2. **How can dynamic soil-spudcan interaction be improved and effectively implemented into the framework?**
3. **What parameters can be identified that will affect the impact between the spudcan and seabed during the going-on-location process of a jack-up vessel?**

The first sub-question focuses on understanding the ways in which a comprehensive framework for modeling the GoL process can contribute to decision-support for jack-up vessels during this critical operation. Accomplishing this question will involve determining how to establish the framework and identifying the key areas within the framework that require focused attention. The second sub-question aims to enhance the dynamic soil-spudcan interaction and its effective implementation within the proposed framework. The third sub-question seeks to identify the parameters that influence the impact between the spudcan and seabed during the GoL process of jack-up vessels. To address the third sub-question, multiple simulation scenarios with a range of sea states are conducted. The objective of this variation is to examine the influence of changing vessel dynamics upon sea-state fluctuation on the impact forces experienced by the spudcan. The ultimate goal is to establish a general guideline for correlating vessel dynamics with the resulting impact forces.
It is worth noting that the gaps and shortcomings in the current decision-making models for the GoL phase are primarily related to the assessment of the soil-spudcan interaction model. By improving the accuracy of this interaction model, it will be possible to reduce conservatism in the decision-making process. The addition of the third sub-question will help to further explore correlations between parameters affecting the impact between the spudcan and seabed.

1.4.2 Research decisions

In advancing the current models for describing the GoL process, certain research decisions and assumptions have been made. These were informed through a comprehensive literature study and during the development of the integrated framework. These decisions include:

- **Multibody-approach**. The methodology underlined in this study embraces a multibody approach, where the spudcan is modeled as an independent object with its own properties. This approach underscores the value of considering the jack-up vessel as a multibody system, diverging from the conventional rigid-body systems. It promotes the decoupling of specialized areas such as geotechnics and structural dynamics, allowing them to be addressed separately.
- **Elasto-plastic soil behaviour**. The soil behavior during impact is found to exhibit significant non-linearity, requiring the incorporation of elasto-plastic behavior into the soil modeling. Consequently, the soil-spudcan interaction model, which characterizes the soil's response to spudcan displacement, is designed to incorporate memory effects to accurately represent these plastic soil deformations.
- **Vertical and horizontal soil resistance**. Separate models are used for vertical and horizontal soil resistance, reflecting the distinct behaviors and characteristics of each direction.

- **Homogeneous soil conditions**. The seabed is assumed to be composed of a single, homogeneous layer of sand with no variations in properties. Additionally, it is assumed that the bathymetry (i.e., the shape and slope of the seabed) is constant.
- **Axial impact force as a limiting factor**. Given the shallow water depths (35 meters) examined in this study, the axial impact forces acting on the spudcan emerge as the constraining force during the going-on-location process.
- **Jack-up vessel characteristics**. 4-Legged jack-up vessels with cylindrical legs and cylindrical spudcans as footings were selected as the vessel characteristics to be considered in this study.
- **Wind and current effects are ignored**. Wind forces were considered to have a minimal impact on jack-up vessel behavior compared to wave forces and were therefore ignored. Current and secondary drift forces can be compensated using a dynamic positioning system (DPS).
- **Use of software**. Python is the preferred programming language for the study. Secondly, Orcaflex is used as a simulation environment for the results.

While it is possible that additional decisions or limitations may arise, they will be explicitly clarified in the respective Chapter.

1.5 Methodology

The methodology for this research comprises three steps: performing a literature study identifying current state-of-the-art GoL analysis, developing a comprehensive framework for GoL modeling from scratch, and using existing industry-standard software for simulation to retrieve results. These three steps are further elaborated on below. The methodology for the establishment of the comprehensive framework and the simulation model can be found in Chapter 4 and Chapter 5. These chapters provide a detailed description of the process involved in creating the framework and the simulation model, highlighting the key elements and considerations in their development. By referring to these Chapters, readers can gain a deeper understanding of the methodologies used and the rationale behind the choices made in constructing the comprehensive framework and simulation model for the Gol process of jack-up vessels.

1.5.1 Literature review; GoL analysis and soil-spudcan interaction

A literature review is conducted to identify and examine the GoL process of jack-up vessels. This review involves a thorough investigation of relevant academic journals and related literature concerning state-of-the-art GoL and soil-spudcan interaction models. Different modeling techniques and soil behavior theories are examined. The purpose of this step is to address the first and partly the second sub-questions. Sections 3.3.3 and 3.4.3 summarize the identified shortcomings of the current state-of-the-art modeling and the characteristics of the soil-spudcan interaction model developed in this thesis, respectively.

1.5.2 Comprehensive framework development

The purpose of this comprehensive framework development is to address the second sub-question, which seeks to understand the potential benefits and improvements of a comprehensive framework for decision-making support. This emphasizes exploring ways in which dynamic soil-spudcan interaction can be effectively implemented into the framework. The approach adopted in this comprehensive framework emphasizes a multibody perspective, characterizing the spudcan as an independent object with distinct properties. This perspective highlights the importance of viewing the jack-up vessel as a multibody system, a different approach from traditional rigid-body systems. It facilitates the separation of specialist fields, including geotechnics and structural dynamics, enabling each to be examined independently. This strategy enables professionals to focus exclusively on their specific field of expertise, thereby optimizing the analytical process.

1.5.3 Simulation model and results

In parallel with the development of the comprehensive framework, a simulation model in Orcaflex is created. OrcaFlex is a widely used software package in the offshore industry for simulating the behavior of offshore structures, including jack-up vessels. This software provides an efficient platform for running simulations and retrieving results. Both regular and irregular sea conditions are taken into account to validate the simulation

model and gather a deeper understanding of the GoL process. Simulations with regular sea states are executed to explore the correlation between the variability in vessel dynamics and the impact forces experienced during the GoL. Additionally, irregular sea state simulations are conducted to represent realistic scenarios and enhance the practical relevance of the study. The results establish a systematic understanding of jack-up vessels' behavior during the GoL process. By accomplishing this step, both the third sub-question and the main question can be addressed.

1.6 Thesis Outline

This Section provides a clear overview of the structure of this thesis.

Chapter 1: Introduction - This Chapter presents the background and motivation behind the research on jack-up vessels and their going-on-location process. It establishes the context, research questions, and objectives of the thesis.

Chapter 2: Theoretical background - This Chapter offers a comprehensive review of existing literature on jack-up vessels, their design, operation, and assessment methodologies. It identifies gaps in the current research and highlights areas for further investigation.

Chapter 3: Soil-spudcan interaction - This Chapter describes the current state-of-the-art models for soil-spudcan interaction. It discusses their advantages and disadvantages in relation to soil behavior and their implementations.

Chapter 4: Developed framework - This Chapter outlines the custom-developed model and explains its design choices and component implementations. A performance check on the Python model is also included.

Chapter 5: Simulation model; verification and validation - This Chapter introduces the simulation model and its coupling with OrcaFlex. A validation study is conducted to ensure the model's accuracy and reliability.

Chapter 6: Results & analysis - In this Chapter, the results of the site-specific assessments are presented and analyzed, offering insights into the performance of the proposed methodologies.

Chapter 7: Discussion & conclusions - This Chapter discusses the implications of the findings and their relevance to the overall objectives of the study. The results, framework, and related assumptions are examined and contextualized within the broader research landscape.

Chapter 8: Recommendations - This final Chapter summarizes the main findings of the research, highlights the contributions to the field and offers recommendations for future work on jack-up vessels and their site-specific assessments.

Chapter 2

Theoretical background

The going-on-location (GoL) process requires careful planning, preparation, and execution to ensure that the vessel is safely and accurately positioned on the seabed. In this context, understanding the design of a jack-up vessel and its motion responses when subjected to wave forces becomes outstanding. This knowledge is vital to ensuring a safe and successful GoL operation.

2.1 Jack-up vessel design and behavior

The primary purpose of a jack-up vessel is to provide a stable work platform for operations in shallow to moderately deep waters. The vessel's hull supports the operations deck and crew accommodations, while the legs are designed to penetrate the seabed, creating a stable and level foundation for operations. Jack-up vessels are used in various industries, including offshore oil and gas drilling, wind farm installation, maintenance, and decommissioning, and other marine construction projects. Different designs are available to ensure that the vessel can perform its intended tasks optimally. For example, jack-up vessels designed for the installation of offshore wind turbines may have different features than those designed for drilling operations. The design choices can include factors such as leg design, spudcan shape, jacking system capacity, and crane capacity.

Leg length is a critical design factor as it determines the water depth in which the jack-up can operate. Longer legs are required for deeper water, while shorter legs can be used in shallower water. Jack-up legs can be either cylindrical or trussed in structure, cylindrical legs are more commonly used in shallow waters, while trussed legs are more suitable for deeper waters (Kaiser & Snyder, 2013). The number of legs on a jack-up vessel can vary but typically ranges between three and six. The current WTIVs mostly have four legs and cylindrical legs.

Spudcans, an integral component of a jack-up vessel, come in various shapes and sizes, tailored to different soil types and operational conditions, see Figure 2.1. The primary function of spudcans is to penetrate the seabed and transfer vertical and horizontal loads to the ground. In softer soils, spudcans with larger surface areas are typically used to distribute the load more effectively, while in harder soils, smaller spudcans are preferred. Spudcans are engineered to endure high-impact loads during the GoL phase, particularly when encountering substantial resistance in sandy environments. Both preloading and free-flooding techniques can be used for the legs and spudcans. In preloading, the legs and spudcans are filled with seawater. This increases the weight of the jack-up unit, which helps to ensure that the spudcans penetrate the seabed and provide the necessary stability. In free-flooding, the legs and spudcans are not filled with any fluid before installation. Instead, they are allowed to fill with seawater during installation.

2.2 Jacking system

The jacking system is a crucial component of the jack-up vessel that enables the hull to be raised and lowered relative to the legs. It comprises of a set of motors, gearboxes, pinions, and racks that engage the teeth of the leg chords. The jacking system plays a critical role during the going-on-location phase as it is where the forces on the spudcan are transmitted to the legs and the hull of the jack-up vessel. The jackhouse is the structure on the jack-up vessel that houses the jacking system components. Two jacking systems can be described depending on the way they transmit force to the legs.
A hydraulic jacking system with movable and resting cylinders is a type of jacking system that uses hydraulic

Figure 2.1: View of the spudcan's underside (Yi & Park, 2023).

force to lift the vessel. This system generally consists of two types of cylinders: a movable cylinder attached to the leg, and a resting cylinder attached to the vessel. When the system is activated, hydraulic fluid is pumped into the movable cylinder, causing the piston inside to extend and lift the vessel. At the same time, hydraulic fluid is released from the resting cylinder, allowing the vessel to be lifted without causing the resting cylinder to move. Once the desired height is reached, the hydraulic cylinders are locked to the leg using a pin-in-the-hole mechanism, which ensures the stability of the system.
The other jacking system, the rack-and-pinion system is electrically powered and uses a series of gears, known as pinions, which engage with a set of teeth along the chords of the legs. As the pinions rotate, they cause the leg chords to move up or down, raising or lowering the hull. The rack and pinion system is the most commonly used jacking system in jack-up units.

During the GoL process, the spudcan of a jack-up vessel penetrates the seabed and creates impact loads that result in shear and bending forces in the legs. To distribute these forces, the upper and lower guides come into play, which act as a horizontal force couple between the legs and the hull of the jack-up vessel (DNV GL, 2015). The guides are vertical steel members attached to the legs and run the entire leg length. They provide stability and prevent excessive lateral movement of the legs during jacking operations. The vertical impact loads on the spudcan generate axial forces in the legs, which are transmitted to the pinions as a vertical force couple (Smith et al., 1995).
The guides and pinions are key components in the jackhouse and are designed to withstand the loads and stresses involved in positioning and stabilizing the vessel. As the jack-up vessel is raised and lowered, the guides provide lateral support and stability to the legs, ensuring that they remain in position and aligned. The pinions, on the other hand, transmit the driving force from the jacking system to the legs, allowing the vessel to be lifted or lowered as required. Due to the high loads and frequent use of these components, they are typically designed to be strong and wear-resistant, to minimize the risk of failure or damage.
The impact loads between the seabed and spudcan are partly absorbed by the horizontal force couple at the upper and lower guides and the vertical force couple at the pinions, with the ratio between them indicated by the parameter β (Zheng, Zhang, & Lai, 2015). This parameter is usually in the range of 0.8 to 1. The guides play a crucial role in the hull-leg connection by establishing the structural limits and withstanding the highest loads. Among the guides, the lower guide is particularly critical due to the significant forces and moments it experiences (Smith et al., 1995) (DNV GL, 2015).

2.3 Vessel motions and Response Amplitude Operators (RAOs)

The hydrodynamic analysis of a free-floating hull involves examining how the hull moves and behaves in the water, considering the various forces that act upon it. The hull is considered to be a rigid body that will oscillate on the free surface of the water. The fluid, water, is assumed to be an ideal fluid (Journée & Massie, 2001). An ideal

fluid is a theoretical concept that is used to simplify the analysis of real fluids. It is a fluid that has no viscosity, meaning it offers no resistance to shear stresses. An ideal fluid also has no surface tension and is incompressible, meaning that its density remains constant regardless of the pressure applied to it (Journée & Massie, 2001).

The vessel in a free-floating state without any constraints has six degrees of freedom (DOF) which refers to the six ways in which a body can move in three-dimensional space, see Figure 2.2 and the degrees of freedom below.

- **Roll** - rotate around an axis running the length of the ship.
- **Pitch** - rotate around an axis running across the ship.
- **Yaw** - rotate around a vertical axis through the ship.
- **Heave** - moves up and down along the yaw axis.
- **Surge** - moves forward and astern along the roll axis.
- **Sway** - moves sideways along the pitch axis.

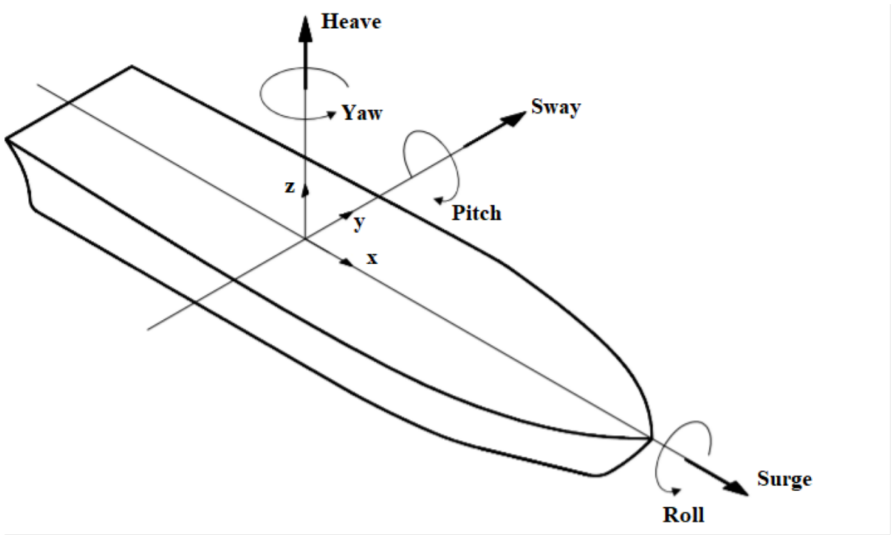

Figure 2.2: Six degrees of freedom vessel (Selimovic et al., 2020).

As jack-up vessels are in free-floating state, they are subjected to incoming waves and tend to move. Response amplitude operators (RAOs) can be determined for each degree of freedom in response to a specific incoming regular wave. An RAO is a dimensionless quantity to predict the motion behavior of a floating body in response to wave excitation. RAOs are calculated as the ratio of the vessel's response to the wave, offering insight into the vessel's characteristics (Le et al., 2021). RAOs serve as a valuable tool in assessing the vessel's performance under different wave conditions, which aids engineers and operators in designing and optimizing vessel configurations for improved stability and functionality in various sea states.

2.4 Environmental loading

Within the context of this thesis, environmental loading pertains to the forces and moments exerted on a ship or floating structure by the surrounding environment, including waves, currents, and wind. During the GoL process of a jack-up vessel, wave loads constitute the most prominent forces compared to current and wind loads (Chakrabarti, 2012). A thorough analysis of environmental loading must account for the effects on various components of the jack-up vessel, such as the hull and legs. In addition, different sea states should also be taken into account, as they each have unique properties such as significant wave height, period, and direction.

2.4.1 Sea state

To describe a specific sea state, several key parameters and characteristics must be provided. These parameters help to quantify and communicate the wave conditions accurately. The essential parameters include significant wave height (Hs), peak period (Tp), and wave direction.
The significant wave height often denoted as Hs represents the average of the highest one-third of the waves within a given wave spectrum. It is a widely used parameter in the maritime industry to describe wave conditions and serves as a practical measure of wave height for engineering purposes. Wave period, typically represented by Tp, refers to the time interval between two consecutive wave crests passing through a fixed point. Accurate knowledge of wave periods allows for better design and operational decision-making to minimize the impact of waves on a vessel. Wave direction is the angle at which waves approach the vessel relative to its heading. This factor affects how the vessel responds to the waves. By considering the wave direction, maritime supervisors can optimize the vessel's orientation and position to reduce the wave-induced motion and improve stability.

Swell conditions and wind waves are two distinct components of a sea state that contribute to the overall wave conditions experienced by the vessel. Swell waves, or swells, are long-wavelength waves that originate from distant storms or winds. Swell waves typically have a more regular and uniform appearance, with long wave periods and smoother crests compared to wind waves. Wind waves are generated by local winds acting on the water's surface. Wind waves tend to have shorter wavelengths and periods, and their crests are more irregular and steep compared to swell waves.
In real-world sea states, swells and wind waves often interact, resulting in a complex wave pattern that affects a vessel's stability. Therefore, it is crucial to analyze both swell and wind wave conditions when describing a sea state and assessing its impact on a vessel. The JONSWAP (Joint North Sea Wave Project) spectrum is a widely used model for describing a realistic sea state that accounts for the combined effects of both swell and wind waves. The JONSWAP spectrum considers the energy distribution of waves as a function of frequency, capturing the characteristics of both swell and wind-generated waves within a single model.

2.4.2 Environmental hull loading

A vessel could experience both translational and rotational oscillatory motions. Each vessel has a unique response to identical wave conditions, as factors like mass, size, and geometry influence both the wave loads and the response of individual units (Izadi & Vazquez, 2021). Vessel loads, hydrodynamic coefficients (added mass/damping), and free-floating motions can be calculated with reasonable accuracy using commercially available software, like Orcaflex (Orcina, 2021). External wave excitation forces are one of the primary sources of environmental hull loading on ships and offshore structures. When a vessel is exposed to incoming waves, the waves generate forces and moments on the hull, which can cause it to experience motions. The total wave force acting on a vessel's hull is the net force resulting from the incident wave forces and the radiation forces (Journée & Massie, 2001).
Incoming wave forces are the forces generated by the waves hitting the hull of the vessel. These forces can be decomposed into two components: the incident wave force, which is the force due to the incoming wave, and the diffracted wave force, which is the force due to the waves that are scattered by the hull. The most basic type of incident wave force is the Froude-Krylov force, which is the force due to the pressure distribution from undisturbed incident waves on the submerged part of the vessel. The diffracted wave force accounts for the changes in wave behavior caused by the presence of the hull.
Radiation forces are the forces generated by the motion of the vessel in the fluid, which create a disturbance in the surrounding water. These forces are dependent on the shape and size of the hull and the velocity of the vessel.

2.4.3 Environmental leg loading

Jack-up legs are characterized as slender structures with lengths that greatly exceed their cross-sectional dimensions. Slender structures have diameters that are relatively small compared to the wavelengths of the fluid in which they are submerged. The fluid interaction with these structures differs from that with a vessel's hull. To compute the wave loads on slender structures such as jack-up legs, the Morison equation is employed. This empirical equation provides a distinct approach to assessing fluid-structure interactions for slender structures. The Morison equation is composed of two components: a linear inertia force, FI, and a non-linear drag force, FD. The drag force is an empirical force that originates from the vortices generated when the fluid moves around the jack-up leg. In contrast, the inertia force arises from the pressure gradient present in an accelerating fluid (M. J. Cassidy, 1999).

The Keulegan-Carpenter (KC) number is used to assess the relative significance of drag and inertia forces, representing the ratio of the inertia force to the drag force. Typically, jack-up structures exhibit high KC numbers, which signifies that they are predominantly influenced by drag forces.

$$F = \underbrace{\rho C_m V \dot{u}}_{F_I} + \underbrace{\frac{1}{2}\rho C_d A u|u|}_{F_D}, \tag{2.1}$$

where:

F = hydrodynamic force acting on the slender structure [N]
ρ = density of the fluid.
C_m = inertia coefficient, which is a measure of the importance of the inertia force relative to the drag force [-]
V = velocity of the fluid relative to the structure [m/s]
u = velocity of the structure relative to the fluid [m/s]
C_d = drag coefficient, which is an empirical constant that depends on the shape and roughness of the structure [-]
A_u = projected frontal area of the structure, perpendicular to the direction of the fluid flow [m^2]
u = magnitude of the velocity of the structure relative to the fluid [m/s]

2.5 Structural jack-up model

Various modeling techniques can be used to represent jack-up units and legs in different design and analysis scenarios. These techniques have different capabilities and limitations in terms of their ability to accurately depict the design and behavior of the units. Common modeling techniques used to depict jack-up and legs are finite element analysis and simplified beam model (Zheng et al., 2015). One way to represent a jack-up is by a simplified beam model, as suggested in research done by (M. J. Cassidy, 2011) (M. Cassidy & Houlsby, 1999) (Smith et al., 1994). This type of model treats the jack-up unit as a series of beams with corresponding stiffness and mass properties, rather than modeling the individual components of the unit in detail. See Figure 2.3 for a simplified beam model of a jack-up. This type of model uses beams to represent the structural elements of the jack-up, such as the legs and the platform, and assigns stiffness and mass values to these beams to reflect the properties of the physical structure. The spudcans and legs are combined and modelled as a single entity rather than as separate components. Besides the hull-leg connection is often represented as a linear spring or, in some cases, as a rigid connection (Van Dalfsen, 2016). An equivalent beam model can be an effective and simple way to represent the overall behavior of a jack-up unit and to analyze its response to different loading conditions.
On the other hand, finite element is a numerical method for solving problems in engineering and applied sciences that involve dividing a complex structure into smaller, simpler parts, known as elements. These elements can be analyzed individually, and the results can be combined to predict the behavior of the overall system. In a study done by Olsson (2014) a representation of leg and spudcan with two different mesh types and densities are evaluated, see Figure 2.4.

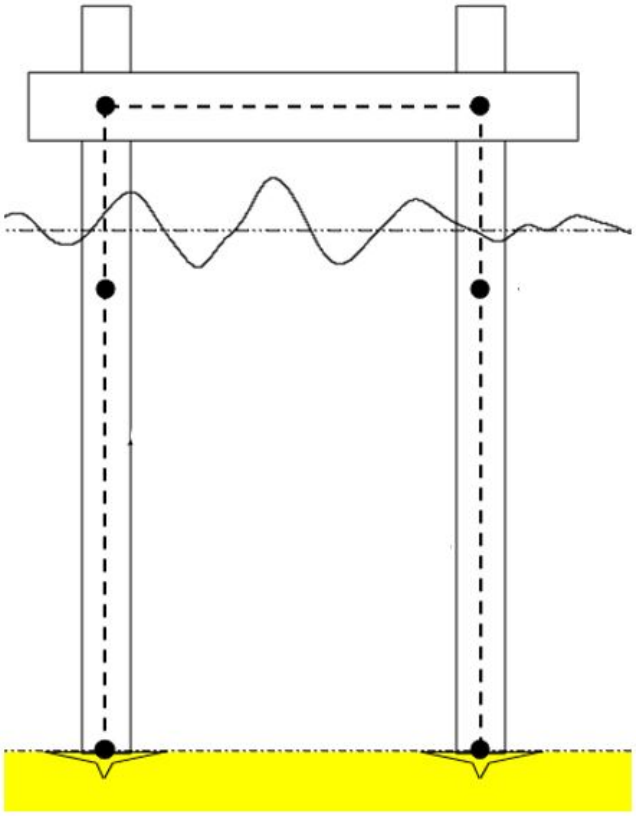

Figure 2.3: Schematic structural representation of a jack-up, simplified beam model (M. Cassidy & Houlsby, 1999).

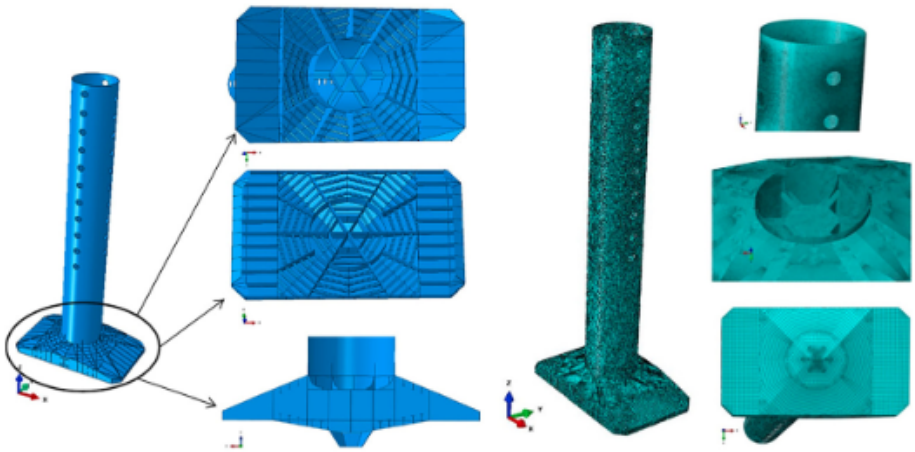

Figure 2.4: The geometry model of the leg and the spudcan made in AUTOCAD (Olsson, 2014).

Chapter 3

Soil-spudcan interaction

Analyzing the impact of a jack-up vessel's legs on the seabed requires an understanding of both the structural and geotechnical elements involved. The structural aspect pertains to the leg and spudcan, and the geotechnical aspect addresses soil behavior. To describe the soil behavior under impact, it is essential to consider the soil's composition and properties, as these factors can significantly influence the response of the soil to the applied load. In this study, the focus is on soil classified as sand, a common seabed material often encountered by jack-up vessels during operation. This Chapter aims to investigate the interaction between the spudcan and sandy seabed conditions. The first section of this Chapter offers a comprehensive overview of soil behavior and modeling approaches. Subsequently, the Chapter outlines the soil-spudcan interaction model developed in this study, which serves as the foundation for in-depth analyses conducted in Chapters 4 and 5.

3.1 Impact analysis

The interaction between the spudcan and the soil starts when the spudcans of a jack-up vessel come into contact with the seabed. Before this contact, the vessel is in a free-floating mode, experiencing translational and rotational oscillatory motions due to incoming regular waves. The spudcans undergo cyclic movements in the free-floating mode before seabed contact, see Figure 3.1. Each of the four spudcans on a jack-up vessel experiences a unique displacement, as they have individual eccentricities relative to the vessel's center of gravity. The amplitude of the horizontal and vertical displacements depends primarily on the vessel's orientation with respect to incoming waves. The spudcan's trajectory in the x-z plane reveals that the spudcan surpasses its initial vertical position (z-direction), potentially resulting in multiple impacts during a single GoL event. This stamping motion has been confirmed to accurately represent the true behavior of a spudcan interacting with the seabed during the GoL process (Vazquez et al., 2017) (Chakrabarti, 2012). Subsequent impacts of the spudcan on the seabed result in the formation of a crater or hole. This phenomenon occurs due to the spudcan displacing and compacting the soil permanently. The spudcan's circular movements create a complex and non-linear dynamic process involving both vertical and horizontal soil forces. Vertical forces arise from the soil's resistance as the spudcan penetrates deeper into the seabed, while horizontal forces are generated by the lateral movement of the spudcan, causing soil displacement and frictional resistance in the opposite direction. The resistance forces, both vertical and horizontal, depending on soil stiffness characteristics, which vary based on the type of soil. These impact loads are dynamic, meaning they vary with time and can cause sudden, high-magnitude forces that act on the jack-up vessel. High-magnitude force impulses can lead to significant stresses on the vessel's structure, potentially causing damage or even failure if the forces exceed the design limits (Izadi & Vazquez, 2021). Through the development of this framework, design limits, such as bending moments and axial forces in the legs, can be established, serving as limits for the GoL process.
In conclusion, the impact analysis in this study entails a two-way examination of the interaction between the jack-up vessel and the seabed soil, incorporating both the structural stiffness of the legs and spudcan, and the non-linear seabed characteristics.

3.2 Soil behavior

An understanding of basic soil behavior principles is crucial for further describing the seabed response. For a correct description, soil behavior and soil deformation as a result of an external force need to be understood. The response of soil depends on both the engineering properties and the nature of the loading applied (Jia,

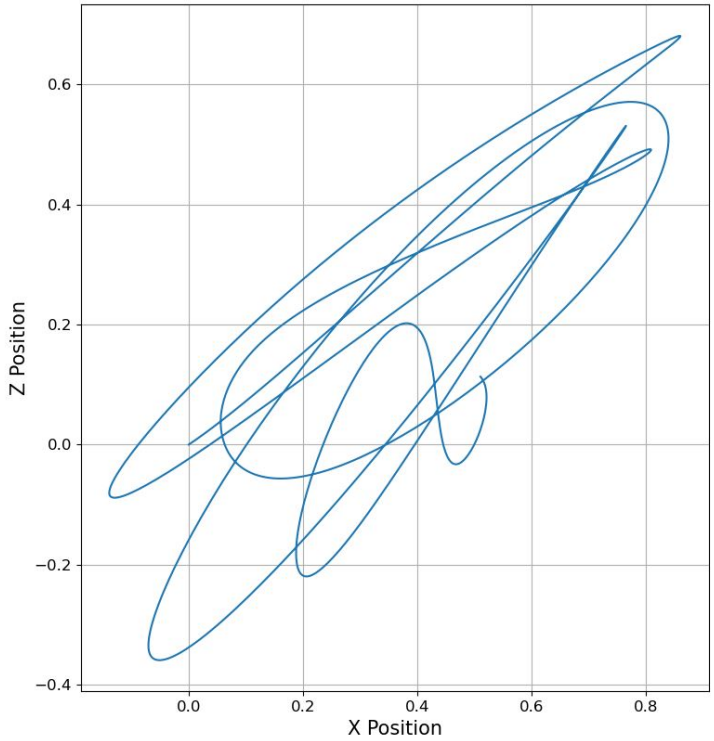

Figure 3.1: Trajectory of the spudcan on a vessel exposed to waves in a free-floating state in the x-z plane.

2018). First, fundamental soil characteristics and soil behavior concepts are elaborated on. Thereafter, soil behavior models are described and framed for this research.

3.2.1 Seabed properties

Soil mechanics is a complex field of study that involves analyzing the response of soil to various external loads and conditions. To accurately analyze and predict soil behavior, it is crucial to understand the properties of soil and how these properties influence its behavior. Soil properties can vary significantly depending on factors such as origin, environment, and loading history, and they play a key role in determining the mechanical behavior of soil. Classifying soils based on their properties and characteristics results in a better understanding of soil mechanics. In soils with low stiffness, like soft clays or loose sands, the soil undergoes great deformation when subjected to an external load. As the soil deforms, it absorbs and dissipates the energy from the applied force, reducing the impact loads transmitted to the legs and spudcans. This energy dissipation process helps minimize the risk of damage to the vessel and its foundation during the GoL in soft soils. In contrast to soft seabeds, hard seabeds such as dense sand, gravel, and bedrock have higher stiffness and resistance to deformation, potentially causing high impact forces. The penetration in these stiff soil may limit the contact area of the spudcan, whereas for soft soils the spudcan will penetrate deep and may bury until equilibrium is reached (Randolph et al., 2006) (Dier et al., 2004). When a jack-up's spudcan makes contact with a stiff seabed, the force exchange between the vessel and the seabed happens much more quickly, as both the seabed and the spudcan are stiff objects. During impact, saturated dense sand typically behaves in an undrained manner. In undrained conditions, the soil does not have sufficient time for water to flow in or out of the soil pores due to the rapid loading that occurs during impact. It is often assumed that the soil layer being studied is uniform, consisting of a single soil type with perfectly horizontal bathymetry. Additionally, no historical footprints are considered, and the soil properties do not change with depth or change laterally.

3.2.2 Elasto-plastic behavior

Understanding the deformation behavior of soil under external stress is essential in geotechnical engineering. Soil can deform in two primary ways, elastic and plastic, which exhibit distinct characteristics. In reality, soil behavior often combines both elastic and plastic responses, resulting in elasto-plastic behavior. When soil, such

as a sandy seabed, is subjected to loading, it initially undergoes elastic deformation. However, as the applied stress exceeds a certain threshold, i.e. yield point, the soil transitions into a plastic deformation region. In this region, even upon unloading, the soil does not fully recover to its initial state, and some permanent deformation remains. These loading and unloading behaviors can be illustrated by stress-strain curves. A stress-strain curve for sand visually represents the relationship between applied stress on the vertical axis and the resulting strain on the horizontal axis. The slope of the curve represents the soil stiffness. The elastic and plastic soil deformations are further described below.

- Elastic soil deformations are fully reversible, with the soil loading and unloading following the same path. In other words, no strains are stored in the soil, and the strain is fully reversible. Elastic behavior is described by Hooke's law $F_s = kx$, which relates the force needed to extend or compress the soil by a distance, with k representing the soil stiffness. Hooke's law can be either linear or nonlinear. In linear cases, strain and force are proportional, while in nonlinear elastic soil behavior, the loading and unloading path follows the stress-strain curve, with varying slopes for different stress states, Figure 3.2 (a) and Figure 3.2 (b) respectively (Jia, 2018).
- Plastic soil behavior involves permanent deformation, with soil loading and unloading following different paths. Upon loading, strain is stored in the soil, and it will not return completely to its original shape. In Figure 3.2 (c), as the applied stress exceeds the yield point Y, the soil undergoes a transition into a region of plastic deformation. To assess the occurrence of plastic strains, the focus lies entirely on the unloading path, as the loading phase does not provide sufficient information to determine the ratio of elastic to plastic deformation.

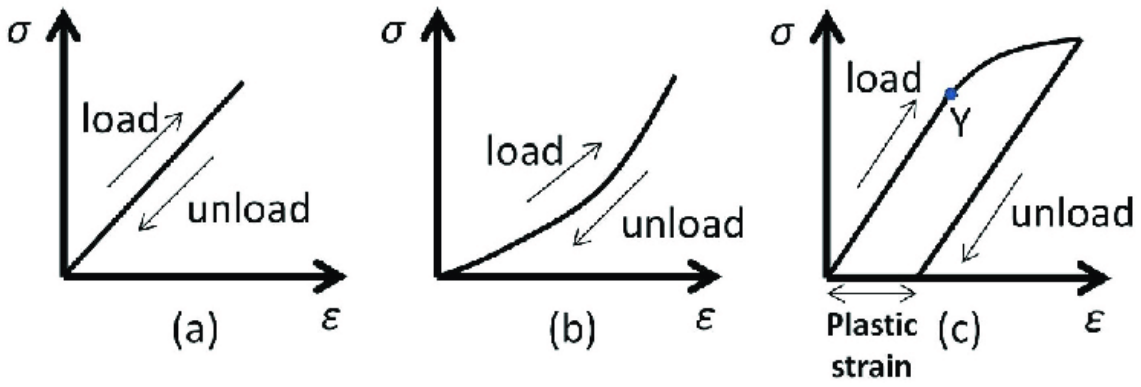

Figure 3.2: (a) Linear loading/unloading path; (b) non-linear loading/unloading path; (c) plastic soil deformation upon loading/unloading.

Real-world soil responses often exhibit a combination of elastic and plastic deformations, known as elasto-plastic behavior. Within elasto-plasticity theory, the total strains of the soil are divided into recoverable and permanent strains, the permanent strain will be determined upon unloading. The yield function is used to classify elastic or plastic deformations, as it is a function of the stress state upon which elastic strain occurs. Beyond the yield function, the strain becomes permanent (Jia, 2018). The yield function will be further elaborated on in Section 3.4.2.

3.3 State-of-the-art dynamic soil-spudcan interaction modeling

3.3.1 Numerical modeling techniques

In an attempt to describe soil under the impact load of a spudcan, in a computerized model, different methodologies and assumptions for describing the soil behavior are used. In a study done by Vazquez and Grasso (2016), Smith et al. (1994) and Smith et al. (1995), the impact is described using a combination of the soil stiffness, leg stiffness, and jacking system stiffness, according to DNV guidelines (DNV GL, 2015). This simplified approach can only describe linear-elastic soil behavior (Figure 3.2 (a)).
Within soil-spudcan interaction, the soil is subjected to time-varying spudcan displacement and therefore behaves as a complex material that displays nonlinear and time-dependent behavior (Chakrabarti, 2012) (Le et al., 2021). Plastic deformation is found to be dominated under impact loading (Chakrabarti, 2012). Therefore, Chakrabarti (2012) and Ringsberg et al. (2017) extended the description of the soil by incorporating plastic soil behavior into their interaction model. These additions aimed to more accurately capture the behavior of the soil during the GoL phase. However in the study done by Ringsberg et al. (2017), no load history is accounted for during impact, therefore every impact is a "new" impact during a single GoL event.

Besides the methodologies described by the studies above, soil can be treated as a continuum to analyze the behavior of soil using finite elements methods. Continuum modeling is a method for describing the behavior of a soil medium that is based on partial differential equations and/or constitutive laws. It is an accurate method for modeling the soil, as it can take into account the complex behavior of the soil and can accurately capture the nonlinearities and nonhomogeneities that may exist in the soil. However, continuum modeling also has some limitations. It can be time-consuming to set up and solve partial differential equations, and it requires specialized commercial software packages and expertise to implement. As a result, it may not be practical for all applications.
Le et al. (2021) and Vazquez et al. (2017) both used commercial software to perform a finite element analysis of the seabed during the GoL process. In their models, Le et al. (2021) used the Mohr-Coulomb constitutive law to describe the behavior of the soil, while Vazquez et al. (2017) used the kinematic hardening law.

3.3.2 Experimental soil impact approaches

Experimental approaches play a crucial role in validating and supplementing numerical models, offering valuable insights into the actual behavior of soil and soil-structure systems. Physical laboratory tests, such as triaxial tests, direct shear tests, and consolidation tests, provide essential data on soil properties and mechanical responses (Jia, 2018). While experimental approaches can be time-consuming and resource-intensive, they are essential for verifying numerical models and ensuring the reliability and accuracy of soil modeling techniques.
In the context of subsequent spudcan impacts during the GoL process, the experimental study by Xie et al. (2016) provides valuable insights into the mechanical behavior of soil subjected to multiple impact loads. The findings suggest that as the number of subsequent impacts by the spudcan on the seabed increases, the settlement of the soil due to each impact becomes less significant. This indicates that the soil beneath the spudcan may experience less plastic deformation over time.
In a benchmark experiment carried out by Yung-Show et al. (2019), the penetration of a spudcan into dense sand was investigated. The saturated dense sand used in the experiment had a unit weight of 20 kN/m^3, a relative density of 70%, and an internal friction angle of 35°. The vertical forces acting on the spudcan computed using equations proposed by SNAME (2008) were found to be in good agreement with the experimental results and the specific details of the model test, as shown in Fig. 3.3. For this research, vertical bearing capacity formulas for conical footprints, which are comparable to the SNAME equations, are also employed to analyze the spudcan penetration and impact. In addition to the previously mentioned benchmark experiments, centrifuge tests can also be conducted to validate and benchmark numerical models. Centrifuge testing is a well-established experimental technique in geotechnical engineering, which involves subjecting scaled-down soil-structure models to increased gravitational forces to replicate the stress conditions experienced in full-scale situations. The insights gained from these two experimental studies provide valuable validation for the numerical modeling techniques employed in this research and studies from Section 3.3.1.

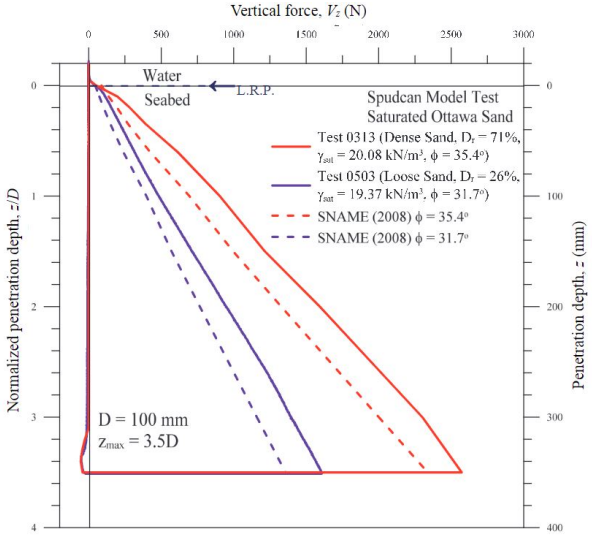

Figure 3.3: Typical spudcan penetration profiles on loose and dense sand. Dashed lines represent the penetration resistance based on the equations proposed by SNAME (2008), while solid lines correspond to the soil resistance obtained from the experimental data by (Yung-Show et al., 2019).

3.3.3 Conclusion; shortcomings and potential improvements

From the various studies conducted, it is evident that numerous methods are available for describing and analyzing soil behavior under spudcan impact. However, the existing soil-spudcan interaction models have some limitations and areas for potential improvement.

- Firstly, none of the models treat the spudcan as a separate body connected to the leg; rather, the spudcan and leg are combined and modeled as a rigid body. To account for the bending of the leg and the performance of the jacking system, an equivalent spring stiffness is defined that incorporates both the leg stiffness and the stiffness of the jacking system. Additionally, linear soil stiffness is integrated into this equivalent spring mechanism as a way to account for soil behavior. However, this approach simplifies the system and is only capable of describing soil behavior that follows a linear-elastic model, as depicted in Figure 3.2 (a).
- Secondly, the models predominantly employ equivalent spring stiffnesses to characterize soil resistance, instead of directly applying soil behavior theories. Incorporating soil behavior theories, elasto-plasticity theory, could offer a more comprehensive understanding of the soil-spudcan interaction and enhance the accuracy of the model predictions. Vazquez et al. (2017) presents the state-of-the-art implementation of soil behavior theory using Abaques. However, plastic soil deformation upon impact is negligible from the results, as it was predominantly assumed to be the case.
- Thirdly, current models do not consider the interaction between the vertical and horizontal soil resistance components. Acknowledging and accounting for this interaction may improve the overall modeling of soil-spudcan interactions, providing a more complete representation of the system's behavior.

The initial part of the first subquestion, which focuses on enhancing soil-spudcan interaction modeling, has been addressed. In the following Section, a comprehensive description of the framework for soil-spudcan interaction modeling is provided, integrating the three improvements summarized above.

3.4 Developed comprehensive soil-spudcan interaction model

In soil mechanics, the vertical and horizontal resistance of soil is often modeled separately due to their different behaviors and characteristics. In essence, both the vertical and horizontal soil resistances can be described by an elasto-plastic behavior. However, the vertical soil resistance of spudcan penetrating the soil is described by the bearing capacity theory, while the horizontal soil sliding resistance is based on bottom friction and side resistance.

3.4.1 Vertical soil resistance

Bearing capacity theory

The bearing capacity of soil is a fundamental concept in geotechnical engineering, as it quantifies the ability of the soil to safely support the load imposed by a foundation or structure. This measure is vital for the design of spudcans, as it governs the selection of the appropriate size and type of spudcan needed to sustain the weight of the jack-up vessel in elevated mode. Several theories have been developed to predict the bearing capacity of the soil, including those by Terzaghi (1943) and Meyerhof (1963). These theories take into account the mechanical properties of the soil, such as stiffness, strength, and deformation characteristics, as well as the shape, size, and depth of the foundation.

The bearing capacity theory is the recommended approach for the prediction of vertical soil resistance by both (ISO) and (SNAME). This theory is used to describe the deformation course of sandy soil and to predict resistance to penetration. The recommended theories in ISO and SNAME are both for conical spudcans vertically penetrating the sandy seabed and are based on the bearing capacity theory developed by Meyerhof (1963) and Terzaghi (1943).

$$F_V = (0.5\gamma' B N_\gamma s_\gamma + p_0' N_q s_q d_q)\, A \tag{3.1}$$

$$\begin{aligned} N_q &= \text{Bearing capacity factor } = e^{\pi \tan\phi} \tan^2(45 + \phi/2) \\ N\gamma &= \text{Bearing capacity factor } = 2\,(\,N_q + 1)\tan\phi \end{aligned} \tag{3.2}$$

B = Effective spudcan diameter at uppermost part of bearing area in contact with the soil
γ' = Effective unit weight of the soil
N_γ = Equation 3.2
s_γ = 0.6, For circular footing
p_0' = Effective overburden pressure
N_q = Equation 3.2
s_q = 1 + tan(ϕ)
d_q = 1+2 $\tan\phi(1-\sin\phi)^2$D/B for D/B $\leq$ 1
A = Spudcan effective bearing area

The vertical soil penetration curve depicts the relationship between the depth of penetration of the spudcan into the sand and the resistance encountered during penetration, see Figure 3.4. The friction angle, often denoted as ϕ, is a crucial parameter in determining the bearing capacity of soil, particularly for granular soils like sand. In general, a larger friction angle corresponds to higher soil strength, which in turn results in a greater bearing capacity. As the spudcan initially contacts the sand surface, there is minimal resistance. At this moment the spudcan partially penetrates the soil, an effective diameter can be used to account for the current bearing area and effectively model the soil resistance experienced during this stage of penetration. As the spudcan progressively penetrates the soil, the effective diameter and the bearing area increase, leading to an increase in the vertical soil resistance acting on the footing, see Figure 3.5.
According to a study by Hu et al. (2021), an analysis of 120 instances of spudcan penetration in sand deposits revealed that 12 cases had a penetration depth of less than 0.5 m, while approximately 71% of the data fell within the 0-3 m range. As a result, during the spudcan's impact and penetration during the GoL, backfill is not considered (Figure 3.5).

Vertical soil resistance model

In this study, the vertical soil resistance is characterized by the elasto-plastic behavior of the soil, taking into account the bearing capacity theory. This approach allows for an accurate representation of the soil response during spudcan penetration, considering both the elastic and plastic soil deformations.
The seabed vertical resistance model in this study employs four distinct penetration modes: no soil contact, virgin soil penetration, unloading, and reloading. Each penetration mode utilizes a different function, and the function parameters are updated whenever a penetration reversal occurs. This approach allows to include elasto-plastic seabed behavior and the spudcan's progressive penetration through cycles of vertical displacement. For each spudcan penetration mode, the soil penetration resistance is determined by a specific derivation and/or formula. The backbone of the penetration resistance is provided by the ultimate penetration resistance of a spudcan in sand. The ultimate penetration resistance for a spudcan in sand is calculated using the bearing

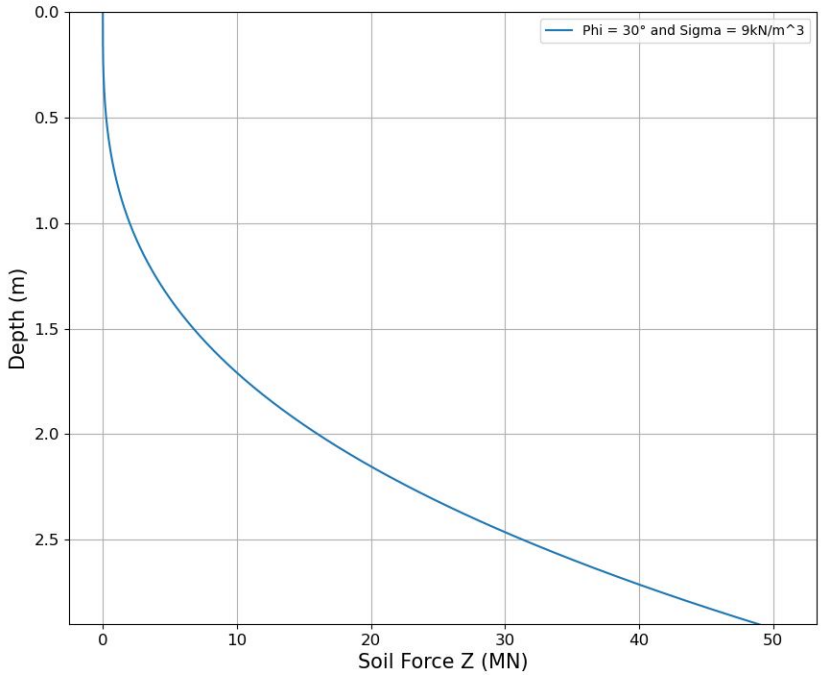

Figure 3.4: Bearing capacity curve for a particular spudcan with for a soil with a friction angle of 30° and a unit weight of 9 kN/m^3.

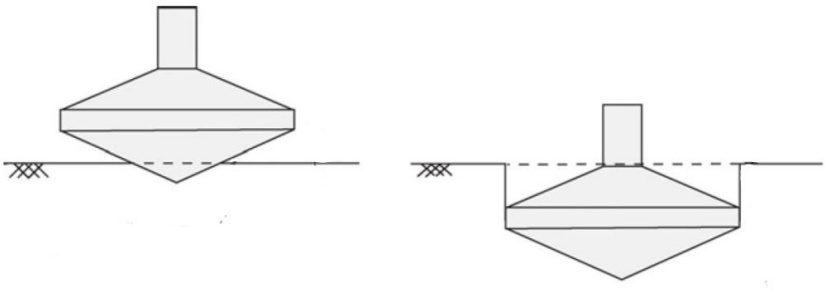

Figure 3.5: Progressive penetration of the spudcan into the soil. The striped line in the left figure represents the effective diameter of a partially penetrating spudcan, accounting for the current effective bearing area. The right Figure illustrates the stage when the spudcan's bearing area reaches its maximum, corresponding to its full bearing area, and no backfill occurs.

capacity formula from equation 3.1 and is schematically visualized by the blue line in Figure 3.6. Figure 3.6 demonstrates the path between the vertical soil resistance modes during a spudcan's vertical motion in the seabed for a single vertical penetration cycle.
A single penetration cycle refers to the complete process of a spudcan's interaction with the seabed during vertical motion, including both penetration and unloading modes. A new cycle starts when the spudcan makes contact with virgin soil, continues as it penetrates into the soil, and concludes when it is extracted or unloaded from the soil. In addressing plastic deformation, the framework considers the historical record of the deepest penetration achieved by the spudcan. The vertical soil resistance begins with the virgin soil penetration mode,

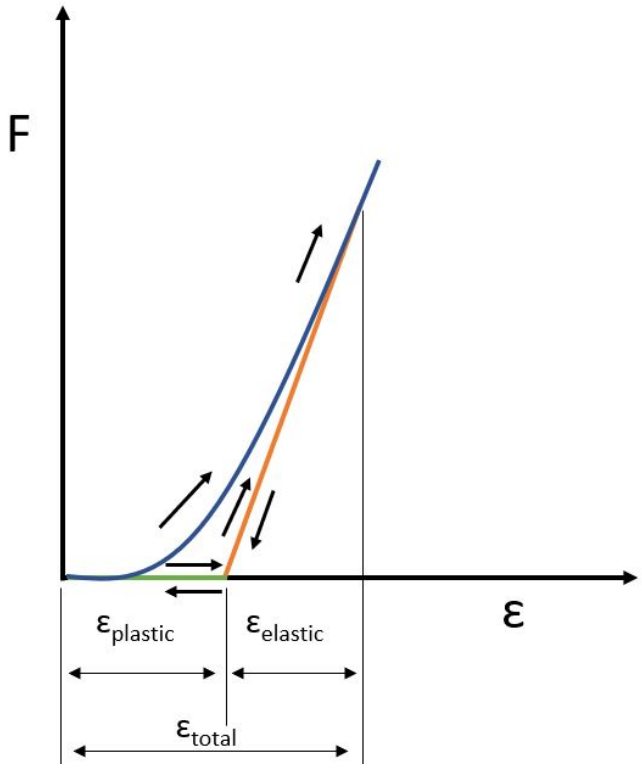

Figure 3.6: Soil model penetration resistance path. The blue line represents the bearing capacity curve, indicating the soil's bearing capacity. Unloading mode and reloading mode follow the same path for a single vertical cycle event, as shown by the orange line. The green line signifies the absence of soil contact, where soil resistance is zero.

where the soil exhibits increasing resistance as the spudcan penetrates further, following the ultimate penetration resistance (blue line). As the spudcan starts to unload, it enters the unloading mode, and the resistance decreases, following the orange line. This orange line represents the perfect elastic resistance during the unloading and subsequent reloading up to the force level previously encountered in the soil prior to unloading. The unloading/reloading modulus $K_u n$, as described in equation 3.3, governs the soil's resistance during these phases. The unloading coefficient, denoted as β, is typically assumed to lie within the range of 5 to 10. However, to determine the exact value, laboratory tests should be conducted. If the spudcan continues to unload and loses contact with the seabed, the soil resistance drops to zero, following the green line. However, when the uplift stops and reloading begins while still in contact with the soil, the resistance is governed by the orange line. As reloading progresses beyond the deepest previous penetration and the spudcan reaches virgin soil, the soil resistance proceeds to the ultimate resistance path, represented by the blue line. The vertical soil resistance should incorporate memory for the deepest penetration achieved by the spudcan.

$$E_{ur} = \beta * \tan\alpha = \beta * \Delta F / \varepsilon_{elastic} \tag{3.3}$$

The plastic deformation, represented by $\epsilon_{plastic}$ in Figure 3.6, corresponds to the spudcan's physical footprint in the soil. The spudcan's physical footprint in the soil refers to the plastic deformation created in the soil as the spudcan penetrates. The soil's elasto-plastic behavior causes the soil to deform permanently around the spudcan's base, leaving an impression or "footprint" in the soil. The ratio of plastic deformation in relation to elastic deformation will be established during the unloading phase since no conclusions can be drawn about

plastic deformation during the loading mode.
In Figure 3.7, the concept described above is expanded to multiple cycles instead of the single cycle considered in Figure 3.6. This cyclic pattern or graph is derived from the vertical soil resistance model developed in this study.

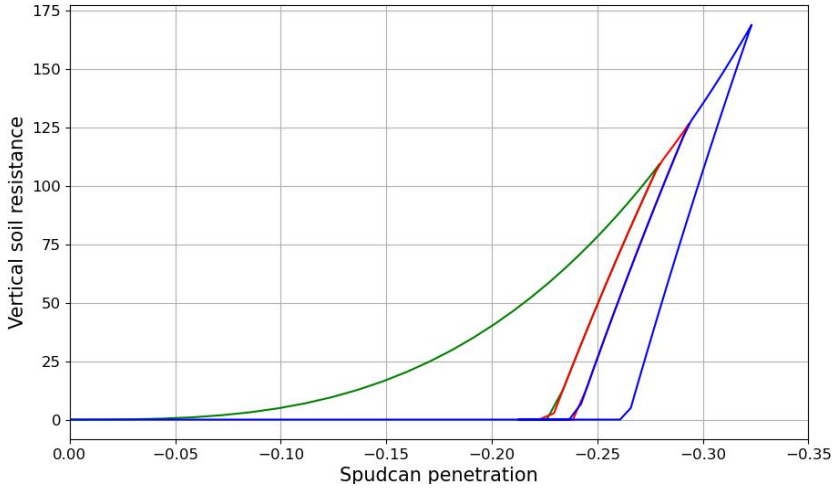

Figure 3.7: Soil model penetration resistance path, illustrating three consecutive new penetration cycles, green, red, blue.

3.4.2 Horizontal soil resistance

As the spudcan undergoes horizontal displacement while in contact with the soil, it encounters horizontal soil resistance. This resistance comprises two components: the side resistance, i.e. the net effect of passive and active soil forces, and the frictional force between the soil and the spudcan's bearing area.

Side resistance

As the spudcan undergoes lateral movement, it generates stresses within the lateral surrounding soil, which in turn produce passive and active earth pressures on the sides of the spudcan. As the spudcan moves away from a soil mass in a lateral direction, a passive earth pressure is exerted on the spudcan, opposing its motion. Conversely, when the spudcan moves laterally towards a soil mass, an active earth pressure is applied to the spudcan, trying to fill the gap created by the spudcan's movement in that direction. The magnitudes of passive and active earth pressures depend on factors such as soil unit weight, spudcan depth, and coefficients. The passive and active coefficients are determined by the soil's friction angle. For sand with a friction angle of 30 degrees, the coefficients for passive and active earth pressures are 3 and 1/3, respectively. The coefficient of passive pressure, K_p, and the coefficient of active pressure, K_a, are calculated in the equations below, where ϕ represents the soil friction angle in radians.

$$\mathrm{K_p} = \tan^2\left(\frac{\pi}{4} + \frac{\phi}{2}\right) \tag{3.4}$$

$$K_a = \frac{1}{K_p} \tag{3.5}$$

As the spudcan moves laterally through the soil, the lateral soil stress experienced is directly related to the spudcan's projected or side area. This projected area is determined by the effective diameter and penetration depth of the spudcan. The larger the effective diameter and deeper the penetration, the greater the projected area and consequently, the greater the lateral soil stress experienced. See Figure 3.5 for the effective diameter.

$$A_{proj} = \int_0^z A(z)dz \tag{3.6}$$

where formula $A(z)$ depends on the spudcan geometry and z is the depth to which the spudcan vertically penetrates the soil. A_{proj} Represents the projected area of the spudcan for a certain depth.

Incorporating the effective soil weight and the factors discussed above, the difference in active and passive soil resistance, F_{side}, can be calculated using the integral 3.7, where γ' is the effective unit weight of soil.

$$F_{side} = \int_0^z \frac{1}{2}\gamma' \left(K_p - K_a\right) A_{proj}(z) dz \tag{3.7}$$

Bottom friction

A lateral displacement of the spudcan, while in contact with the soil, is often referred to as a sliding motion. Sliding friction resistance is the resistance to sliding between two surfaces in contact with each other. The frictional resistance between the spudcan's bearing area and the soil plays an important factor in analyzing lateral soil resistance. The friction resistance arises due to the interaction between soil particles and the spudcan's bearing area, creating a force that opposes the spudcan's lateral movement. The magnitude of this frictional resistance is directly proportional to the normal force acting between the spudcan and the soil. The vertical resistance force between the spudcan and the soil, as discussed in Section 3.4.1, determines the normal force on the spudcan. The friction surface is limited to the bearing area of the spudcan, as the passive and active soil pressures account for the lateral sides of the spudcan.
The sliding friction resistance depends on the steel/soil friction angle (δ). For a flat plate, the friction angle is typically expressed as $\delta = \phi - 5°$, while for a rough-surfaced, conically shaped spudcan, the friction angle is $\delta = \phi$, where ϕ is the soil's internal friction angle (SNAME, 2008) (ISO-19905-1). Accurate determination of the friction angle between the soil and the spudcan laboratory testing should be performed. The horizontal friction resistance ($F_{friction}$) can be calculated using the following equation:

$$F_{friction} = F_V \tan\delta \tag{3.8}$$

where $F_{friction}$ is the horizontal frictional resistance, F_V is the vertical force between the spudcan and the soil, and δ is the steel/soil friction angle.

Horizontal soil resistance model

During the GoL process of a jack-up vessel, the ultimate horizontal soil resistance encountered by a spudcan during lateral displacement while penetrating sand is modelled by taking into account the combination of two components: the net effect of passive and active soil resistances, Section 3.4.2, and the frictional resistance between the soil and the spudcan's bearing area, Section 3.4.2. The total horizontal resistance force can be calculated using equation 3.9.
It is essential to recognize that both components of the horizontal soil resistance depend on the vertical penetration depth of the spudcan, as vertical penetration is required for the development of horizontal resistance forces. The friction force is proportionally related to the vertical force acting between the spudcan and the soil, which links the horizontal soil resistance to its vertical counterpart. The net effect of passive and active soil resistances depends on the vertical penetration of the spudcan.

$$F_H = F_{friction} + F_{side} \tag{3.9}$$

To model the horizontal sliding resistance of the spudcan during the GoL phase, again elasto-plastic soil behavior is applied. This approach assumes that the spudcan initially elastically deform the soil, and as the applied displacement increases, the horizontal resistance reaches a yield value, causing the spudcan to slide and plastically deform the soil.
In the elastic region, the soil resistance follows Hooke's law (Section 3.2.2), in which the resistance has a nonlinear relationship with the lateral displacement. In the plastic region, where sliding occurs, the soil resistance is governed by equation 3.9. The transition from elastic deformation to plastic deformation in the soil is marked by yield lines, which separates the two regions. The yield lines establish the limits of the elastic region, corresponding to the maximum positive and minimum negative soil resistance before plastic deformation of the soil occurs. These two yield lines are initially established upon contact with the soil and are subsequently updated each time they are surpassed. Refer to the top graph in Figure 3.8, which illustrates the elastic region, the plastic region, and the yield surfaces.
The midpoint between the two yield lines represents the reference position of the spudcan, i.e. the spudcan's origin. The distance between the spudcan's origin and either of the yield lines constitutes a constant value, characterizing the extent of the elastic region. In practical applications, the elastic response of the soil is often considered small, as the soil exhibits predominantly plastic behavior under load conditions (Chakrabarti, 2012).

This implies that the soil's deformation tends to be more permanent and irreversible, rather than recovering its original shape after the removal of the load. As a result, the distance between the spudcan's origin and either of the yield lines is assumed to be equal and relatively small. This assumption reflects the practical conditions where the elastic behavior of the soil is minor, and the focus is primarily on the plastic behavior in soil-structure interactions.
As the spudcan undergoes displacement over time along the x- or y-axis, the elastic region moves in tandem, as it is considered to be constant in size. This implies that the distance between the spudcan's origin and the yield lines, which define the elastic region, remains unchanged. However, the position of the elastic region translates along the axis in response to the spudcan's movement, maintaining its constant size while adjusting to the changing global location of the spudcan in the soil. Refer to the bottom graph in Figure 3.8, which demonstrates the translation of the elastic region, as indicated by the red arrows. Additionally, the red lines represent the new yield surfaces that encompass the elastic region. If the yield surface translates without changing in size as plastic strain occurs, this exhibits characteristics of kinematic hardening (Houlsby & Puzrin, 2006). The maximum yield is the same for both negative and positive elastic regions. Every time the positive

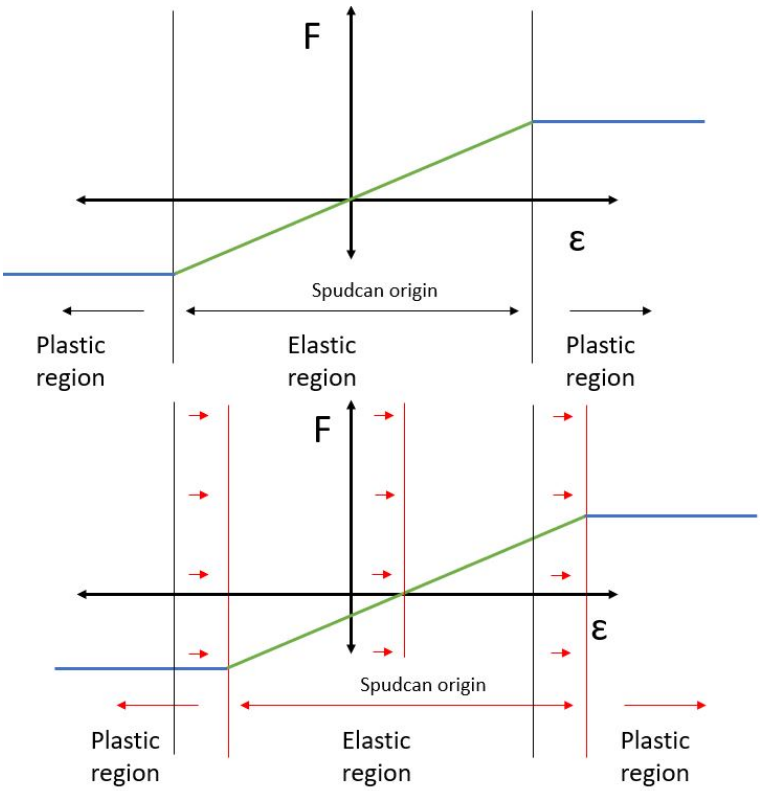

Figure 3.8: The upper graph illustrates the elastic region, plastic region, and yield surfaces, while the lower graph demonstrates the translation of the elastic region (indicated by red arrows) and the new yield surfaces (represented by red lines) that encompass the elastic region.

or negative displacement crosses the yield lines, the elastic region translates along, maintaining its constant size while adjusting to the changing global location of the spudcan in the soil. It is essential to note that the above description applies to a single displacement cycle. For another subsequent cycle with a changing spudcan origin, the elastic region continues to adapt and translate in response to the spudcan's displacement, ensuring accurate modeling of soil resistance during multiple cycles of lateral movement.

3.4.3 Soil-spudcan interaction model characteristics

The following section outlines the unique characteristics of the soil-spudcan interaction model, highlighting its particular design principles and theoretical theories. The model, designed to capture soil resistance in response to spudcan displacement, features several critical components and attributes which are listed below.

- The setup for the soil-spudcan interaction model is specifically designed to yield soil resistance in response to spudcan displacement. In this design, the spudcan is treated as a separate body, rather than a part of a rigid jack-up system. Neither leg stiffness nor jacking system stiffness is integrated into this soil-spudcan model. This design choice implies that a wide range of soil models could be incorporated without the need for adjustments to the jack-up system, i.e. leg stiffness or jacking system stiffness.
- Soil resistance models for vertical and horizontal displacement are established independently, each incorporating distinct underlying theories. This separation is due to the unique characteristics of soil behavior observed in each respective direction.
- Both the vertical and horizontal soil resistance models adhere to the elasto-plasticity theory. This is because, during impact forces, plastic deformation in the soil is predominantly observed. To accurately incorporate plastic soil behavior, the soil model may incorporate a memory mechanism.
- The yield surface for horizontal elasto-plastic soil description moves without altering its size as plastic strain occurs, demonstrating the properties of kinematic hardening (Houlsby & Puzrin, 2006).

The soil-spudcan interaction component, as elaborated upon in this Chapter, should be incorporated into the framework, a structure that also includes both the hydrodynamic and structural elements. The interaction between these components is crucial, as they form an integrated system. Chapter 4 will provide a detailed description of this framework, offering an in-depth explanation of the structural and hydrodynamic elements in relation to the soil-spudcan interaction.

Chapter 4

Developed framework

The content of this Chapter is focused on the mathematical description of the model described in Chapter 3. This Chapter begins by introducing the mathematical method applied and continues to explain the implementation of the individual components that make up the model. The explanation of the components is facilitated through their realization in Python, which is the primary simulation environment. The model is implemented using the Python programming language. Python was chosen for its ease of use, extensive libraries, and open-source nature.

4.1 Base model and description

A multibody system approach is employed to model the dynamics of a jack-up vessel, treating it as a collection of rigid bodies connected by beams. This approach underscores the importance of treating the jack-up vessel as a multibody system, distinct from rigid body systems. It facilitates the decoupling of various areas of expertise, such as geotechnics and structural dynamics, enabling them to be addressed separately. This system of decoupling permits specialists to concentrate solely on their particular area of expertise, thereby optimizing the analysis process. The base model of the jack-up vessel comprises a single hull and two spudcans, which are modelled as separate rigid bodies in a 2D plane, see Figure 4.1. By simplifying the vessel model to the 2D plane, its degrees of freedom (DOFs) are reduced from 6 to 3: surge, heave, and pitch. Each of the two spudcans has three DOFs: two for translation along the x and z axes, and one for rotation in the x-z plane. A DOF in a system represents an independent motion a single object within the system may exhibit. In total, the model encompasses 9 DOFs: three for the hull and three for each spudcan. The legs of the jack-up vessel are modelled as massless beams connecting the spudcans to the hull, eliminating the need for additional DOFs related to the legs. This simplifies the model. Overall, the 2D model offers a straightforward yet accurate representation of the jack-up vessel's dynamics, enabling the simulation of its behavior during GoL.

The fundamental equations that govern physics-based models are known as governing equations. For this specific model, the governing equation is Newton's second law of motion. Newton's second law is a fundamental principle in physics and states that the acceleration of an object is determined by the force acting on it and the mass of the object. In other words, a change in force will result in a change in the object's motion. The relationship between force, mass, and acceleration is commonly expressed as the equation $F = ma$, where F denotes the force exerted on an object, m represents the object's mass, and a signifies the object's acceleration. This equation states that an object's acceleration is directly proportional to the applied force and inversely proportional to its mass. In essence, applying a larger force to an object results in a higher acceleration. It is crucial to recognize that the applied force may consist of a combination of forces originating from various directions. To determine the acceleration of an object, it is necessary, to sum up, all the forces acting on it and subsequently divide the result by the object's mass.

Newton's second law forms the basis for understanding how an object's motion changes due to a changing net force acting on the object. From this fundamental law, the equations of motion can be derived, providing a mathematical framework for predicting an object's position, velocity, and acceleration over time under the influence of various forces. These equations enable us to analyze an object's motion systematically by considering its initial conditions and the forces acting upon it. In the context of this research, equations of motion are used to understand the motion of the three objects in the system. The equation of motions of a single object is often written:

$$m\ddot{u} + c\dot{u} + ku = \sum F(t) \tag{4.1}$$

where:

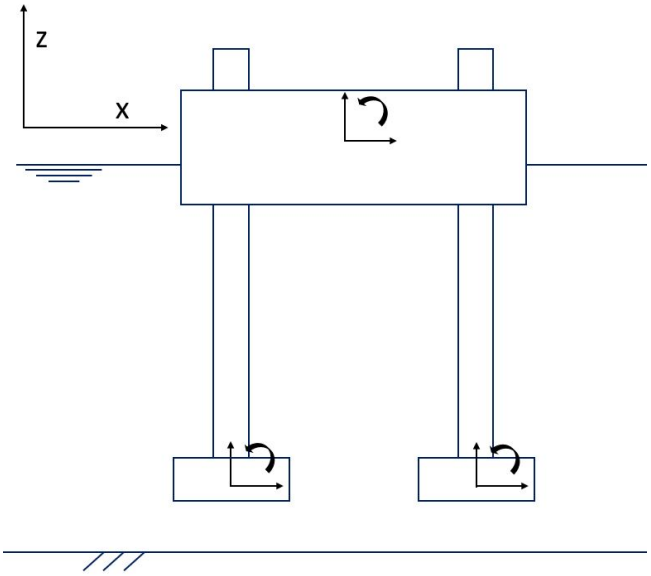

Figure 4.1: A 2D side view representation of the jack-up vessel with 9 DOF (3 for the hull and 3 for each spudcan) in the x-z plane.

m = the mass of the object [kg]
$\ddot{u}$ = the object's acceleration [m/s^2]
c = the damping coefficient [N/(m/s)]
$\dot{u}$ = the object's velocity [m/s]
k = the stiffness [N/m]
u = the object's displacement [m]
$\sum F(t)$ = net force acting on the object as a function of time [N].

Integrating the acceleration over time results in the velocity of an object. The velocity, $\dot{u}$, represents the time rate of change of the position. Consequently, integrating the velocity provides the displacement, u. The resulting equation is a second-order differential equation, which describes the dynamic behavior of the object over time. It is common to rewrite the equation in terms of acceleration, as shown in equation 4.2.

$$\ddot{u} = \frac{(\sum F(t) - c\dot{u} - ku)}{m} \tag{4.2}$$

To determine the motions of the jack-up vessel and the spudcans within the 2D model, accounting for the 9 DOF, it is essential to establish the equations of motion for each DOF in the system. Therefore, 9 equations of motion should be established. A systematic and organized representation of multiple equations of motion can be achieved through a matrix notation, which involves the mass, damping, and stiffness matrices.

$$\mathbf{M\ddot{u}} + \mathbf{C\dot{u}} + \mathbf{Ku} = \mathbf{F}(t) \tag{4.3}$$

where $\mathbf{M}$ represents the mass matrix, $\mathbf{C}$ and $\mathbf{K}$ are matrices representing the damping and stiffness coefficients, respectively. $\mathbf{u}$ And $\mathbf{F}(t)$ are vectors representing the displacement and external forces, respectively. The second derivative of $\mathbf{u}$ with respect to time, $\ddot{\mathbf{u}}$, represents the acceleration. This method enables the efficient analysis of complex systems and can be employed to predict the behavior of the model under various conditions. Given that the system has 9 DOF, and that the motion of the objects within the system interacts with each other, the equations of motion in each DOF are not independent. The interactions between the different objects within the system of equations are interconnected through the stiffness matrix, damping matrix, and mass matrix. These matrices play a vital role in defining the model's dynamic behavior.

Stiffness matrix: This matrix represents the system's resistance to deformation and is dependent on the structural and material properties of the system components. The elements of the stiffness matrix capture the stiffness coefficients of the various DOF, representing the relationship between displacements and the restoring forces.

Damping matrix: This matrix represents the energy dissipation within the system due to factors such as friction, fluid drag, and material damping. The elements of the damping matrix capture the damping coefficients of the various DOF, representing the relationship between velocities and the damping forces.

Mass matrix: This matrix represents the distribution of mass within the system, accounting for both the translational and rotational inertia. The elements of the mass matrix capture the mass and inertia coefficients of the various DOF, representing the relationship between accelerations and inertial forces.

The matrices are always [nxn] for n-DOFs, signifying that the matrices are square, with the dimensions corresponding to the number of degrees of freedom within the system. The dependency between the various objects' DOFs within the system is represented by the non-diagonal terms in the matrices. Solving the entire system of equations of motion, which are in the form of ordinary differential equations (ODEs), can be a complex and time-consuming process.
An ODE involves functions of only one independent variable and one or more of its derivatives with respect to that variable. The equation of motion 4.1 is an ODE because it involves a single independent variable, t, and only one dependent variable, u, along with its derivatives concerning t. Furthermore, it is a second-order ODE, as the acceleration, $\ddot{u}$, represents the second derivative of displacement.

Various methods exist for solving ODEs, including analytical and numerical techniques. In this model, a numerical method is employed to approximate the dynamic solutions of the system, specifically as an initial value problem for the velocity and displacement of the separate bodies in the system. Numerical approximations offer a practical way to solve an ODE over time. Several numerical methods for solving ODEs, such as the Euler method and Runge-Kutta methods, provide accurate approximate solutions, each with its benefits and drawbacks. The Euler method is relatively simple to implement but may be less accurate over extended periods. In contrast, Runge-Kutta methods offer improved accuracy but are generally more computationally expensive. Numerical approximations of ODEs can be computationally demanding, particularly for complex ODEs or when high accuracy is required. Python is commonly utilized for solving ODEs numerically, for its inbuilt ODE solvers to handle complex calculations efficiently.

4.2 Stiffness matrix

The stiffness matrix serves as a mathematical representation of the stiffness properties inherent to the system. As a square matrix of dimensions [NxN] (N-DOFs), it establishes the linear relationship between forces and moments concerning the displacements or rotations of the degrees of freedom within a linear system. The diagonal entries of the stiffness matrix correspond to the stiffness values of each degree of freedom, which represent the system's resistance to deformation in their respective directions. The off-diagonal elements of the matrix represent the coupling between DOFs, the effect of displacement in one direction on the forces in another direction. A non-zero non-diagonal entry indicates that there is a coupling between the corresponding DOFs, while a zero non-diagonal entry indicates that there is no coupling between them. The stiffness matrix is symmetric along its diagonal, and by definition the entries on the diagonal are positive. If a diagonal entry of the stiffness matrix were to be negative would result in an unstable or unconstrained system
The process of deriving the stiffness matrix can be intricate; nevertheless, standard deflection formulas, also known as "De vergeet me nietjes," are commonly employed. These formulas offer a straightforward, closed-form solution to determine the stiffness of a beam subjected to specific loading conditions. Within a system, beams are frequently described using the Euler-Bernoulli beam theory.

4.2.1 Euler-Bernoulli beam theory

The system described in Section 4.1 is a simplified two-dimensional representation of the jack-up vessel, consisting of the hull and two spudcans. The hull is modelled as a basic geometric shape, a rectangle, while the spudcans, featuring a cylindrical geometry, are positioned at the corners of the hull. To facilitate load transfer, cylindrical beams, known as the jack-up legs, connect the hull and spudcans. These legs, typically constructed from materials such as steel, are designed to withstand bending, buckling, and other forms of deformation. They play a crucial role in transmitting forces and moments from the spudcan to the hull and vice versa. The legs are modelled using the Euler-Bernoulli beam theory, with rigid connections to both the hull and the spudcans, ensuring an accurate representation of the structural behavior.

The Euler-Bernoulli beam theory is a model that examines the behavior of slender beams under bending and

deflection. It assumes that the beam is made of isotropic materials, exhibits linear-elastic behavior, and experiences only small deformations such that its cross-section remains plane and perpendicular to its longitudinal axis.
Internal moments and shear forces in a beam represented by the Euler-Bernoulli theory are the results of bending and deflection in the beam. Internal moments and forces exist within the beam as a result of external bending and deflection applied to the beam. They represent the resistance to bending, shearing, and axial loading of the beam.
The internal bending moment is the force acting along the beam's cross-section that produces bending and is calculated by multiplying the applied load by the distance from the load to the neutral axis of the beam's cross-section. The internal shear force is the force acting along the beam's cross-section that produces shear. The axial load is the force acting along the longitudinal axis of the beam and is caused by compression or tension forces applied to the beam. Together, the internal moments, shear forces, and axial forces provide a complete description of the internal state of the beam, allowing for the prediction of its behavior under different external load conditions. The relative direction of these forces and the rotation direction of the moments are important. Therefore sign conventions play a crucial role in the analysis of two- and three-dimensional beams. They establish a standardized system for specifying the direction of the forces, moments, and translational or rotational displacements. Adhering to a consistent sign convention throughout the analysis process is crucial to obtaining accurate and reliable results.

4.2.2 Leg properties

The properties of the legs are important to understand to design and analyze the structural behavior under different loads. The basic leg properties include cross-sectional shape, length, Young's modulus, the surface moment of inertia, and boundary conditions. These properties are used to calculate the internal moments and forces, that occur when the leg is subjected to various deflections and bending. The design of a leg must consider the loads it will experience, the strength of the material, and the deformation that is acceptable in the structure. This thin-walled cylindrical leg can be analyzed using the Euler-Bernoulli beam theory described previously. A schematic representation of a leg segment is shown in Figure 4.2. The leg properties depend on design choices.

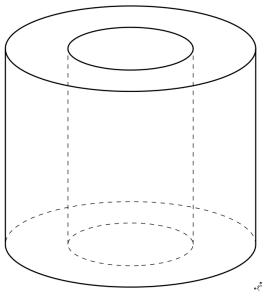

Figure 4.2: Segment of cylindrical beam connection spudcan and jack-up hull.

Young's modulus is a measure of the stiffness or elasticity of a material. It is defined as the ratio of longitudinal stress to longitudinal strain within the elastic limit, typically Young's modulus of steel is approximately 210 GPa. The cross-sectional area of a thin-walled cylinder can be represented using, $A = \pi \left(R_2^2 - R_1^2\right)$ where: R_2 is the outer radius of the cylinder, and R_2 is the inner radius of the cylinder. The length of the leg is l, and can be varied.
The axial stiffness of a leg is a measure of the resistance of the beam to axial deformation when a force is applied along its length, this can either be a compression or a tension force. The axial leg stiffness is assumed to have a linear behavior and can be calculated with:

$$K_{axial} = \frac{E * A}{\ell} \tag{4.4}$$

Where E is Young's modulus of steel, and A and l are the cross-section area and length of the leg, respectively. The boundary conditions of the leg connections at the hull and spudcans are further elaborated in the next Section.

4.2.3 Boundary conditions

In Euler-Bernoulli beam theory, boundary conditions are essential to defining the problem and accurately predicting the behavior of the beam. The boundary conditions specify the values of the deflection, slope, shear force, and moment at the endpoints of the beam. The boundary conditions restrict the number of unknowns in the mathematical model, making it possible to solve for the desired outcome. The three basic boundary conditions for Euler-Bernoulli beam theory are:

1. Free: The beam is free to rotate and translate. The shear force at end of the beam is zero and the bending moment changes continuously along the length of the beam.
2. Hinge supported: The support can sustain shear forces but no bending moments. This means that the support will allow rotation at the support point, but will not allow the bending of the beam at that point.
3. Fixed: The beam is fixed and can sustain both shear forces and bending moments. There will be no rotations and translations.

In the context of the 2D jack-up representation, applying a small displacement to one of the three masses - the hull or one of the two spudcans - leads to a change in the internal forces and moments within the beam connecting the masses. The reaction forces at the supports can be calculated by considering the balance of forces and moments at each boundary condition, utilizing standard deflection formulas.
Two standard deflection formulas are employed to derive the internal beam forces and moments of the legs. The first standard deflection formula, Figure 4.3, relates the rotation, θ, and applied torque, T, at boundary 2 to the shear forces and bending moments in the beam. At boundary 2, there is no translation, resulting in the presence of a shear force. Conversely, at boundary 1, the beam is fixed and incapable of undergoing any rotations or translations. Consequently, the beam can support shear forces and bending moments at this boundary. The formulas associated with internal shear forces, bending moments, and rotations are derived from the Euler-Bernoulli beam theory and are presented in the equations 4.5.

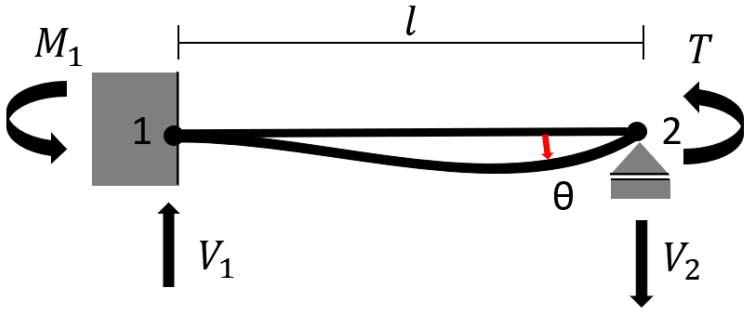

Figure 4.3: Schematic representing of standard deflection formula 1. Applied rotation, θ, and torque T, at boundary 2.

$$\theta = \frac{1}{4}\frac{T\ell}{EI}; \quad M_1 = \frac{1}{2}T; \quad V_1 = V_2 = \frac{3}{2}\frac{T}{\ell} \tag{4.5}$$

The second standard deflection formula, 4.4, involves the application of a translation, w, at boundary 2. Both endpoints of the beam are fixed and unable to undergo rotations or translations due to their rigid constraints. As a result of the translation, w, both boundaries experience shear forces and bending moments. The formulas related to shear forces, bending moments, and translation are derived from the Euler-Bernoulli beam theory and are described in the equations 4.6.

$$M_1 = M_2 = \frac{6EI}{\ell^2}w; \quad V_1 = V_2 = \frac{12EI}{\ell^3}w \tag{4.6}$$

The application of the standard deflection formulas involves making two main simplifying assumptions. First, the relationship between the applied loads and the resulting displacements is linearly proportional. Secondly, the standard deflection formulas are only valid for small displacements and rotations. The deployment of small displacements results in the linear approximation of the Taylor series expansion of both the sinus and cosine, in which $sin(\theta) \approx \theta$ and $cos(\theta) \approx 1 - \frac{x^2}{2} \approx 1$.

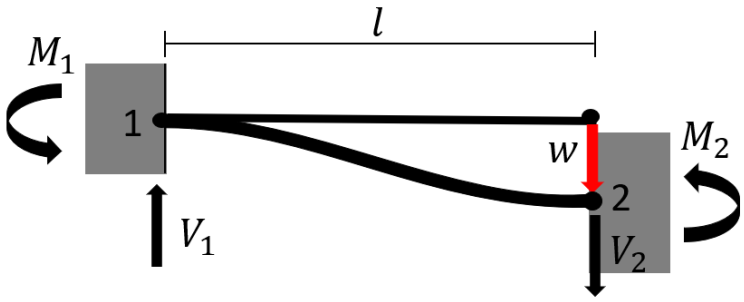

Figure 4.4: Schematic representing of standard deflection formula 2. Applied translation, w, at boundary 2.

4.2.4 Setting up stiffness matrix

The stiffness values for the respective degrees of freedom, as well as the coupling terms between them, can be determined by utilizing the theories discussed in the previous Sections. Several assumptions regarding the 2D structural system of the jack-up should be made before deploying the theories. Firstly, the legs of the jack-up are treated as massless beams, with their primary purpose being to transfer moments and shear forces between the hull and the spudcans. The properties of the leg are described are isotropic. Secondly, there is no coupling between the two spudcans.

The stiffness matrix can be established by collecting all the forces and moments from the results of the displaced situations, described and collected in Appendix A. Each column in the stiffness matrix corresponds to the forces and moments that result from a unit displacement in a particular DOF. These forces and moments are the reaction forces and moments that the structure generates in response to the displacement in that DOF. Therefore, each column of the matrix represents the contribution of a particular DOF to the overall stiffness of the structure. On the other hand, each row in the stiffness matrix corresponds to the forces and moments acting in a particular DOF due to a unit displacement in another DOF. These forces and moments are the results of the coupling between different degrees of freedom, and they represent how a displacement in one direction affects the forces and moments in another direction. Therefore, each row of the matrix represents the relationship between the forces and moments acting in a particular DOF and the displacements in other degrees of freedom.
The first three rows represent the forces and moments on the hull, x_1, z_1, θ_1, rows three to six represent the forces and moments on the right spducan, x_2, z_2, θ_2, and rows six to nine represent the forces and moments on the left spudcan, x_3, z_3, θ_3. See Figure 4.5 for the local reference systems, for the hull and spudcans. The magnitudes of the shear forces and bending moments resulting from the translation or rotation of one of the spudcans are equivalent for both spudcans, because the system is symmetric through the vertical plane intersecting the center of gravity (COG) of the hull.

Table 4.1: The 9 degrees of freedom and their respective signs and units for the jack-up vessel model.

Degree of Freedom	**Description**	**Unit**
x_1	Horizontal displacement of hull	m
y_1	Vertical displacement of hull	m
θ_1	Rotation of hull	rad
x_2	Horizontal displacement of right spudcan	m
y_2	Vertical displacement of right spudcan	m
θ_2	Rotation of right spudcan	rad
x_3	Horizontal displacement of left spudcan	m
y_3	Vertical displacement of left spudcan	m
θ_3	Rotation of left spudcan	rad

Incorporating only the internal stiffness of structures within a model yields an unrealistic representation, as it neglects any form of connection or interaction with the external environment. In the 2D jack-up representation, the jack-up vessel is floating in water; thus, it is essential to account for forces arising from its contact with the

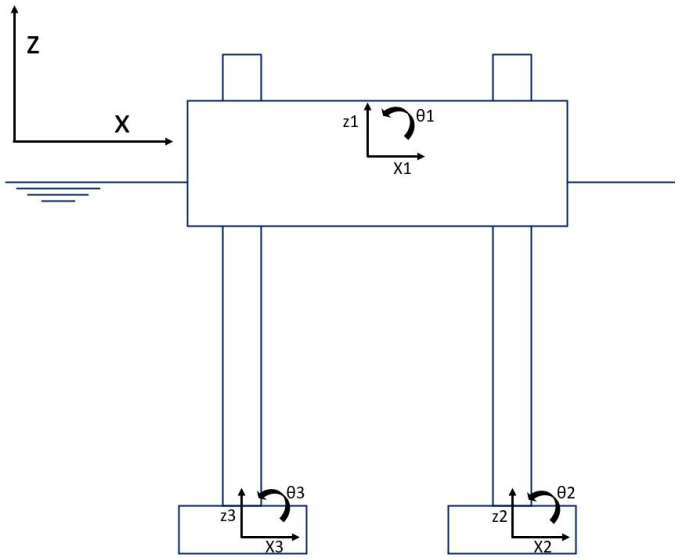

Figure 4.5: A 2D side view representation of the jack-up vessel illustrating the 9 degrees of freedom in the x-z plane, along with the local reference systems for each of the three components (hull and two spudcans).

water. This can be achieved by incorporating hydrostatic restoring stiffness into the matrix. The hydrostatic restoring stiffness of a vessel represents the restoring forces acting on the hull due to its displacement in water. This parameter is determined by the vessel's geometry and weight distribution and is closely related to the hydrostatic properties of the hull. Incorporating the restoring stiffness in all three DOFs - heave, surge, and pitch -ensures a more accurate and realistic representation of the jack-up vessel's behavior in its operational environment.

For the heave motion of the hull, the hydrostatic restoring stiffness represents the resistance to the buoyancy force. Equation 4.7 estimates the hydrostatic heave restoring stiffness acting on the hull due to its vertical displacement in water. This equation assumes that the hull can be approximated as a rectangular barge with a specified length and width. The heave restoring force operates in the vertical direction of the hull and is therefore incorporated into the stiffness matrix at the entry [2,2], which corresponds to the intersection of the z_1 column and row.

$$k_{heave} = \rho \cdot g \cdot length \cdot width \tag{4.7}$$

The hydrostatic restoring stiffness in the surge direction is negligible for free-floating vessels, as there is no lateral projection of the buoyancy force acting on the hull in the surge direction. Consequently, the vessel can move freely in the surge direction without resistance from the water. However, having zero stiffness in a specific direction may result in numerical instability. Thus, for implementation purposes, a small non-zero hydrostatic surge stiffness value will be utilized. The surge restoring force acts in the horizontal direction of the hull and is incorporated into the stiffness matrix at entry [1,1], corresponding to the intersection of the x_1 column and row.

The hydrostatic restoring stiffness acting on a free-floating vessel in the pitch direction results from the buoyancy force acting on the hull. When a vessel heels, the weight of the displaced water generates a moment counteracting the heeling motion, tending to restore the vessel to its upright position. For a free-floating vessel, the hydrostatic restoring stiffness in pitch is determined by the buoyancy force acting on the hull and can be calculated using equation 4.8. In this equation, GM denotes the metacentric height of the vessel, representing the distance between the ship's center of gravity and its metacenter. The pitch restoring moment operates in the pitch rotation of the hull and is included in the stiffness matrix at entry [3,3], corresponding to the intersection of the θ_1 column and row.

$$k_{pitch} = \rho \cdot g \cdot GM \cdot width \cdot length \tag{4.8}$$

$$\left[\begin{array}{cccccccccc|c}
\frac{12(EI)}{l^3}+k_{surge} & 0 & \frac{6(EI)}{l^2} & -\frac{12(EI)}{l^3} & 0 & \frac{6(EI)}{l^2} & -\frac{12(EI)}{l^3} & 0 & \frac{6(EI)}{l^2} & x_1 \\
0 & \frac{AE}{l}+k_{heave} & 0 & 0 & -\frac{AE}{l} & 0 & 0 & -\frac{AE}{l} & 0 & z_1 \\
\frac{6(EI)}{l^2} & 0 & \frac{4(EI)}{l}+2a^2\frac{AE}{l}+k_{pitch} & \frac{-6(EI)}{l^2} & -a\frac{AE}{l} & \frac{2(EI)}{l} & \frac{-6(EI)}{l^2} & a\frac{AE}{l} & \frac{2(EI)}{l} & \theta_1 \\
-\frac{12(EI)}{l^3} & 0 & \frac{-6(EI)}{l^2} & \frac{12(EI)}{l^3} & 0 & \frac{-6(EI)}{l^2} & 0 & 0 & 0 & x_2 \\
0 & -\frac{AE}{l} & -a\frac{AE}{l} & 0 & \frac{AE}{l} & 0 & 0 & 0 & 0 & z_2 \\
\frac{6(EI)}{l^2} & 0 & \frac{2(EI)}{l} & \frac{-6(EI)}{l^2} & 0 & \frac{4(EI)}{l} & 0 & 0 & 0 & \theta_2 \\
-\frac{12(EI)}{l^3} & 0 & -\frac{6(EI)}{l^2} & 0 & 0 & 0 & \frac{12(EI)}{l^3} & 0 & \frac{-6(EI)}{l^2} & x_3 \\
0 & -\frac{AE}{l} & a\frac{AE}{l} & 0 & 0 & 0 & 0 & \frac{AE}{l} & 0 & z_3 \\
\frac{6(EI)}{l^2} & 0 & \frac{2(EI)}{l} & 0 & 0 & 0 & \frac{-6(EI)}{l^2} & 0 & \frac{4(EI)}{l} & \theta_3
\end{array}\right]$$

4.3 Mass matrix

The mass matrix is an essential component in the analysis of the multi-degree-of-freedom system, representing the distribution of mass and inertial properties of the individual objects within the system. Constructing the mass matrix involves determining the masses and inertia associated with each DOF, which are essential for understanding the system's dynamic behavior under various conditions.
In the mass matrix, the diagonal elements correspond to the masses and inertia of the individual DOF. The diagonal entries represent the mass for a translation motion and the moment of inertia for a rotational motion. These diagonal elements describe the direct relationship between the applied forces or moments and the resulting accelerations or angular accelerations, respectively. The mass matrix is diagonal, meaning that only the diagonal elements are non-zero, as depicted below.

For floating structures, it is also important to consider the added mass matrix. The added mass is an additional mass that arises due to the interaction between the structure and the surrounding water. The added mass coefficients, (a_{nn}), are a function of the structure's geometry and water properties. These coefficients can be added to the mass matrix to account for the hydrodynamic effects on the structure's motion. To incorporate the added mass coefficients, they can be placed on the diagonal elements of the mass matrix, corresponding to their respective DOF. This updated mass matrix then accounts for both the structure's inherent mass and the additional mass due to fluid interaction.

$$\left[\begin{array}{ccccccccc|c}
m_1+a_{11} & 0 & 0 & 0 & 0 & 0 & 0 & 0 & 0 & \ddot{x_1} \\
0 & m_1+a_{22} & 0 & 0 & 0 & 0 & 0 & 0 & 0 & \ddot{z_1} \\
0 & 0 & I_1+a_{33} & 0 & 0 & 0 & 0 & 0 & 0 & \ddot{\theta_1} \\
0 & 0 & 0 & m_2+a_{44} & 0 & 0 & 0 & 0 & 0 & \ddot{x_2} \\
0 & 0 & 0 & 0 & m_2+a_{55} & 0 & 0 & 0 & 0 & \ddot{z_2} \\
0 & 0 & 0 & 0 & 0 & I_2+a_{66} & 0 & 0 & 0 & \ddot{\theta_2} \\
0 & 0 & 0 & 0 & 0 & 0 & m_3+a_{77} & 0 & 0 & \ddot{x_3} \\
0 & 0 & 0 & 0 & 0 & 0 & 0 & m_3+a_{88} & 0 & \ddot{z_3} \\
0 & 0 & 0 & 0 & 0 & 0 & 0 & 0 & I_3+a_{99} & \ddot{\theta_3}
\end{array}\right]$$

4.4 Damping matrix

The damping matrix represents the energy dissipation within the system due to factors such as friction, fluid drag, and material damping. It describes the relationship between velocities and damping forces for each DOF in the system. The damping matrix is square and has dimensions equal to the number of DOF in the system. In the context of a floating structure like a jack-up vessel, the damping matrix not only incorporates the system damping, which originates from the structural and mechanical components but also the hydrodynamic damping. Hydrodynamic damping is the damping that results from the interaction between the vessel and the surrounding water. System damping is typically associated with the internal energy dissipation within the structural materials, connections, and mechanical components of the system. Hydrodynamic damping, on the other hand, arises due to fluid resistance forces acting on the vessel as it moves through the water. It is a complex phenomenon influenced by several factors such as the shape and geometry of the hull, the water depth, and the fluid properties.
For this custom-developed framework an initial value problem is solved, and the framework allows for the

implementation of damping components. However, the determination of complex wave damping and structural damping coefficient is not included in the model.

$$\left[\begin{array}{ccccccccc|c} b_1 & 0 & 0 & 0 & 0 & 0 & 0 & 0 & 0 & \dot{x_1} \\ 0 & b_2 & 0 & 0 & 0 & 0 & 0 & 0 & 0 & \dot{z_1} \\ 0 & 0 & b_3 & 0 & 0 & 0 & 0 & 0 & 0 & \dot{\theta_1} \\ 0 & 0 & 0 & b_4 & 0 & 0 & 0 & 0 & 0 & \dot{x_2} \\ 0 & 0 & 0 & 0 & b_5 & 0 & 0 & 0 & 0 & \dot{z_2} \\ 0 & 0 & 0 & 0 & 0 & b_6 & 0 & 0 & 0 & \dot{\theta_2} \\ 0 & 0 & 0 & 0 & 0 & 0 & b_7 & 0 & 0 & \dot{x_3} \\ 0 & 0 & 0 & 0 & 0 & 0 & 0 & b_8 & 0 & \dot{z_3} \\ 0 & 0 & 0 & 0 & 0 & 0 & 0 & 0 & b_9 & \dot{\theta_3} \end{array}\right]$$

4.5 External force vector

The external force vector, $F(t)$, in equation 4.3 represents the summation of all external forces acting on the system. These external forces arise from the environmental loads, such as wave-induced forces and soil resistance forces. These forces are time-dependent and are recalculated every time step during the numerical approximations. Importantly, the soil forces resulting from the soil-spudcan interaction model are integrated into the framework through the external force vector. The respective vertical and horizontal soil forces are calculated for the spudcan displacement at every moment in time, and they are subsequently added to the force vector. This ensures that the effects of these interactions are accurately captured and considered in the dynamic analysis of the system.
The set-up of this framework allows the user to include all external forces in the external force vector. This enables the addition of numerous functions to the framework, as long as they result in a force acting on an object within the system. Consequently, this adaptability permits the integration of various force-generating mechanisms, enhancing the framework's capacity to account for a wide range of scenarios and environmental conditions.

4.6 Dynamic analysis

The dynamic analysis of the jack-up vessel system focuses on understanding the system's behavior over time to assess its response to external loads. To conduct this analysis, it is necessary to solve the system's equations of motion (EOM), which consist of nine second-order differential equations. These equations incorporate the mass, stiffness, damping of the system, and the external loads acting upon it. A modal analysis of the system is performed to gain insights into its behavior, natural periods, and mode shapes of dynamic system, find in Appendix B. A time-domain analysis involves employing numerical integration techniques to approximate the solution to the EOM over a specified time interval. By conducting dynamic analysis, GoL can be simulated, and relevant parameters can be examined.

4.6.1 Time domain analysis

There are two techniques for solving numerical models: time domain (Td) and frequency domain (Fd). Each method offers unique advantages and disadvantages, with the choice between them depending on the problem at hand. Time domain analysis is focused on how a signal changes over time. It involves measuring the amplitude of a signal at different points in time and plotting it over a time axis. This method is useful for understanding the dynamic behavior of a system and identifying trends over time. Frequency domain analysis, on the other hand, examines a signal concerning frequency. It employs a Fourier transformation function to decompose a time-based input into its constituent frequency components. This method is beneficial for determining the amount of a signal present within each given frequency band across a range of frequencies.

In the context of this study, the interaction between spudcan and soil during the GoL is best simulated in the time domain, as it is a highly non-linear and dynamic process. Time-domain analysis can be computationally expensive, but for the duration of the GoL, which typically lasts up to several minutes, simulations in the time domain are appropriate.

4.6.2 Numerical integration

Numeric integration methods are computational techniques used to approximate the solution of mathematical problems that involve integration. These methods are employed when analytical integration is too complex. Numeric integration techniques discretize the continuous problem into smaller time steps and estimate the integral. Within Python, the "ode" package in the "scipy.integrate" library is specifically designed for solving systems of ODEs. The system of equations of motion, involves a single independent variable, time, and one or more of its derivatives with respect to time.
The "ode" package offers a method for integrating the derivatives over a specified time interval, using the initial conditions provided. This approach is an example of solving an initial-value problem. An initial-value problem involves finding a solution that satisfies both the equation of motion and the initial conditions. In equation 4.2, the initial values for velocity, $\dot{u}_0$, and displacement, u_0, must be provided, along with the mass, damping, and stiffness matrices. The ODE solver numerically integrates the ODE, determining the acceleration solution that corresponds to the given initial conditions. Figure 4.6 shows a flowchart outlining the numerical time integration process for the Python model.

The system of equations of motion is a system of second-order ODEs. To solve this system of equations, it is necessary to transform it into a system of first-order ODEs. This mathematical transformation is known as the state-space transformation. The state-space form is a mathematical representation of a dynamic system that characterizes the system's behavior in terms of its states and their derivatives. This form represents the system of equations of motion in a concise matrix form. The state-space transformation introduces two new variables, which are functions of the original function and its first derivative, X and $\dot{X}$, respectively (as in Equation 4.9).

$$X = \begin{bmatrix} u \\ \dot{u} \end{bmatrix} \leftrightarrow \dot{X} = \begin{bmatrix} \dot{u} \\ \ddot{u} \end{bmatrix} \tag{4.9}$$

In addition, for the system to be written in state-space, two matrices are made, A and B, see 4.10. The A-matrix in the state-space formulation includes the object's mass matrix, zeroes matrix, and an identity matrix to establish the constraints of the system. The B-matrix is composed of the damping matrix, the stiffness matrix, an identity matrix, and zeroes matrix.

$$A = \begin{bmatrix} M & 0 \\ 0 & I \end{bmatrix} B = \begin{bmatrix} c & K \\ -I & 0 \end{bmatrix} \tag{4.10}$$

Using state-space formulation, the second-order differential equation 4.1, can be written in first-order equations 4.11.

$$\underbrace{\overrightarrow{F(t)}}_{\text{External forces}} = \underbrace{[A]}_{\text{A-matrix}} \cdot \underbrace{\overrightarrow{X}}_{\text{Output}} + \underbrace{[B]}_{\substack{\text{B-matrix} \\ \text{2n x 2n}}} \cdot \underbrace{\overrightarrow{X}}_{\text{Input}} \tag{4.11}$$

Expressing the matrix notation as two separate equations results in equations 4.12 and 4.13.

$$\begin{bmatrix} F \\ 0 \end{bmatrix} = \begin{bmatrix} \mathbf{M} & 0 \\ 0 & I \end{bmatrix} \cdot \begin{bmatrix} \ddot{u} \\ \dot{u} \end{bmatrix} + \begin{bmatrix} \mathbf{C} & \mathbf{K} \\ \mathbf{-I} & 0 \end{bmatrix} \cdot \begin{bmatrix} \dot{u} \\ u \end{bmatrix} \tag{4.12}$$

$$\begin{aligned} F &= \mathbf{M}\ddot{u} + \mathbf{C}\dot{u} + \mathbf{K}u \\ 0 &= \mathbf{I}\dot{u} - \mathbf{I}\dot{u} \end{aligned} \tag{4.13}$$

Again it is convenient to write equation 4.11 with respect to acceleration, or $\dot{X}$, see equation 4.14. The state-space representation is a simple and alternative way of presenting the equations of motion. The first-order differential equations can then be further computed with the "ode" package in the "scipy.integrate" library, which is designed for solving systems of first-order ODEs.

$$\overrightarrow{\dot{X}} = [A]^{-1} \cdot (\overrightarrow{F} - [B] \cdot \overrightarrow{X}) \tag{4.14}$$

4.7 Framework setup and performance

In Figure 4.6, a flowchart of the framework is provided, summarizing all components described in this Chapter. The numerical integrator solves the system over time, utilizing time-invariant mass, and damping matrices.

These matrices originate from the pre-calculations outlined in Sections stiffness, 4.2, 4.3, and 4.4, and are incorporated within the first-order equations of motion (EOM) state-space formulation in the numerical integrator. Initial values must be provided for the integrator, serving as the starting point.
The blue area in the flowchart represents the numerical integration performed at each time step. Consequently, the outputs of the integrator are the displacements and velocities of the objects in the system. These displacements are then input into the soil-spudcan interaction model to calculate the corresponding soil forces acting on the spudcan objects. These soil forces are subsequently incorporated into the external force vector, ensuring that the soil forces are accurately accounted for and solved over time.

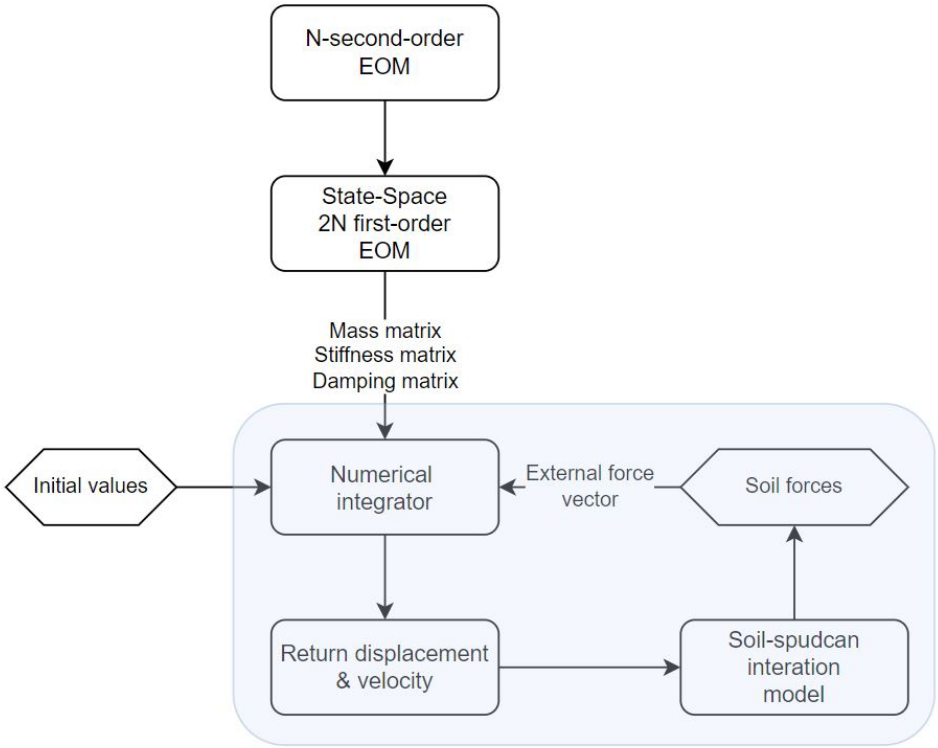

Figure 4.6: Flowchart depicting the time integration process within the Python model. The blue area highlights the numerical integration performed at each time step.

The developed framework can be numerically solved within the Python environment. However, there are limitations when solving solely in Python. For instance, the vessel is significantly simplified. No wave loads and wave damping terms can be incorporated, which means wave-induced vessel motions cannot be analyzed. The primary objective of using Python in this framework is to verify the soil-spudcan interaction model by initializing displacements of the objects in the multibody system.
Figure 4.7 illustrates the vertical soil force upon initializing the system in its third mode, which corresponds to the heave mode shown in Figure B.1. As mode 3 represents a rigid body mode, all the individual objects exhibit a similar behavior pattern, as all the displacement lines in the upper graph of Figure 4.7 overlap. The spudcans exhibit a stamping-like behavior just above the seabed, as the entire system is positioned 1 meter above the seabed as per initial conditions. No damping term is included, and rigid harmonic displacement of the multi-body system is observed, with corresponding vertical soil forces. In reality, the soil-spudcan interaction extracts energy from the system as it opposes the kinetic and potential energy components of the jack-up vessel. To account for this, a damping coefficient in the heave direction equal to 5% of its critical damping coefficient is introduced in Figure 4.8. After 20 seconds, the vertical displacement of the spudcans is insufficient to reach the seabed, as the seabed has experienced plastic soil deformation due to spudcan penetration. It should be noted that no spudcan lowering is applied in both the simulation.
To account for dynamic vessel responses in real sea-state, Orcaflex is used and introduced in Chapter 5.

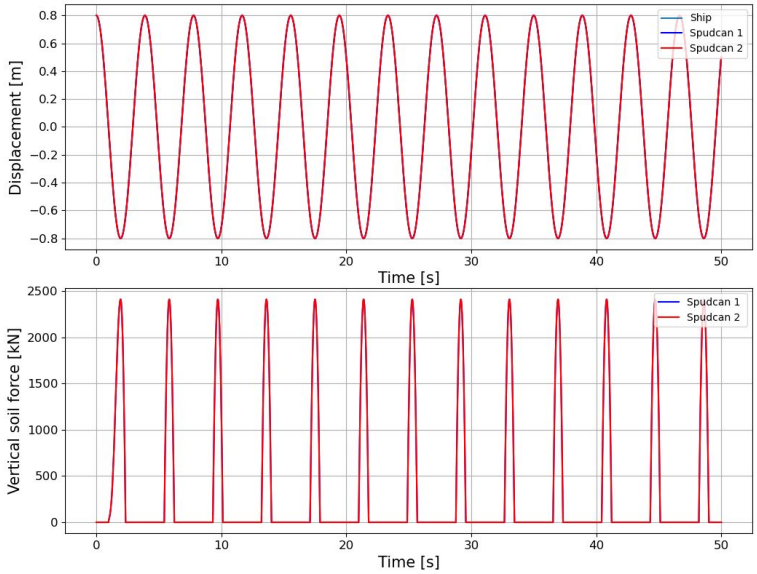

Figure 4.7: The upper graph displays the vertical displacement of the three bodies over time, while the lower graph presents the corresponding soil forces on the spudcans.

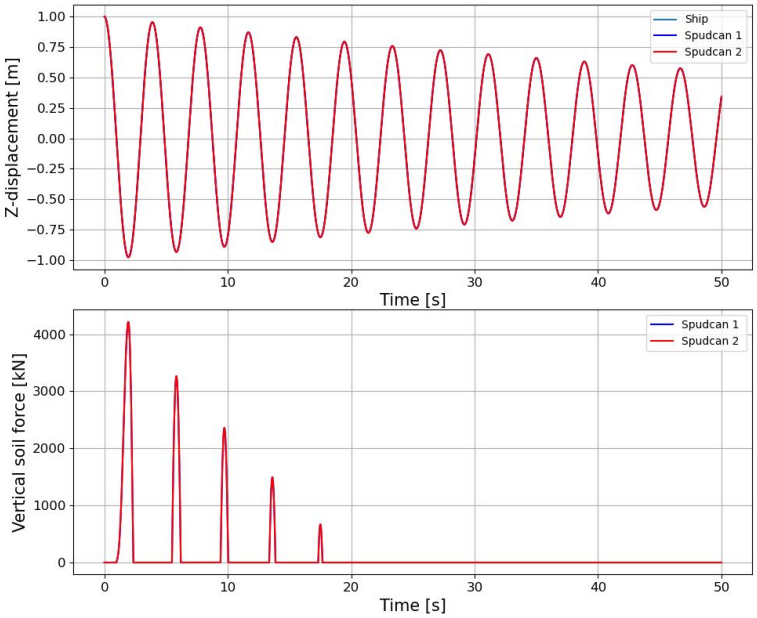

Figure 4.8: Heave mode vertical soil force with 5% critical damping. The upper graph displays the vertical displacement of the three bodies over time, while the lower graph presents the corresponding soil forces on the spudcans.

Chapter 5

Simulation model; verification and validation

The first phase of this thesis involved the complete development and implementation of the framework within the Python environment, where each component was developed from scratch. In this chapter, the soil-spudcan interaction model, initially developed in Python, is integrated into OrcaFlex. OrcaFlex, a software solution by Orcina, is extensively utilized within the offshore and maritime sectors for the dynamic analysis and design of systems (Orcina, 2021). The software is capable of simulating a variety of offshore structures, including jack-up vessels, providing precise results under different environmental circumstances. The second focus of this chapter involves the verification and validation of the implementation, designed to simulate the behavior of jack-up vessels during the GoL process.

5.1 Orcaflex

OrcaFlex is powerful software for simulating jack-up vessel dynamics and behavior, offering numerous advantages to complement the custom Python model. Its comprehensive functionality and user-friendly interface make it an ideal choice for modeling and simulating going on location and obtaining detailed insights into a jack-up vessel's behavior. By utilizing OrcaFlex for simulations, a benchmark study with the Python model can be performed, to ensure accuracy and reliability. OrcaFlex is specifically designed for efficient numerical simulations, and its computational engine has been optimized for performance. As a result, OrcaFlex can perform simulations quickly and provide good visuals of the results.
OrcaFlex uses a time-domain approach for the dynamic analysis of structures, taking into account the effects of nonlinearities and time-varying loads. The software employs a numerical integration method for solving the equations of motion, following the same methodology within the Python model (Chapter 4). Orcaflex allows defining various types of objects, such as nodes, lines, buoys, and vessels, to represent the structural components of the system. The user can specify the geometrical and material properties of these objects, as well as the boundary conditions and constraints. In addition, the software provides an extensive library of hydrodynamics, enabling users to simulate the environmental loads acting on the structure accurately.

5.2 Simulation model setup

OrcaFlex is a powerful simulation tool that can model various aspects of marine operations, including the soil-structure interaction. While it offers built-in seabed representations, these representations lack the ability to account for plastic deformation, especially important in scenarios involving multiple soil impacts and varying loading conditions. This limitation means that the simulation results may not fully capture the complex behavior of the soil-spudcan interaction, especially in scenarios involving multiple impacts and varying loading conditions.

Fortunately, OrcaFlex allows for the integration of external functions from other applications, such as Python. This feature facilitates the integration of the soil-spudcan interaction model into the OrcaFlex simulation, resulting in a more accurate representation of the soil-spudcan interaction. By incorporating the soil-spudcan interaction model in Python within the GoL simulation, the spudcan motions from the OrcaFlex GoL simulation are imposed on the soil-spudcan model in Python, see the flowchart in Figure 5.1. For every time step in the

numerical integrator, the soil forces from the Python are retrieved and incorporated as an external force on the spudcan within Orcaflex.

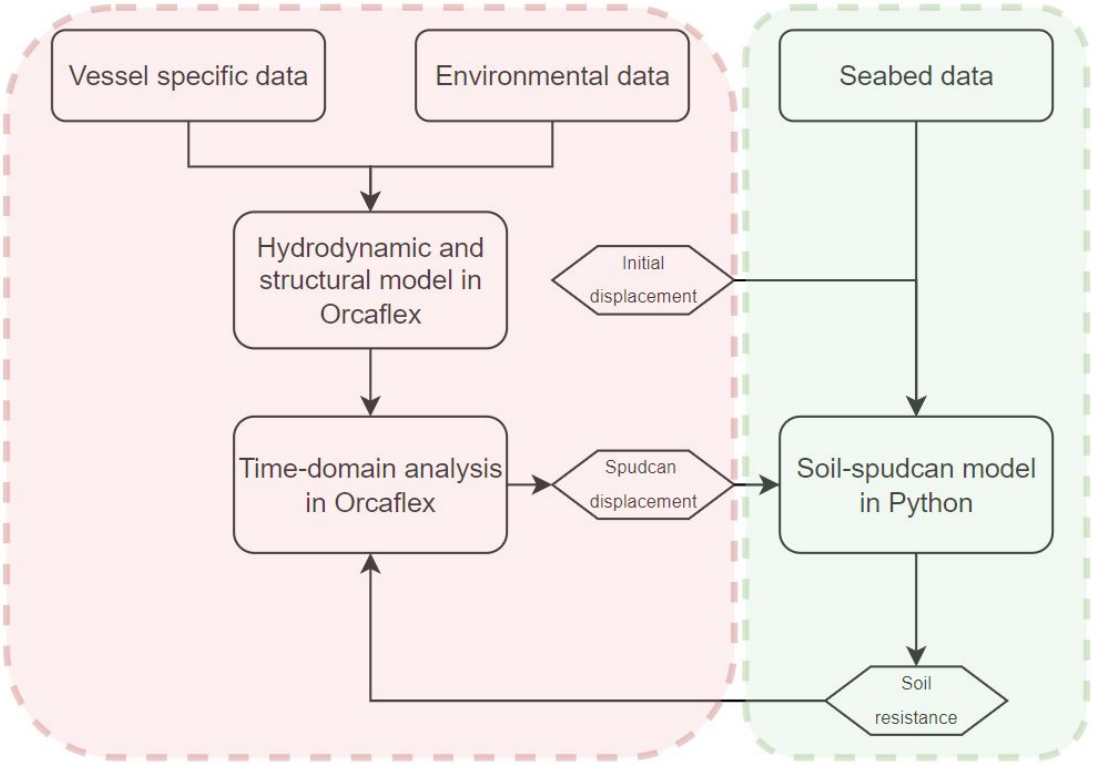

Figure 5.1: Flowchart illustrating the interconnection between OrcaFlex and Python. The green area represents calculations and data processing performed within Python, while the red area indicates the calculations and data provided by OrcaFlex.

5.3 Input data

This Section provides an overview of the various input parameters that can be varied in the model. The input parameters encompass soil properties, vessel characteristics, spudcan dimensions, and wave data. It is important to note that the framework's setup and purpose enable easy adjustments and variations in input parameters.

5.3.1 Soil data

In this research, the focus is on studying sandy seabed conditions, for which three main soil states can be classified: loose, medium, and dense sand. Table 5.1 presents the friction angle and effective unit weight of these soil types.

Table 5.1: Three soil types considered: loose, medium, and dense sand (Smith et al., 1995) (Jia, 2018).

Type of sand	**Friction angle** $(\phi)[degrees^{\circ}]$	**Effective unit weight** $(\gamma')[kN/m^3]$
Loose sand	30	9
Medium sand	35	11
Dense sand	40	13

The friction angle and effective unit weight of the soil are the primary parameters influencing soil bearing capacity. Figure 5.2 illustrates the bearing capacity curves for the three different soil states. It is evident that an increase in friction angle and effective unit weight leads to an increase in the soil's bearing capacity.

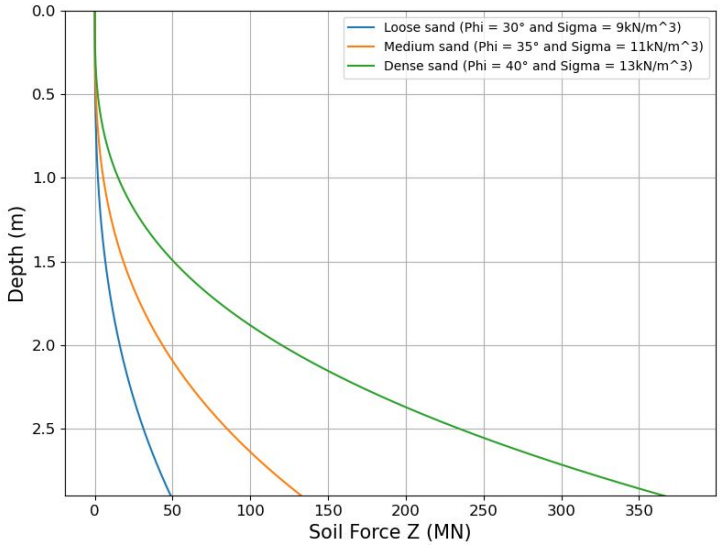

Figure 5.2: Bearing capacity curves of the three sandy soil states.

5.3.2 Spudcan data

Various spudcan geometries can be applied to model. In this research, the spudcan features a conical shape with a specific diameter and cone angle. Spudcans typically exhibit cone angles around 15 or 25 degrees and diameters varying up to 14 meters. The effective bottom area of the spudcan, a crucial parameter for computing the soil force acting on the spudcan, can be determined for any penetration depth of the spudcan within the soil. Figure 5.3 illustrates the geometry of the spudcan, indicating its effective diameter and bearing capacity upon penetration, as well as its cone angle θ.

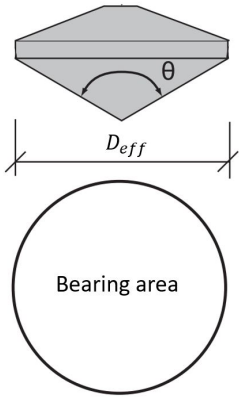

Figure 5.3: Example of spudcan configuration; D, diameter of the equivalent circular foundation; θ, cone angle.

5.3.3 Vessel data

The vessel's hull should be defined with its appropriate mass and dimensions. The hydrodynamic coefficients added mass, and damping should also be specified to account for the interaction between the hull and the surrounding water. To obtain the complete set of hydrodynamic coefficients for a vessel, it is essential to conduct thorough research and analysis on the specific vessel geometry. For this study, an existing jack-up hull model is utilized, which includes all the necessary data required for accurate simulation. The legs should be defined with their respective lengths, cross-sectional properties, and material properties.

5.3.4 Regular sea state

Regular waves, often referred to as Airy waves or linear waves, provide a straightforward representation of wave propagation. Originating from Airy wave theory, these waves are idealized versions of real sea conditions,

characterized by a sinusoidal shape. Their wave characteristics, such as wave height (half of the amplitude) and wave period (duration of one wave cycle), remain fixed and unchanging, making their behavior predictable. The plot, Figure 5.4, displays a wave over time, demonstrating the regular, sinusoidal pattern.
It's important to note, however, that regular sea states, as described by Airy wave theory, are primarily used to develop engineering understanding. They help to find relationships between vessel motions induced by incoming regular waves and the potential impact loads. Despite its usefulness, Airy wave theory does not fully represent real sea states. Real sea conditions are often irregular, which need further analysis beyond the scope of the linear wave theory In the following section, the application of irregular sea states is described.

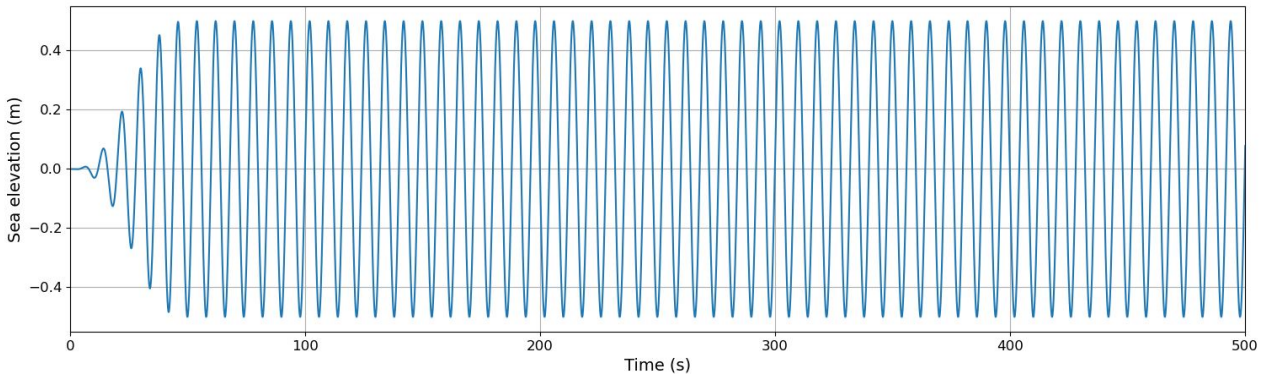

Figure 5.4: Simulation of a regular wave using the Airy wave theory. The figure demonstrates wave propagation over time, with Hs = 1m and Tp = 8s.

5.3.5 Irregular sea state

While the Airy wave theory can accurately describe simple periodic waves, real sea states are typically more complex. Waves in the ocean are rarely regular or periodic; they vary in height, period, and direction, leading to what is known as an irregular sea state. The irregular sea state is a superposition of several regular waves, each with its own period and wave height. The plot, Figure 5.5, displays a wave over time, showing the irregular wave patterns characteristic of real-world sea conditions.
In an irregular sea state, wave data comprises a mix of characteristics. The significant wave height (Hs) measures the average height of the highest third of the waves. The wave period (Tp) describes the time between the passage of two successive wave crests. The wave direction indicates the origin of the waves. Lastly, the wave spectrum, such as Joint North Sea Wave Project (JONSWAP), illustrates the distribution of wave energy across different wave frequencies. The wave spectrum provides a description of the sea state by illustrating how wave energy is distributed across different frequencies. The most common spectrum used for this purpose is the JONSWAP spectrum.
By incorporating these wave parameters into the simulation model, the dynamic behavior of the jack-up vessel under different irregular sea states can be accurately analyzed. This enables the evaluation of the system's performance and the assessment of a typical sea state's suitability for specific operations. Table 5.2 provides an

Table 5.2: Typical wave characteristics for swell and wind waves

	Swell wave	**Wind wave**
Significant wave height (Hs)	2 m	0.5 m
Wave period (Tp)	9 s	5 s
Wave direction	$0 - 360°$	$0 - 360°$
Wave spectrum	JONSWAP	JONSWAP

example of typical wave characteristics for swell and wind waves. These parameters can be used to simulate and analyze a realistic irregular sea state that a jack-up vessel may encounter during operations. It's worth noting that despite the complexity of irregular sea states, they are essential for conducting realistic simulations and assessments of marine structures like jack-up vessels. A good understanding of irregular sea states, along with the use of appropriate wave spectra, can significantly improve the reliability and accuracy of such simulations.

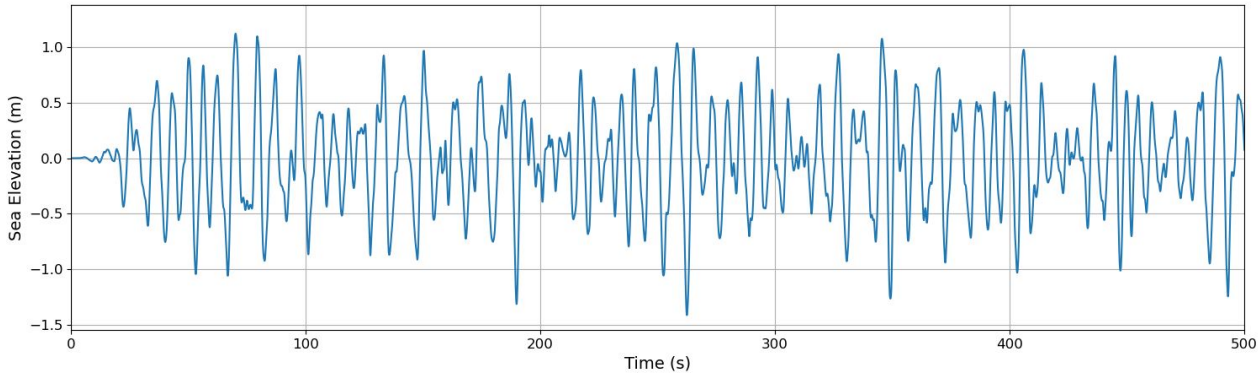

Figure 5.5: Simulation of an irregular incoming wave using the JONSWAP spectrum. The figure illustrates the complex wave patterns.

5.4 Full simulation; GoL stages

A typical OrcaFlex simulation of a jack-up vessel's going-on-location (GoL) process can be divided into four distinct stages: ramping, free-floating, impact, and pinned (Vazquez et al., 2017). In Figure 5.6 the 4 stages are indicated, ramping [I], free-floating [II], impact [III], and pinned [IV]. The ramping stage occurs prior to the actual simulation. In this stage, wave heights are progressively introduced into the simulation to prevent abrupt changes and ensure a smooth transition to the subsequent stage. In the free-floating stage, the jack-up vessel is allowed to float freely on the water's surface, responding to the wave loads. During this stage, there is no interaction between the seabed and the spudcans. The impact stage involves the spudcans making first contact with the seabed until the spudcan is pinned. This stage is critical in assessing the vessel's performance during the spudcan penetration process and evaluating the structural integrity of the legs and spudcans. Finally, in the pinned stage, the spudcans remain in contact with the seabed. The wave loads on the hull become minimal as the jack-up elevates itself above the mean sea level.

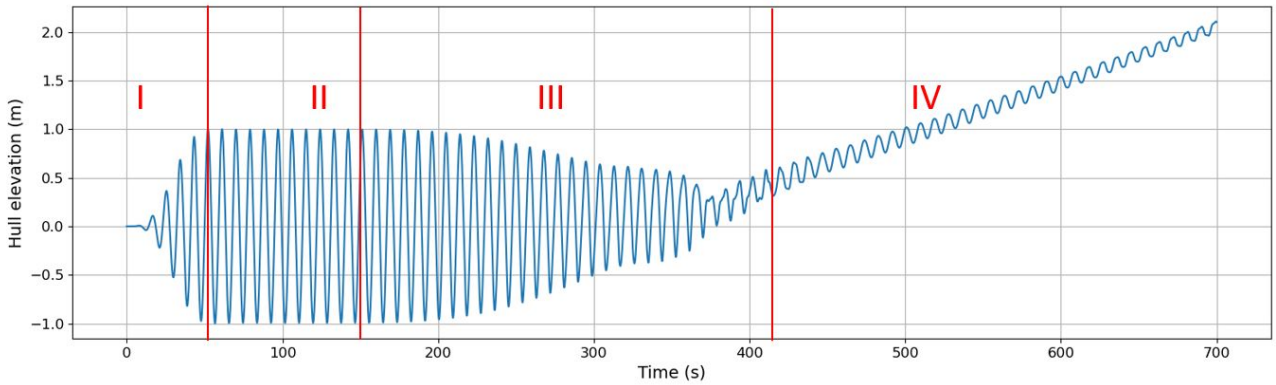

Figure 5.6: Simulation stages of GoL: ramping [I], free-floating [II], impact [III], and pinned [IV].

5.5 Soil-spudcan model verification

Verification ensures that the soil-spudcan interaction model has been implemented correctly and consistently in accordance with the underlying theory and assumptions made in Chapter 3. A verification simulation is conducted to explore and capture the descriptive vertical and horizontal soil behaviors. This simulation is performed using regular incoming waves characterized by a significant wave height (Hs) of 2 meters and a wave period (Tp) of 9 seconds, with the waves approaching on beam side. These sinusoidal waves represent a regular incoming wave as described by the Airy wave theory, providing a controlled and predictable environment. The regular sea state is described in section 5.3.4. Through this process, we aim to validate our model's functionality under controlled conditions, ensuring its capability to accurately represent soil-spudcan interactions under the influence of incoming waves. Subsequent analysis in Chapter 6, will delve into more complex and realistic sea states, employing irregular wave models to better simulate real-world conditions.

5.5.1 Vertical soil model

Figure 5.7 illustrates the vertical soil force acting on the forward-starboard spudcan during the hull GoL simulation. The plot provides a visual representation of the dynamic interaction between the spudcan and the soil under regular waves. It is important to note the oscillatory nature of the force response, reflecting the cyclic loading conditions induced by the wave action. Detailed analysis and discussion of the observed soil behavior will follow.

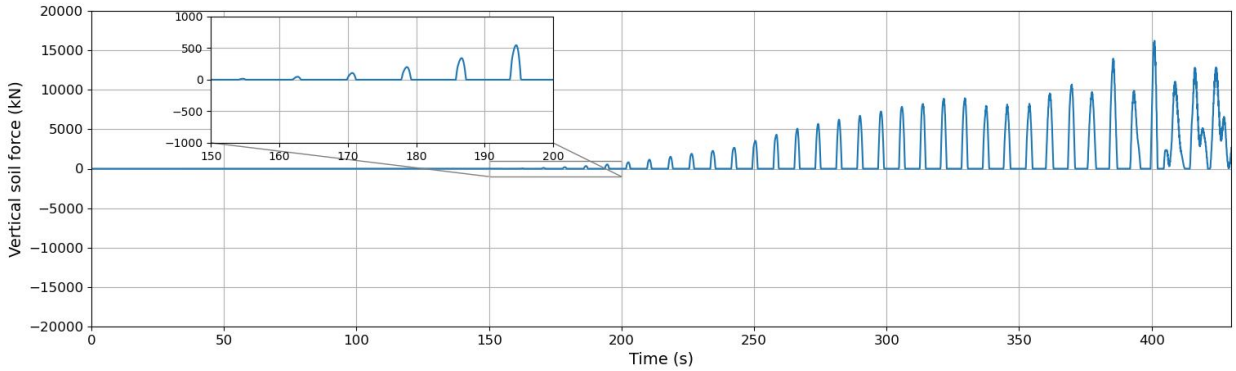

Figure 5.7: Vertical soil force acting on the forward-starboard spudcan.

The vertical soil forces can be described through the resistance path outlined by the four modes depicted in the flowchart presented in Figure 5.8. Initially, the model's configuration does not incorporate unloading and reloading modes. Instead, the penetration mode is set to either "virgin soil penetration" if the spudcan penetration is positive (i.e., below the seabed), or "no soil contact" if the spudcan penetration is zero or negative. In the dynamic simulation of the GoL, the spudcan begins to simulate in the "no soil contact" mode, it transitions to the "virgin soil penetration" mode once the spudcan penetration becomes positive.

The spudcan remains in the "virgin soil penetration" mode until it starts to lift out of the seabed and proceeds to "unloading" mode. The spudcan stays in the "unloading" mode until there is a loss of contact with the soil, the unloading will proceed to "no soil contact" mode. If the spudcan penetrates the soil again, the system will proceed to "reloading" mode.
The "Reloading" mode persists until the spudcan starts to unload again, at which point it transitions to the "Unloading" mode. If the spudcan maintains contact with the soil but oscillates up and down, it alternates between the "Unloading" and "Reloading" modes. When the spudcan loses contact with the soil and subsequently reestablishes contact in the following cycle, it operates under the "Reloading" mode. However, if the spudcan penetrates deeper into the soil during the "Reloading" mode than it did during its previous "Virgin soil penetration" mode, it comes into contact with virgin soil and reverts back to the "Virgin soil penetration" mode.

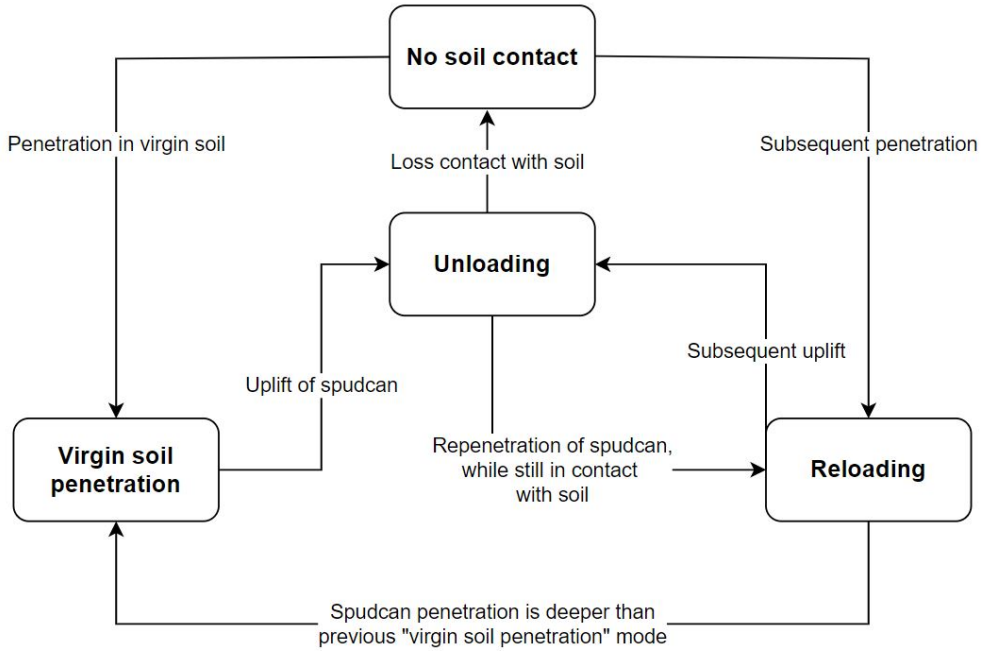

Figure 5.8: Vertical penetration modes of the spudcan in soil. The diagram distinguishes four main penetration modes, with arrows indicating the progression paths between them.

5.5.2 Horizontal soil impact

In Figure 5.7, the horizontal soil force in the x-direction acting on the forward-starboard spudcan is depicted as a function of time for the same simulation shown in Figure 5.6. The primary requirement for lateral soil

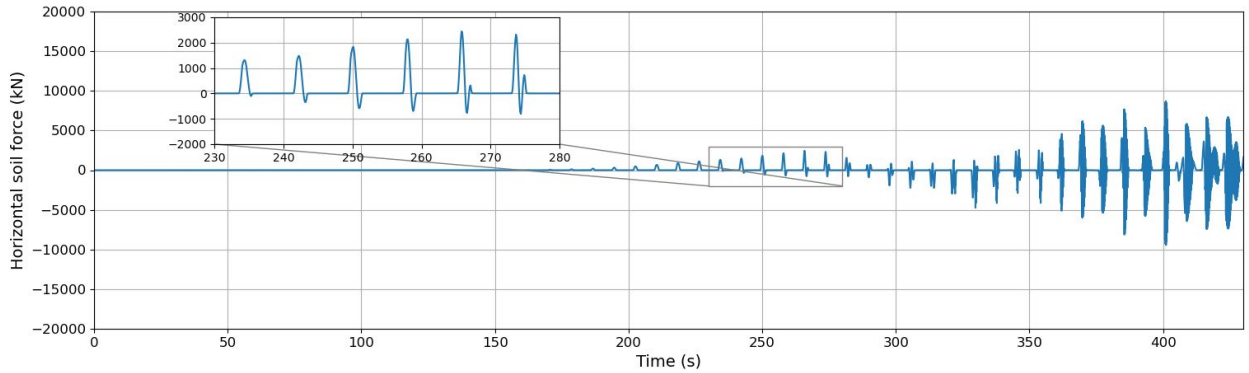

Figure 5.9: Horizontal soil force acting on the forward-starboard spudcan. The inset highlights interesting impacts between the seabed and the spudcan.

resistance is the simultaneous occurrence of vertical soil penetration. Vertical penetration embeds the spudcan, establishing a vertical soil resistance force. When considering lateral displacement, it is essential to recognize that during spudcan penetration, the soil can exert resistance on the spudcan in both positive and negative directions, depending on the direction of displacement. Within a single penetration cycle, the spudcan may move in two opposing directions, leading to soil resistance exhibiting both positive and negative signs in a short subsequent order, as seen in the inset. Figure 5.10 shows the horizontal soil force path for a single penetration cycle.

As the spudcan moves in the positive y-direction, the lateral soil resistance increases positively. When the spudcan moves in the opposite direction but remains on the positive side of its origin, the soil force is still positive. However, when the spudcan crosses its origin and moves into the negative side, the soil force is established within the negative elastic soil resistance. It is important to note that the negative sign does not indicate a pulling soil force.

Towards the end of the impact phase and the start of the pinned stage, the spudcans begin to exhibit vibrations,

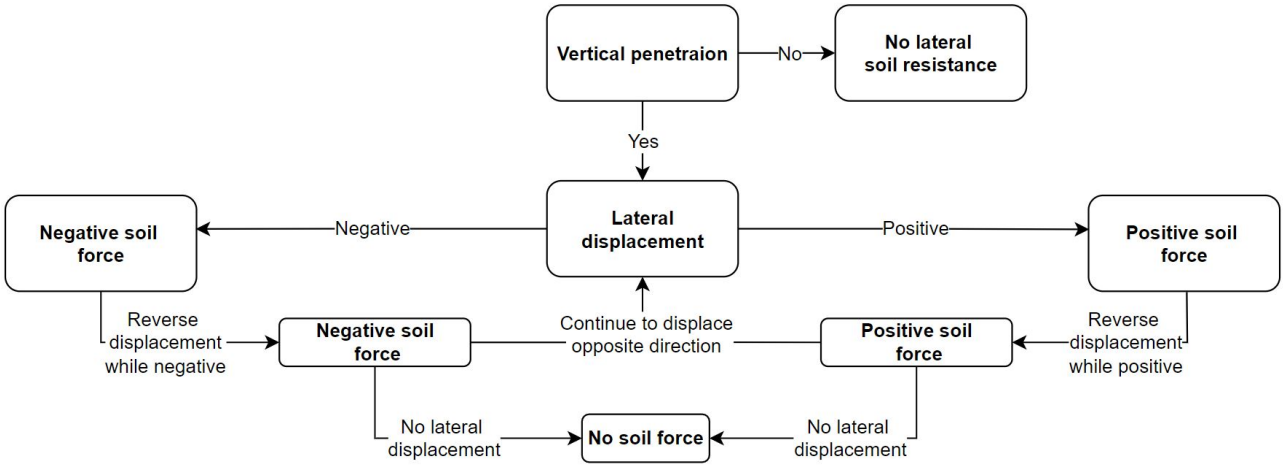

Figure 5.10: Horizontal displacement modes of the spudcan and soil forces.

evident from the frequent surpassing of their mean force. The horizontal soil forces exhibit a vibrating pattern over time, as the spudcan becomes increasingly embedded in the soil. This vibrating behavior is typical for such situations as stiffness is increasing. During the initial horizontal soil forces, as seen in the inset of Figure 5.9, no vibration is yet visible. This vibratory behavior can also be attributed to the numerical aspects of the modelling.

5.6 Summery

This section consolidates the key findings and conclusions from the implementation of the framework in OrcaFlex, before proceeding to the results chapter. It also highlights the crucial input variables used in the process.

In contrast to the implementation in Python, the time-domain solver within OrcaFlex was employed to accomplish the integration. Figure 5.1 graphically presents the division of the three elements between OrcaFlex and Python. Notably, the entire soil-spudcan interaction model operates independently from OrcaFlex, again, underscoring the flexibility of this approach in allowing easy modifications and integration of alternative soil-spudcan interaction models.

All simulations performed in the upcoming result Chapter employ data corresponding to medium-dense sand for soil characteristics, see Table 5.1. Additionally, the two distinct sea states introduced in this Chapter, regular and irregular, are utilized for simulations and will specify the particular sea state used in each instance. A comprehensive overview of all additional vessel data is provided in Section 6.3. Lastly, the simulation stages have been refined by combining the free-floating and ramping stages, as neither of these stages involves soil-spudcan interaction.

Chapter 6

Results & analysis

In the results Chapter, findings will be presented based on a specific model that adheres to the model framework outlined in Chapter 5. To gain a better understanding of the model and its physical implications, an energy-based perspective will be established. According to the outcomes and observations of the results, key events will be highlighted and can be further examined by varying specific parameters or by delving deeper into particular aspects of the model. This approach allows for a more comprehensive interpretation of the results and sheds light on the underlying mechanisms at play.

6.1 Complete going-on-Location simulation

In the initial section of the Chapter, a complete going-on-location (GoL) simulation is presented. For a deeper understanding and identification of key events of the GoL, both regular and irregular sea states are considered. Detailed discussions of these sea states can be found in Section 5.3.4 and Section 5.3.5, respectively. Regular sea states serve as a simplified model for engineering analysis, whereas irregular sea states better mimic the complexity of actual sea conditions.

In both sea states, the axial impact forces on the four spudcans over time are analyzed, see Figures 6.1 and 6.2. The axial forces on the spudcans adhere to the soil-spudcan interaction model as described in Chapters 3 and 5. The focus of this study lies on the axial forces exerted on the spudcans, as these are more likely to be limiting factors compared to horizontal soil forces. As such, the vertical soil forces on the spudcans are illustrated. Furthermore, wave elevations for each scenario are also displayed, clearly comparing wave elevation between regular and irregular sea states.
Figure 5.6 in Section 5.4 illustrates the GoL stages, representing them through the elevation or z-displacement of the vessel above the seabed. However, these stages are also visible through a multitude of other graphical representations in the context of a complete GoL. The first two stages, namely ramping and free-floating, are combined and referred to as the free-floating stage. This consolidation is due to the absence of any soil contact during both of these stages. The stages are sequenced as follows: the first stage represents free-floating, the second stage marks the impact phase, and the third stage indicates the pinned condition. In the simulation, the GoL starts with a free-floating stage, which includes the ramping phase. This initial stage lasts until the first instance of soil-spudcan interaction. This interaction marks the start of the impact phase, distinguished by recurring contacts between the spudcans and the seabed. At a certain point, a continuous axial force is established on the spudcans due to sustained contact with the seabed. This occurrence signals the end of the impact phase and the onset of the pinned stage. During this final stage, the draft reduces and the vessel ascends above the waterline. The two figures, 6.1 and 6.2, clearly distinguished the three distinct stages, indicated by red numbers in the upper graph of each figure.
For the regular sea state, the axial forces on the spudcans progressively increase as the spudcans descend towards the seabed. The maximum impact force exerted on spudcan 4 (indicated by the red line) is approximately 26,000 kN. The transition into the pinned stage begins at the 500-second mark. In the case of the irregular sea state, the increase in impact forces is not gradual and displays a more random pattern. The start of the impact stage is slightly delayed, but like in the regular state, the transition to the pinned stage begins at the 500-second mark. The maximum impact force in this scenario is approximately 25,000 kN. From the simulations, several key observations can be made.

1. The axial impact forces tend to escalate as the impact phase progresses towards its end.

2. For irregular sea states, as the spudcans are progressively lowered towards the seabed, the frequency and magnitude of the impacts increase. For regular sea states, the frequency remains consistent and corresponds to the wave period.

3. In these specific simulations, the axial forces exerted on the aft-starboard spudcan appear to be the most significant. Nevertheless, depending on the sea states and notably varying wave directions, any spudcan could potentially become the critical factor.

4. During the pinned stage, the axial forces initially decrease as the ship's dynamics are reduced, leading to a quasi-static system. The graph in Figure 6.3 shows the roll angle of the jack-up vessel for the regular sea state simulation, illustrating the almost complete reduction of the roll angle and the associated decrease in the vessel's dynamics. However, after 600 seconds, the axial forces become greater than the maximum impact forces as the vessel's mass gradually shifts from being supported by buoyancy to being supported by the axial soil forces, for both regular and irregular sea states.

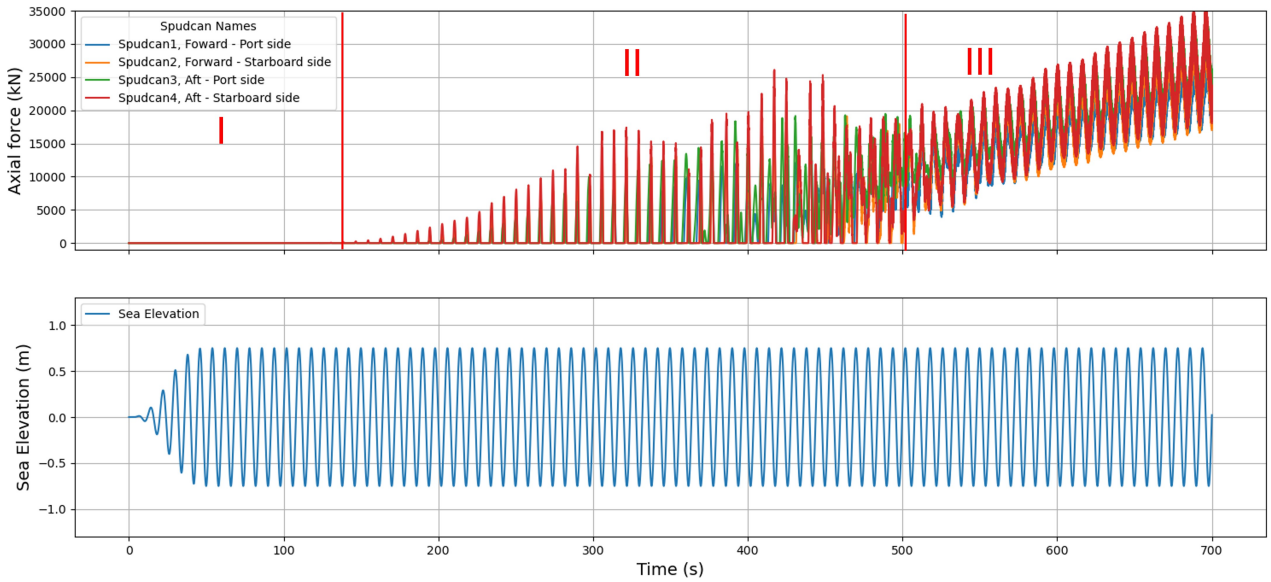

Figure 6.1: The axial impact forces on the spudcans for a complete going-on-location process of the jack-up vessel subjected to regular beam waves with Hs = 1,5m and Tp = 8 seconds

6.2 Energy-based analysis

An alternative method of system analysis involves examining its energy, rather than focusing solely on the impact forces. This approach offers valuable insight into the soil-spudcan interaction and the vessel's behavior during impacts. By defining the system as the entire jack-up vessel, including spudcans and legs, we can potentially establish a relationship between the system's energy and the soil-spudcan impact forces.
The energy-based analysis, as also discussed in the paper by Vazquez and Grasso (2016), emphasizes the significance of understanding the energy exchange between the vessel's motion and its interaction with the seabed. The paper by Vazquez and Grasso (2016) is based on the DNV guidelines (DNV GL, 2015). By focusing on the conservation of energy and the transformation of different forms of energy, Vazquez and Grasso (2016) demonstrates the effectiveness of this approach in analyzing the sudden soil impacts on free-floating vessels. The analysis of the free-floating mode and a sudden introduction of the seabed for four different load cases demonstrates that the first impact is the most significant. This result can be attributed to the fact that the energy in system during free-floating is released upon the first contact with the seabed, causing the greatest force to be exerted during the first touchdown. With numerous subsequent impacts, the system energy approaches zero as the impacts dissipate energy from the system and exhibit a damping effect. The energy-based analysis effectively represents the dissipation of energy upon impact and will be utilized in further analysis in this research.

The energy in the jack-up system can be determined by considering both potential and kinetic energy. Kinetic energy is associated with the motion of the jack-up and is calculated based on its moment of inertia

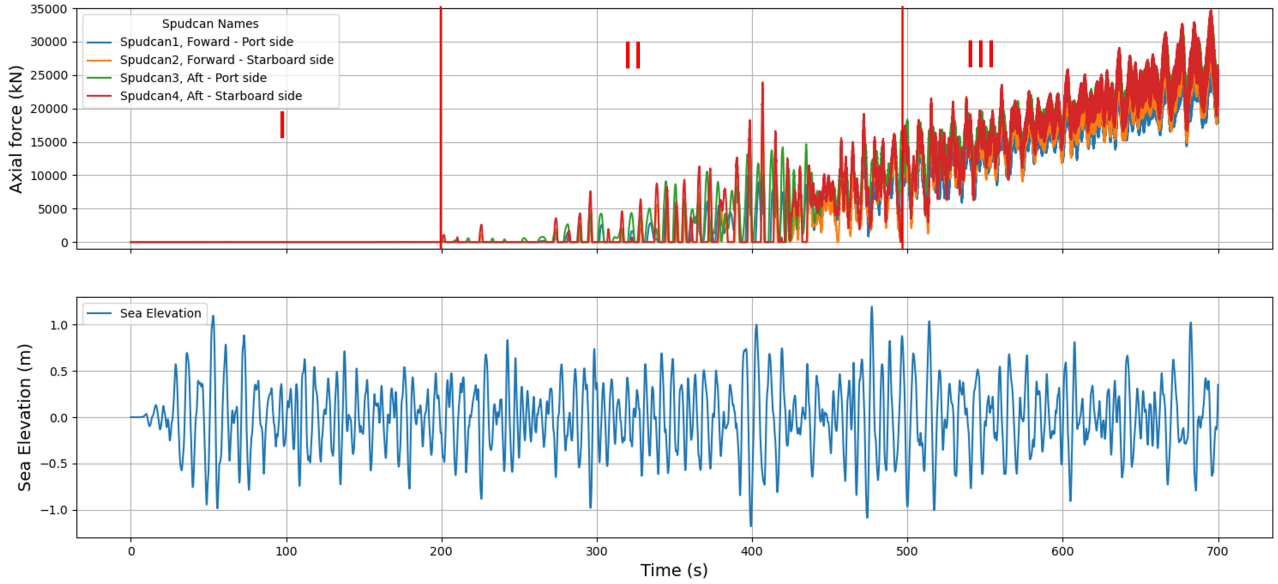

Figure 6.2: The axial impact forces on the spudcans for a complete going-on-location process of the jack-up vessel subjected to irregular beam waves with Hs = 1,5m and Tp = 8 seconds

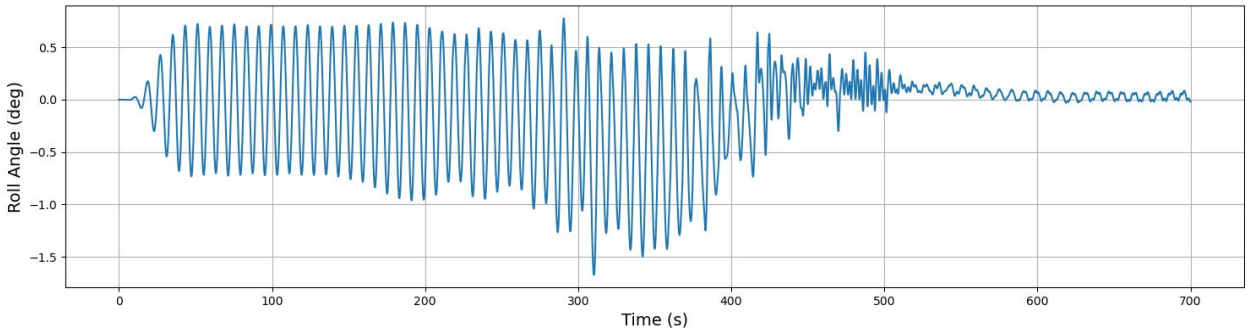

Figure 6.3: Roll angle of the jack-up in a regular sea state.

around the respective axes and its angular velocities, or for a translational displacement and its velocity. The potential energy can be described by the stiffness in a particular degree of freedom (DOF) and the angular or translational displacement. The ship's motion, and consequently the spudcan dynamics, are mainly governed by the angular motions of the vessel in pitch and roll (Chakrabarti, 2012). The equations for the potential and kinetic energy for the roll motion are as follows:

$$E_p = \frac{1}{2} k\theta^2 \tag{6.1}$$

$$E_k = \frac{1}{2} I_x \dot{\theta}^2 \tag{6.2}$$

In these equations, E_p represents the potential energy, k is the stiffness, θ is the angular displacement, E_k is the kinetic energy, I_x is the moment of inertia around the x-axis, and $\dot{\theta}$ is angular velocity. For the pitch motions, the corresponding pitch angular stiffness and moment of inertia around the y-axis should be used.

6.3 Specific model

Before comparing different simulation scenarios and results, a specific jack-up model and environmental parameters must be selected. A jack-up model has been developed in accordance with the model framework presented in this research. A diffracted jack-up model with legs and spudcans is used for simulations, see Figure 6.4. All specific jack-up parameters and soil parameters that are defined within the framework are summarized in Table 6.1. While the specific jack-up model is used for presenting results in the subsequent Sections, the framework

offers flexibility for easy modification of the input data.
In this research beam seas are established with a varying significant wave height and a wave period, for both regular and irregular waves. These wave conditions generate a maximum roll response, resulting in the largest roll motions. The vessel's natural roll period is close to 12 seconds, so with a wave period of 12 seconds, the roll motion will be primarily present. To accurately capture the range of possible responses, different seeds can be performed for the irregular waves. Each seed represents a different random realization of the wave conditions, allowing for a comprehensive analysis of the vessel's behavior under various wave scenarios.

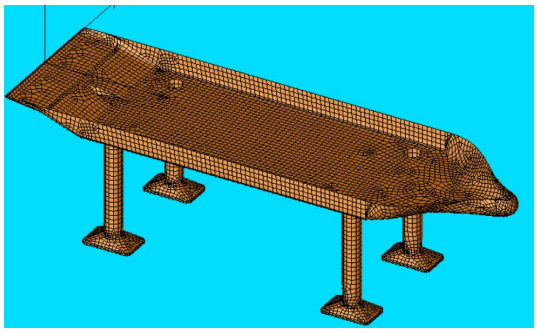

Figure 6.4: Illustration of the hydrodynamic panel model for the jack-up vessel used for the simulations.

Table 6.1: Vessel and leg data parameters.

Parameter	**Value**
Vessel Data	
Length $[m]$	103
Mass $[te]$	24.6×10^3
Leg data	
Outer diameter $[m]$	3
Inner diameter$[m]$	2.93
Mass per unit length $[te/m]$	5
Bending stiffness X $[kN \cdot m^2]$	103.9×10^9
Bending stiffness Y $[kN \cdot m^2]$	103.9×10^9
Axial-stiffness Y $[kN \cdot m^2]$	94.5×10^9
Initial leg length $[m]$	30
Continuous payout rate leg (downward velocity) $[m/s]$	0.0075
Spudcan data	
Diameter D_{eff} $[m]$	12.6
Cone angle θ $[degrees°]$	25
Max bearing area $[m^2]$	124.7
Soil data: Medium dense sand	
Friction angle $[degrees°]$	35
Effective unit weight $(\gamma')[kN/m^3]$	11
Wave data; regular and irregular	
Water depth $[m]$	35
Significant Wave Height (Hs) $[m]$	1 - 4
Wave Period (Tp)	6 - 12 s
Wave Direction $[degrees°]$	90
Seed $[-]$	1 - 50

6.4 Simulation scenarios

Three simulation scenarios will be introduced in this Section; undisturbed vessel, disturbed vessel and pinned vessel. An overview of the involved stages per simulation scenario is visualized in Table 6.2. The three simulation

scenarios have been established to depict the boundary stages of a jack-up vessel during the going-on-location. The process of going-on-location (GoL) represents a transition from a free-floating mode to an elevated or pinned mode. In between these modes, the impact phase occurs, which has been attempted to be modeled in this study. The three scenarios are introduced as a means of validation and to establish boundary conditions for the impact phase. The energy-based approach (Section 6.2) will be applied to two simulation scenarios: an undisturbed vessel and a disturbed vessel.
The analysis of the undisturbed, disturbed, and pinned stages will provide an understanding of the jack-up system's dynamic behavior. By examining the differences and resemblance of these three situations, valuable insights into the impact of soil-spudcan interactions on the vessel's energy distribution and overall dynamics will be gained. The following sections will provide a more detailed description of the three scenarios.

Table 6.2: The table provides a concise overview of the sequence of the 'Free-floating', 'Impact', and 'Pinned' stages for each scenario: undisturbed vessel, disturbed vessel, and pinned vessel.

Scenario	**Time →**		
1. Undisturbed vessel	Free-floating		
2. Disturbed vessel	Free-floating	Impact phase	Pinned
3. Pinned vessel	Pinned		

6.4.1 Undisturbed vessel

In the scenario of the undisturbed vessel simulation, the vessel remains continuously in a free-floating mode. This is a significant phase as every vessel begins in this state before proceeding to going-on-location. This particular simulation scenario allows for a comparison of an undisturbed continuous free-floating mode with the free-floating mode seen in the disturbed scenario.
The energy-based approach, as outlined in Section 6.2, has been employed to this scenario. Since the incoming beam waves predominantly excite the vessel's roll motions, the total roll energy consists of the kinetic and potential energy associated with the roll motion, as described in equations 6.2 and 6.1. The total roll energy of the ship is closely related to the incoming waves, as higher waves exert a load on the vessel, causing it to roll and accumulate energy. However, incoming waves can also provide damping as they oppose the vessel's motion. This damping effect occurs when the wave-induced forces and moments counteract the vessel's movements, leading to a reduction in the vessel's roll energy. In this dynamic process, the ship's energy continuously oscillates between potential and kinetic energy under the influence of the incoming waves. In Figure 6.5, the roll energy is plotted over time and the wave height for an irregular incoming wave. The graph shows the accumulation and damping of roll energy, which depends on the vessel's position relative to the incoming wave at any given moment. During the simulation, no soil-spudcan interaction occurs because the spudcans remain above the seabed throughout the entire simulation.

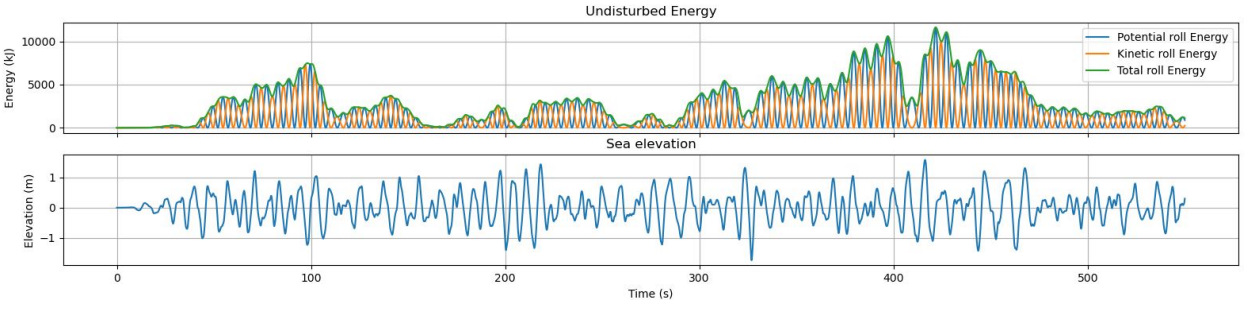

Figure 6.5: Undisturbed roll energy and the wave height at the COG of the vessel.

6.4.2 Disturbed vessel

The disturbed simulation scenario fully adheres to the framework introduced in Chapter 5, encompassing all three stages: free-floating, impact, and pinned modes. Hence, the disturbed simulation scenario fully captures the entire going-on-location (GoL) process.
In Figure 5.6, the various stages of the GoL process are illustrated. The jack-up vessel always begins the GoL in the free-floating or undisturbed mode, as described in Section 6.4.1. The legs are progressively lowered until they

make contact with the seabed, initiating the soil-spudcan interaction. From the moment the first touch-down occurs, the vessel experiences disturbance. In the free-floating vessel mode, potential and kinetic energy are constantly exchanged, with the total energy changing gradually over time without abrupt fluctuations. However, upon soil-spudcan interaction, an additional energy component is introduced to the system. With each impact between the four spudcans and the seabed, energy is dissipated from the vessel's total energy, causing the soil to exhibit a damping effect on the system, see Figure 6.6. By the end of the impact phase (approximately 460 seconds), or at the start of the pinned situation, the total energy in the system approaches zero as the energy is absorbed through soil interactions.
When plastic deformation occurs in the soil, energy dissipation arises due to the hysteresis loop. This loop symbolizes the energy lost from the system because of the soil's irreversible structural changes, a manifestation of the soil's non-linearity. Refer to Section 3.4.1 for a deeper understanding of the soil-spudcan interaction model or Section 6.5.3.

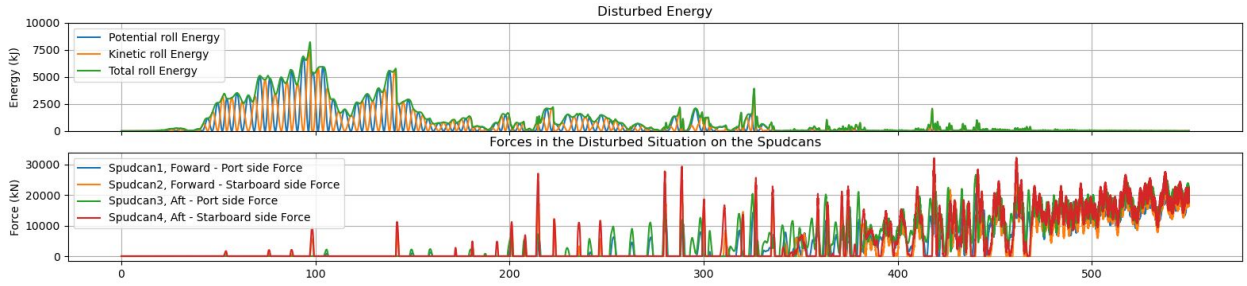

Figure 6.6: Disturbed roll energy and impact forces on the spudcans.

6.4.3 Pinned vessel

In the simulation scenario where the jack-up vessel is in a pinned situation, the spudcans are constrained to the seabed. While they are allowed to rotate, their translational motion is restricted. Consequently, no roll motions will be present in the system. The incoming wave loads are directly transmitted through the spudcans to the constrain, effectively bypassing any potential for roll energy accumulation. As a result, the forces between the spudcans and the seabed form a quasi-static force balance, counteracting the incoming wave loads. In Figure 6.7, the forces acting on the spudcans are illustrated. In the pinned scenario, the forces on the spudcans can exhibit both positive and negative values, resulting in tension and compression forces. The outlined pinned system simulates the situation following the impact phase, where the jack-up has elevated and the spudcans are in continuous contact with the seabed. This scenario acts as the endpoint boundary condition for the disturbed scenario, symbolizing the vessel's final state after successful positioning on location.

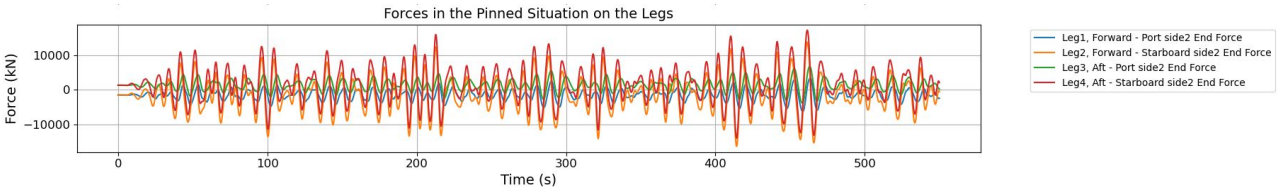

Figure 6.7: Forces exerted on the spudcan during the pinned situation.

6.5 Comparative analysis of simulation scenarios

The results of the three simulation scenarios are analyzed to identify similarities and to evaluate the performance of the soil-spudcan interaction model. The primary purpose of presenting these distinct simulation scenarios is to ensure the accurate establishment of the boundary conditions —free-floating and pinned— for the disturbed vessel simulation. By comparing these scenarios, we can confirm that the transitions between stages in the disturbed vessel simulation have been modeled accurately, providing a robust foundation for studying the impact phase. Furthermore, the roll-energy graphs discussed in Sections 6.4.1 and 6.4.2, and the forces on the pinned spudcans represent separate simulations for the same seed number, making it possible to overlay them for a comparison of their behavior over time. In Figure 6.10 the outcomes of three simulation scenarios are

shown together. Two key-events stand out in this context, specifically the energy dissipation and the peak impact.

6.5.1 Free-floating boundary; undisturbed and disturbed

The first and second plot of Figure 6.10 presents the roll energy of the disturbed and undisturbed vessel simulation. Upon the initiation of soil-spudcan interaction, the energy plots of the two simulations start to diverge, illustrating the beginning of the impact phase around the 60-second mark. This is where the disturbed simulation scenario demonstrates its first soil-spudcan impact. In the disturbed vessel simulation, these impacts influence the total energy of the system, marking a clear deviation from the undisturbed scenario. Since the plots are identical up to the 60-second mark, indicates that the free-floating stage has been successfully modeled and validated, as the two plots match perfectly before the onset of the impact phase. Therefore, the free-floating boundary conditions of the disturbed scenario are confirmed as accurately modeled. Hence, it becomes evident that during the impact phase, the soil-spudcan interaction significantly alters the energy dynamics of the system, see section 6.5.3.

6.5.2 Pinned boundary; disturbed and pinned

As the impact phase of the disturbed scenario concludes and transitions towards a pinned situation, a quasi-static system starts to establish itself. From this stage, the quasi-static forces in the pinned scenario become comparable to the axial spudcan forces in the disturbed situation. The similarities between the two simulation scenarios are evident in the plots depicted in 6.8, which illustrate the axial forces on spudcan 4 over time under regular wave conditions. In both the disturbed and pinned simulations, the trajectory of the axial forces is similar, as highlighted by the inset, i.e. a zoomed-in view of the final 30 seconds of the simulation. While a trend is observed in the plot for the disturbed spudcan forces, the general pattern and trajectory of both simulations exhibit considerable consistency. This implies that the soil-spudcan interaction model aligns well with the established framework in the pinned simulation scenario.
The same consistency is observable in Figure 6.10, which depicts the simulation results for irregular wave conditions. During the period from 465 seconds until the end of the simulation, the forces on the spudcan in the third plot show a gradual increase with a noticeable trend associated with the spudcan's downward velocity. In the pinned scenario, represented by the fourth plot, the forces on the spudcan follow a pattern related to the incoming wave heights.

6.5.3 Energy dissipation

At the end of the impact phase, at 465 seconds, the disturbed energy plot reaches zero, as there is no roll energy in the system, in Figure 6.10. This contrasts with the undisturbed vessel, which accumulates roll energy, indicating that the impact forces on the soil are responsible for energy dissipation. In Figure 6.9, the energy dissipation is visible as the total roll energy decreases for two subsequent impacts, first on the starboard spudcan pair and then on the portside spudcan pair.
The energy dissipation observed is closely related to the non-linearity of the soil-spudcan interaction model. As the spudcans impact the soil, plastic deformation occurs, leading to energy dissipation and extraction from the vessel system. This is distinctly different from a scenario involving velocity-dependent damping. The non-linear characteristics of the soil-spudcan system, specifically the plastic deformation of the soil upon impact, act as a damping mechanism, absorbing the vessel's kinetic energy. This is evident in Figure 6.9, where the total roll energy decreases sequentially with the impact of the starboard spudcan pair, followed by the portside spudcan pair.

6.5.4 Maximum impact

The maximum impact force occurs on spudcan 4 towards the end of the impact phase at approximately 460 seconds, in Figure 6.10. At the end of the impact phase, the system behavior can be described by both the disturbed system and the pinned system, see Section 6.5.2. As the impact phase is nearly completed, and no spudcan loses contact with the seabed, short periods of pinned vessel behavior occur alternating with uplift resulting in no soil contact. These periods can vary up to 30 seconds. The highest impacts occur during the final stage of the impact phase, as the vessel behaviors alternate pinned and no soil contact, resulting in a complex interplay between static and dynamic forces that ultimately shape the maximum impact between the soil and spudcan. This observation holds for both regular and irregular sea states, see Figures 6.1 and 6.2, respectively.

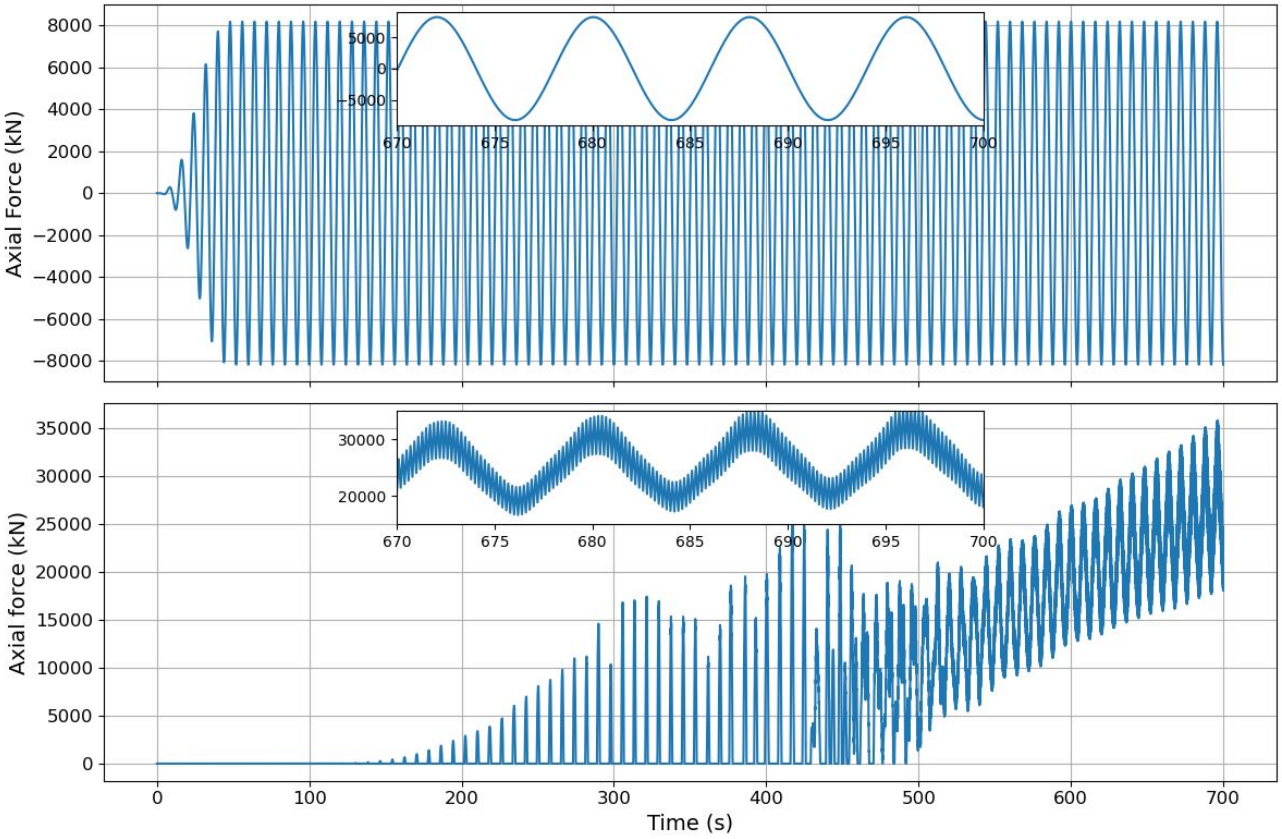

Figure 6.8: The first plot presents the axial forces exerted on spudcan 4 in the scenario of the pinned simulation. The second plot illustrates the axial forces applied to spudcan 4 when the vessel is in a disturbed state. The insets provide a zoomed-in view of the plots, specifically focusing on the final 30 seconds of the simulation.

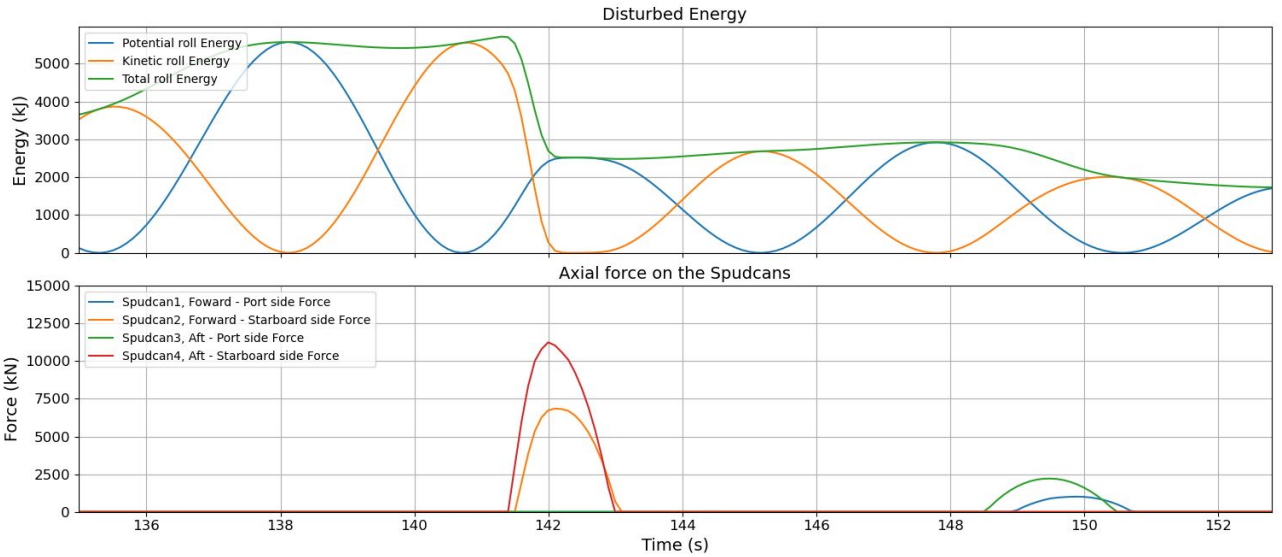

Figure 6.9: Energy dissipation during impact. The first energy drop is attributable to spudcans 2 and 4, both on the starboard side, as they simultaneously make contact with the seabed. The second decrease in energy is due to spudcans 1 and 3 on the port side.

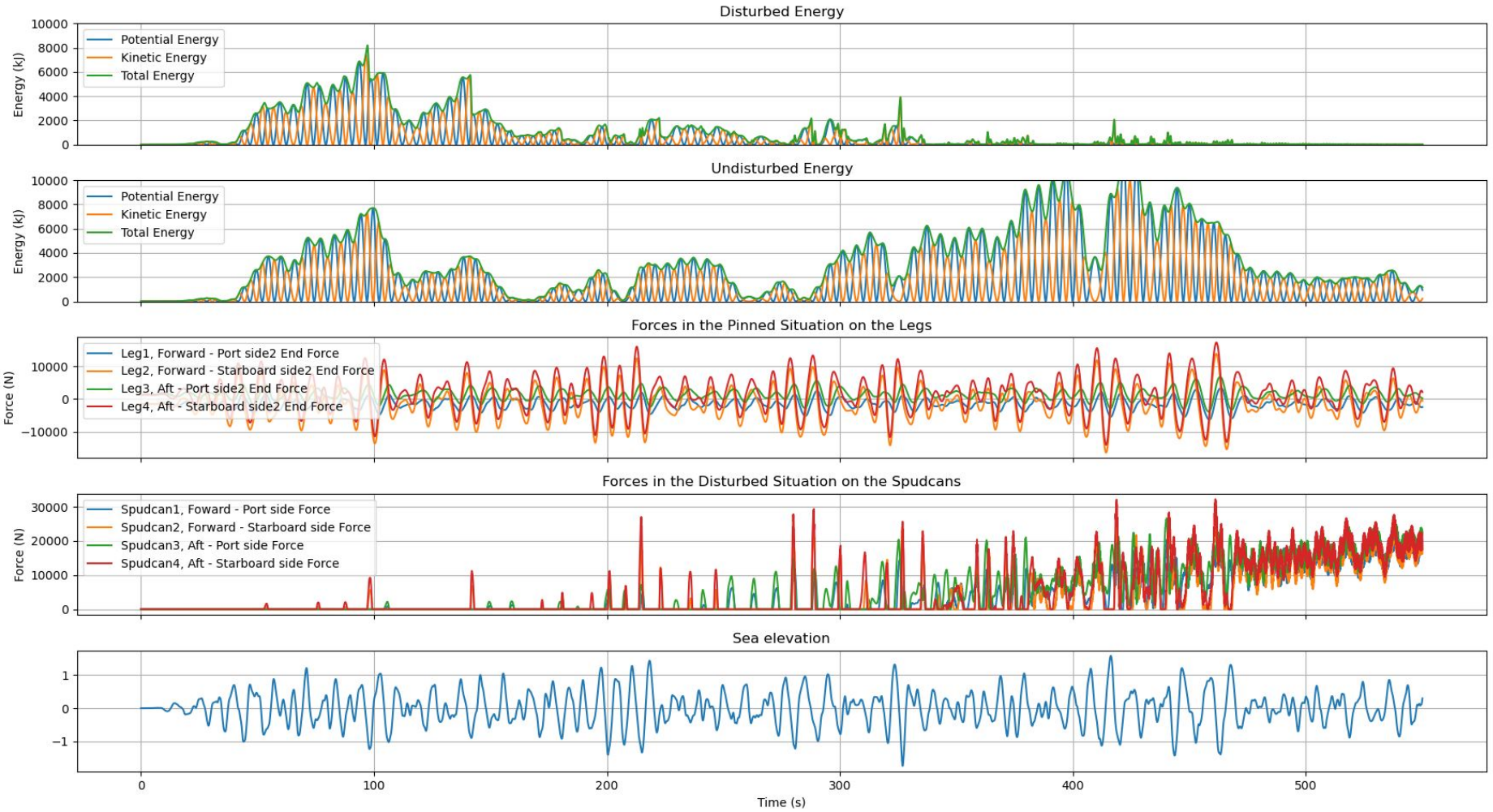

Figure 6.10: First plot; Disturbed vessel roll energy. Second plot; Undisturbed vessel roll energy. Third plot; Pinned vessel spudcan forces. Fourth plot; Impact forces spudcan during disturbed vessel simulation. Fifth plot; wave elevation data.

6.6 Varying sea states

The key events and boundary scenarios discussed thus far in this Chapter apply to both regular and irregular sea states, with results primarily shown from a single simulation run. The findings and key events outlined are applicable across all simulation scenarios run so far. However, research is being conducted into how these results may change when varying sea state parameters are introduced, for both regular and irregular conditions. Applying variations to regular sea states in the jack-up system helps deepen the understanding of the system's response and its interaction with the seabed. Regular sea states offer a more straightforward approach and comprehension, making them an ideal starting point. For regular sea states, variations are introduced primarily in the wave height and period to examine their effects. In the case of irregular sea states, the investigation expands to include six different load cases, each subjected to numerous iterations, or 'seeds', to ensure a comprehensive understanding of the system's behavior under diverse conditions.

6.6.1 Regular sea state; Vessel dynamic vs. impact force

The central principle in this analysis is the correlation of vessel dynamics with impact forces. This can be achieved by examining the impact forces for varying regular sea states. By adjusting the wave height and wave period for regular incoming waves, the dynamics of the vessel are likely to vary, leading to corresponding changes in the impact forces and their magnitudes. The fundamental idea behind analyzing and correlating vessel dynamics with impact forces is to enable to predict impact forces, even under conditions where information about the sea state (like wave height, direction, or speed) might not be fully known. In traditional workability studies, certain parameters like wave height can set limitations to when the going-on-location process can proceed. If these conditions are exceeded, operations would typically be halted for safety and operational integrity reasons. However, with the approach suggested in this Section, the focus shifts from solely relying on external conditions like wave height, to a more understanding of how the vessel's own dynamics can influence the forces it experiences during the impact phase. So, even in situations where the wave height exceeds traditional safety limits, if the vessel's dynamics are understood to be within safe bounds for withstanding the resulting impact forces, operations could continue. This approach could potentially enhance workability.

For analyzing the vessel dynamics, the maximim downward velocities of the spudcan during impact are considered, alongside the peak impact forces experienced by the spudcan throughout the entire impact phase. In the case of incoming beam waves, the most significant effects are observed on the spudcans situated on the starboard side. Therefore, the dynamics of spudcans numbered 2 and 4 located on the starboard side are focussed on.
The wave height is adjusted in a range from 1 to 2.5 meters, with increments of 0.5 meters, while the wave period is modified between 6 to 12 seconds, with step increments of 1 second. The direction of the incoming waves is held constant, coming in as beam waves. In all, 36 different scenarios are considered involving regular wave patterns. In Figure 6.12, the scatter plot showcases the maximum axial impact force experienced by the two starboard spudcans during the impact phase, plotted against its maximum downward spudcan velocity (DSV). Thus, for each simulation, two data points will be displayed. This correlation implies an intrinsic relationship between the vessel's dynamics and the resulting impact forces under different wave conditions.
A clear trend becomes apparent when observing the distribution of data points. This trend reveals that as the maximum DSV increases, so too do the impact forces. Furthermore, higher wave heights contribute to an increase in both these parameters: impact forces and DSV. This suggests a correlation where greater wave heights induce higher downward velocities in the spudcan, which in turn incurs more substantial impact forces. The underlying thought of relating vessel dynamics with impact forces is to predict impact force unknown of information about the sea state.
In order to validate the data employed for the results of the regular wave data, a straightforward assessment can be carried out by determining the associated spudcan displacements and plotting these values against the corresponding impact forces. The interaction model between the soil and the spudcan is reliant on displacement, and the prevailing theory that guides this vertical interaction is the bearing capacity theory, see Figure 3.4 and Section 3.4.1. Creating a plot of the displacements against the impact forces should therefore reflect the underlying bearing capacity curve as shown in Figure 6.13.

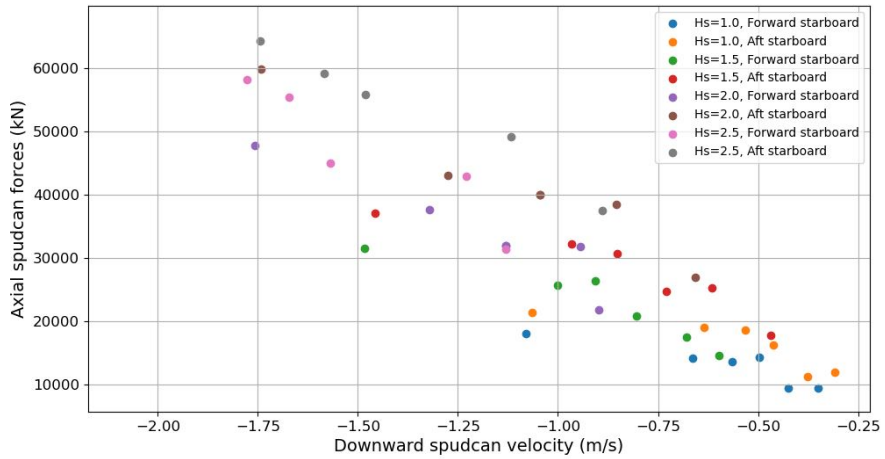

Figure 6.12: Scatter plot between maximum DSV and impact forces for varying regular waves.

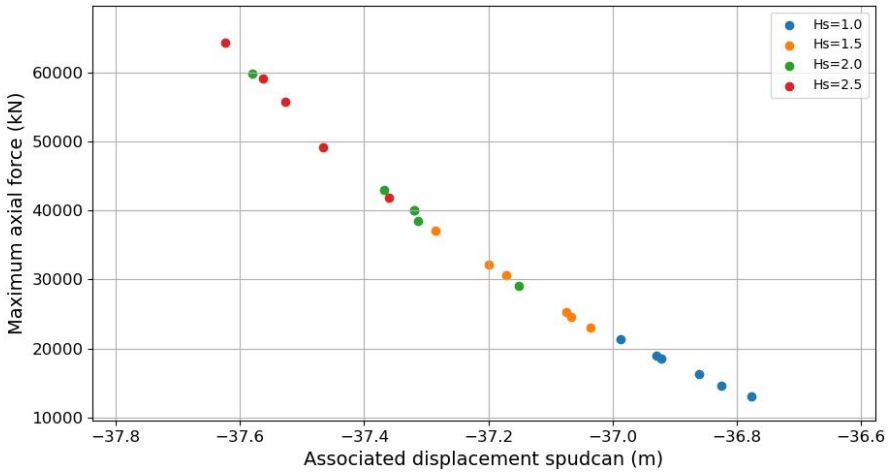

Figure 6.13: Displacement against impact force plot. The curve reflects the underlying bearing capacity theory, demonstrating the displacement-dependent nature of the soil-spudcan interaction model.

6.6.2 Varying irregular sea state

While regular sea states provide a simplified wave model that serves engineering understanding and computations, regular waves do not accurately depict the complexities of real-world sea states. Real sea state conditions are characterized by irregular waves with wide-ranging wave characteristics such as varying wave heights, periods, and occasionally, directions. These more unpredictable conditions are what vessels face in actual going-on-location operations. This section focuses on analyzing these irregular sea states.

The correlation between the downward spudcan velocity and maximum impact force, from the regular wave simulations, as discussed in Section 6.6.1, does not straightforwardly translate to the irregular wave simulations. The high level of randomness and statistical variance inherent to irregular sea states prevents the formation of such clear correlations within this research. This uncertainty, however, does not preclude us from gaining insights into the system's behavior.

In Section 6.5, key events are discussed with the aim of understanding the framework and interpreting the results based on a single simulation. To determine if these key events are valid and generally applicable numerous simulations of irregular sea states should be performed with varying environmental conditions. Two primary wave parameters are altered: significant wave height (Hs) and wave period (Tp), find in Table 6.3. One of the key challenges of studying irregular sea states is the inherent randomness of the wave. This randomness is represented in Orcaflex simulations through a pseudorandom number generator, by a variable called a "seed". Different seeds generate different sequences of random numbers, and thus different waves, even when other input variables remain the same. To fully capture the system's response to certain input parameters it's necessary to run multiple simulations, each initialized with a different seed. By analyzing the aggregate results from these batches, one could obtain a statistically significant result. Therefore for each load case, 50 seeds are performed.

The purpose of analyzing irregular sea states is to examine the impact phase, focusing on its duration and the timing of the maximum impact. The summarized findings of the different load cases are presented in Table 6.4.

Table 6.3: Varying significant wave height (Hs) and wave period (Tp) values for different load cases.

Load case (LC)	**Hs** [m]	**Tp** [s]
1	2	6
2	3	6
3	2	9
4	3	9
5	2	12
6	3	12

Table 6.4: Averaged impact times and forces for the 6 load cases, each considering 50 seeds.

Avaraged parameter	**LC 1**	**LC 2**	**LC3**	**LC 4**	**LC 5**	**LC 6**
Time of the first impact [s]	109	90	58	55	56	53
Max first impact force [kN]	0.01	0.06	1161	778	1431	6471
Impact phase duration [s]	390	402	342	389	404	425
Maximum force of whole impact phase [kN]	19e3	30e3	34e3	70e3	56e3	97e3
Duration of GoL [s]	407	453	420	534	520	612

6.6.3 Varying Hs

Two distinct significant wave heights are simulated for varying wave periods. A significant wave height (Hs) of 2 meters is often considered the limiting wave height for proceeding with the going-on-location (GoL) operation, whereas a Hs of 3 meters would most likely be a sea state for which the GoL will not proceed.

When comparing the difference in wave height while keeping the wave period constant, several observations can be made based on the overall results from the 50 seeds. As the wave height increases, the duration of the GoL, or the impact phase, becomes longer, leading to a later stage of a pinned vessel. The average duration of the impact phase is longer for higher Hs. This can be attributed to the fact that the first impact occurs earlier for higher wave heights. The increased wave height leads to larger ship dynamics, resulting in greater roll motions of the vessel. These roll motions, in turn, cause the impact phase to initiate sooner, an initial touchdown may arise even as the steady-state distance between the spudcan and the seabed is relatively large. Additionally, for higher incoming wave heights, the vessel tends to lose contact with the seabed even when it is considered to be in the pinned situation, see Figure 6.14. Furthermore, for Hs = 3, the maximum impact occurs over a more extended period, while for Hs = 2, the most significant impact is concentrated just before the pinned situation is reached. This can be observed in the scatter plots 6.15a and 6.15b, where the spread in the x-dimension is larger for plot 6.15a compared to the dense point cloud in plot 6.15b. Lastly, the maximum impact is greater for Hs = 3. This can be attributed to the increased ship dynamics, as higher waves lead to more significant roll motions of the vessel, which in turn results in greater impact forces.

6.6.4 Varying Tp

This study considers three distinct wave periods, as the wave period can have a significant influence on the roll motion of the vessel. When the wave period approaches the vessel's natural roll period, resonance occurs, leading to increased roll motion amplitudes and corresponding energy in the system. For this specific jack-up model, the natural roll period is close to 12 seconds. Consequently, a wave period of 12 seconds excites the vessel more than wave periods of 6 or 9 seconds, given the same wave height. The increase in the roll motion has a direct influence on the impact forces. The impact forces for increasing wave period shows an increase of the impact forces, for both the initial and the maximum impact force. The spread of the maximum impact forces as found for increasing wave height, where found for increasing wave period.

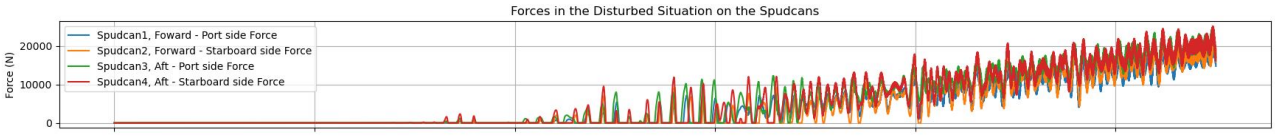

(a) Impact forces over time Hs = 2

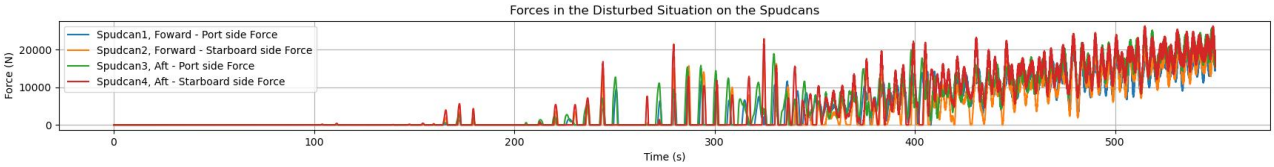

(b) Impact forces over time Hs = 3

Figure 6.14: Comparison of the impacts forces and the duration of the GoL of Hs = 2 and Hs = 3 with a constant wave period (Tp = 6).

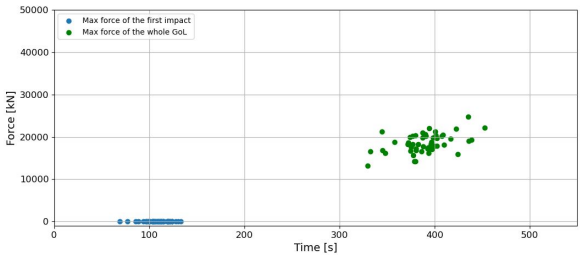

(a) Initial and maximum impact forces for Hs = 2 and Tp = 6

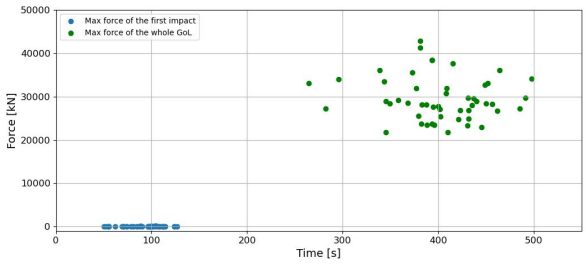

(b) Initial and maximum impact forces for Hs = 3 and Tp = 6

Figure 6.15: Comparison of initial and maximum impact forces for different wave heights (Hs) with a constant wave period (Tp = 6).

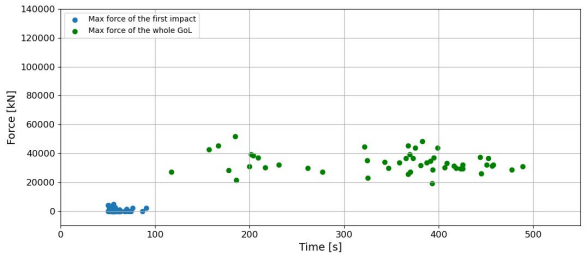

(a) Initial and maximum impact forces for Hs = 2 and Tp = 9

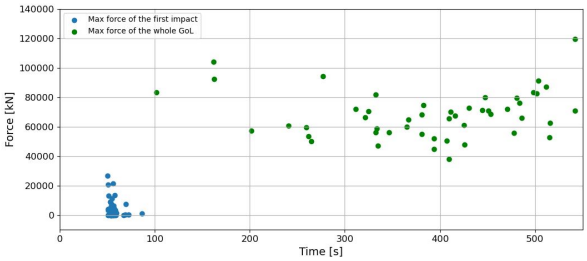

(b) Initial and maximum impact forces for Hs = 3 and Tp = 9

Figure 6.16: Comparison of initial and maximum impact forces for different wave heights (Hs) with a constant wave period (Tp = 9).

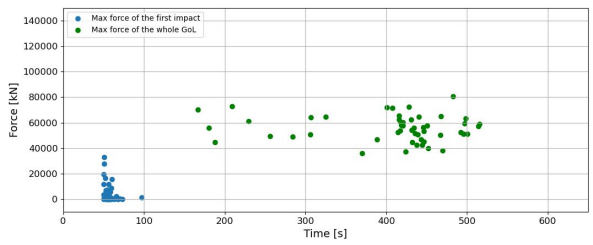

(a) Initial and maximum impact forces for Hs = 2 and Tp = 12

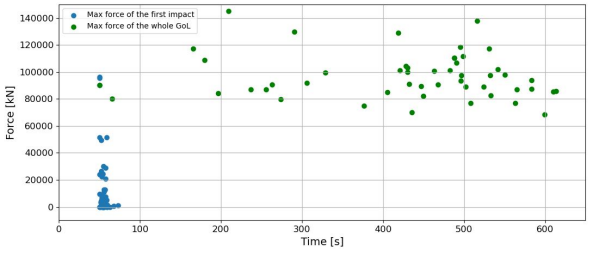

(b) Initial and maximum impact forces for Hs = 3 and Tp = 12

Figure 6.17: Comparison of initial and maximum impact forces for different wave heights (Hs) with a constant wave period (Tp = 12).

Chapter 7

Discussion & conclusions

This Chapter is a comprehensive examination of the insights and conclusions drawn from the results presented in the report. Several components are addressed separately, ensuring that the connections between outcomes from the previous Chapter, the interpretations, and the approaches and assumptions used in the framework are thoroughly understood. Consequently, this Chapter adeptly highlights the interplay between expected results, observed simulations, and the thought process behind understanding their outcomes. In the end, the main conclusions are stated.

7.1 The limitations of comprehensive framework

All models or frameworks serve as simplified representations of reality, and through the process of making assumptions and determining which phenomena are significant enough to include or exclude, predictions can be generated about real-world applications and challenges. The primary purpose of the framework is to establish a comprehensive framework that clearly differentiates the three sub-elements; structural, hydrodynamic, and soil-spudcan interaction elements. The framework is designed to allow easy modification or removal of various components within each elements. Two different framework implementations are performed - one using Python and the other using OrcaFlex. The performance and the limitations of the framework will be examined and discussed by looking at the different components of each of the two implementations.

7.1.1 Implementaion using Python

The custom-developed model, detailed in Chapter 4, utilizes an integrated Python solver that incorporates the three sub-elements: structural, hydrodynamic, and soil-spudcan interaction models. The implementation of the framework entirely within the Python environment marked the first phase of this thesis, with each component being developed from scratch. The knowledge gained from the engineering and development processes laid the groundwork for all subsequent tasks and implementations. As the entire code was developed in-house, without the use of pre-existing snippets, there are several assumptions, simplifications, and limitations associated with this implementation.
This framework implementation, i.e. 2D-model, represents a jack-up vessel featuring two spudcans in a 2D plane, with 9 degrees of freedom (DOFs). The three objects, the hull and two spudcans, all have three DOFs. The main limitation of this framework is that it operates within a 2D plane, which is a significant simplification compared to real-world scenarios. Limiting the simulation to two dimensions could result in the loss of crucial information and may not accurately represent the actual scenario. While adding an additional dimension for 3D simulations could enhance the accuracy and realism of results, it is important to note that it significantly increases the complexity of the framework implementation compared to the 2D version. The 2D constraint should always be considered when utilizing and interpreting the results obtained from this framework.
The primary emphasis in the developed framework lies in the soil-spudcan interaction model. This unique element is an integral part of the framework and is indispensable to its functioning. A substantial part of the research was dedicated to the soil-structure interaction component, making it the cornerstone of this research. Therefore, the 2D model substantially simplifies the hydrodynamic and structural components. These components are adapted and created primarily to make the model function for simulating the going-on-location process.

The vessel's hull is depicted as a rectangular barge, and the hydrodynamic stiffnesses are computed accordingly.

While this simplification aids computational efficiency, it may not fully capture the actual hydrodynamics at play, considering the unique design of jack-up vessels. Moreover, velocity-dependent damping coefficients are not utilized, as they originate from complex hydrodynamic analyses. Not including these could limit the model's ability to accurately predict the response of the vessel to complex wave actions. However, these comprehensive hydrodynamic evaluations extend beyond the focus of this thesis.

The structural representation of the jack-up vessel in the model consists of three rigid bodies interconnected by beam-modeled legs. While this setup offers a reasonable approximation of the vessel's structure, it can be enhanced for increased accuracy. Specifically, introducing more nodes could help reduce element sizes, thereby providing a more refined and precise representation of the vessel's structure. Additionally, structural limits within a jacking system are neither defined nor considered.

In the current simulation setup, actual incoming waves cannot be accurately simulated due to the simplifications in the hydrodynamic component. The 2D model is effectively equipped to handle initial value problems related to displacement, velocity, or externally applied force. However, it lacks to account for velocity-dependent coefficients, such as damping. This is a notable limitation as it impacts the model's capacity to accurately simulate the vessel's response to dynamic sea states. Figures 4.7 and 4.8 display two preliminary simulations, the second of which includes damping effects.

The soil-spudcan interaction component serves as the keystone of the framework and is incorporated in every framework implementation. Any technical constraints associated with the soil-spudcan interaction model will be addressed in Section 7.1.2. The primary limitations identified in the 2D model primarily concern the structural and hydrodynamic aspects. Given these constraints, the research progressed by incorporating commercial simulation software, OrcaFlex, to enhance both structural and hydrodynamic components.

7.1.2 Simulation model using OrcaFlex

The growing complexity and need for more detailed analysis of hydrodynamic and structural elements necessitated the use of commercial software. OrcaFlex was employed to carry out time-domain simulations to assess impact forces during the GoL process. Using OrcaFlex for system analysis requires creating a mathematical representation of the real-world system. This model includes chosen environmental conditions and a selected number of objects symbolizing the jack-up vessel. The environment dictates the wave excitation, while the objects respond accordingly. The three distinct components within the simulation model will be explored, and the simulation outcomes will be discussed.

Soil-spudcan interaction element

It's important to mention that the soil-spudcan interaction component is incorporated into both the 2D model and the OrcaFlex implementation. So the discussion below considers both the simulation implementations. The key principle of the soil-spudcan interaction model is its dependence on displacement, whereby it returns a soil force (impact force) for a specific spudcan displacement. This crucial characteristic of displacement-dependency not only adds flexibility but also facilitates the integration of other displacement-dependent soil models in the future. The soil-spudcan interaction model distinctly models the vertical and horizontal soil resistance components due to their individual characteristics. Both the vertical and horizontal soil resistance models adopt the fundamental principles of elasto-plastic behavior.

The vertical impact forces acting on the spudcans are simulated using the bearing capacity theory, a widely accepted method employed in various soil-spudcan studies. However, these studies primarily investigate preloading, as the loads on the spudcan gradually increase. Impact forces typically feature short periods with rapidly escalating high forces. The rate of loading can significantly influence soil behavior. The bearing capacity theory does not incorporate the effects of loading rate, which could be found to be a more important factor.
Secondly, the bearing capacity theory is used only for the soil resistance in virgin soil. However, the complex circular motion of the spudcan just above and within the soil, as illustrated in Figure 3.1, results in rapid loading and reloading of the soil. The soil resistance during unloading and reloading is modeled as linearly elastic. The β coefficient influences the ratio between plastic and elastic soil deformation. Determining the unloading/reloading coefficient β is challenging and introduces a significant degree of uncertainty. In order to accurately determine the β coefficient, detailed soil investigations, and laboratory studies are required.
In a study by Randolph and Quiggin (2009), a framework was developed for a nonlinear hysteretic seabed model in the context of catenary pipeline contact. This model incorporated resistance during uplift from the seabed,

which resulted from the pressure difference above and below the catenary. The geometry of the spudcan suggests that under pressure could develop below the spudcan which may be relevant during frequent uplift following an impact, particularly as the impact and unloading are considered to be rapid. This could potentially make it necessary to integrate suction resistance into the analysis.

The horizontal soil resistance is dependent on both elastic and plastic regions. The yield surface, which separates these regions, translates along the horizontal axis and is considered constant. This implies a changing stiffness coefficient within the elastic region. An alternative approach would involve maintaining a constant elastic soil stiffness while allowing the elastic region to vary. In addition, the spudcan is allowed to displace within the whole horizontal plane therefore combining the x and y components in the horizontal plane would be more intuitive. Within the soil-spudcan interaction model, the x and y components in the horizontal plane are treated independently. Combining the x and y components will incorporate a translating locus-like yield surface within the horizontal plane. This soil behavior is described by Houlsby and Puzrin (2006) and indicates kinematic hardening of the soil.

Structural element

In the 2D framework, the structural component is deemed limited. For the OrcaFlex implementation, it doesn't use the pre-established stiffness matrix from Section 4.2.4. Instead, OrcaFlex creates its own stiffness matrix, which includes all the necessary properties and components. The hull is depicted as a rigid body with specified motion. This includes incorporating response amplitude operators (RAOs) for each of its six degrees of freedom. The model features four spudcans, each represented as a 6D buoy. They are connected to the hull via leg components, which are depicted as line objects. Each of these line objects is subdivided into segments, each segment is 5 meters in length. These segments represent portions of the line, with properties such as mass, buoyancy, and drag consolidated within each one. While the structural modeling approach utilized in OrcaFlex is more sophisticated than the one applied in the 2D model, it's worth discussing potential limitations.
In particular, the leg-hull interface might be the constraining structural factor during the GoL, as the impact forces on the spudcan increase. Sections 2.2 and 2.5 provide an overview of the structural limitations inherent in a jacking system and the leg-hull interface. Within the framework, the leg-hull connection is assumed to be fixed, and the soil impacts are not absorbed by the hull or jacking system. A study conducted by Zheng et al. (2015) investigates the load distribution within the leg-hull interface. In this paper, the characteristics of hull-leg interaction are explored, and a simplified method using gap elements is proposed. Incorporating a more detailed structural component that considers the leg-hull interface could offer additional insights into determining the limiting factor during the going-on-location process. Secondly, the model doesn't take into account possible leg failures like buckling. Given that the legs are subjected to substantial forces during the GoL process, such failures could indeed be a limiting factor for the system's performance. Considering these failure modes in the model could thus provide a more comprehensive understanding of the system's structural limits.

Hydrodynamic element

Although the preliminary 2D model adopts a significantly simplified representation of the hydrodynamic component, as a 2D barge on a water plane, the framework set up in OrcaFlex offers a more refined approach, including a comprehensive analysis of a real jack-up vessel with all the hydrodynamic coefficients. The primary motivation for integrating the framework into OrcaFlex was to enhance the hydrodynamic element of the model. Nevertheless, it's crucial to note that the hydrodynamic model in the current setup does not take into account factors such as wind and currents. While their relevance during the GoL process may be debatable, for a more complete and realistic model, incorporating these effects could be considered in future studies.

7.1.3 Interpretation of simulations results and conclusions

First, the simulation scenarios concerning the validation of the boundary stages -free-floating and pinned- are evaluated, followed by a series of simulations that were conducted to evaluate the sensitivity of the modeling framework and outcomes to variations in input wave parameters.
An energy-based analysis was established to validate the free-floating boundary stage of the going-on-location. It should be noted that the energy plots presented in this thesis only represent the vessel's roll motion energy and do not account for other energy components, related to the pitch and heave motion. Since the jack-up is primarily subjected to beam waves, it will predominantly exhibit roll motion. However, the disregarded heave

motions can still have an impact on the system's total energy. For a more comprehensive understanding of the system's energy balance, it would be necessary to include the potential and kinetic energy contributions from all relevant degrees of freedom. This would involve calculating the potential and kinetic energies for each motion component and summing them up to obtain the total energy of the system. However, the roll energy-based approach provides a clear demonstration of the correct modeling of the free-floating stage in the disturbed vessel simulation. As a result, we can validate the free-floating boundary stage of the going-on-location in the disturbed vessel scenario. The scenario featuring the disturbed vessel encompasses all stages of the going-on-location procedure in accordance with the established framework.
The scenario involving the pinned vessel is proposed as a means to validate the pinned boundary conditions at the end of the going-on-location. As the disturbed vessel scenario transitions into the pinned stage, it's observed that the forces applied on the spudcans follow a similar path as the pinned vessel scenario, as depicted in Figure 6.8. This outcome confirms the validation of the pinned phase at the end of the going-on-location. However, the values of the axial forces do not align due to the continuous increase in axial forces in the disturbed scenario, a result of the ongoing descent of the spudcans. While for the pinned vessel scenario no leg lowering is applied, as the spudcans are constrained to the seabed.

The regular wave simulations were performed to establish potential correlations between the vessel dynamics and the forces during spudcan impacts. Such correlations could serve as a basis for informed decision-making during the vessel's transit to location. With the methodology proposed here, the emphasis shifts from a sole dependence on external factors such as wave height, towards an understanding of how the vessel's own dynamics affect the forces it encounters. Consequently, even under circumstances where the wave height surpasses conventional safety thresholds, operations might still proceed if it's determined that the vessel's dynamics remain within safe parameters to endure the subsequent impact forces.
Interestingly, a clear correlation was observed between the downward spudcan velocity (DSV) and the impact forces. It was noted that an increase in the DSV correspondingly increased the impact forces.
However, the correlation was made using the maximum DSV of the disturbed vessel scenario, where the interaction between the soil and the spudcan is taken into account. It may be more relevant to consider the dynamics of the free-floating vessel for this correlation, as opposed to the dynamics of the vessel under disturbance. This emphasis is mainly due to the capability of predicting the free-floating vessel dynamics before installation, thereby making it an important consideration for on-board decision-making regarding the proceeding of the GoL process. The correlation between the free-floating DSV and the corresponding impact forces of the vessel in the undisturbed scenario was not as evident as illustrated in Figure 6.12. Often, the maximum DSV in the disturbed scenario is found to be greater than the DSV in a free-floating state, see Figure 7.1. It's worth noting that the soil-structure interaction could not only dampen the system but also potentially excite the vessel dynamics. However, no specific pattern was identified for when this dynamic excitation occurs, as it appears randomly for typical wave height (Hs) and peak period (Tp) values. Hence, the relationship between the (DSV) of the undisturbed (free-floating) vessel and the maximum impact forces represents a promising topic for future research. Moreover, it's important to note that this correlation hasn't yet been observed in the simulations of

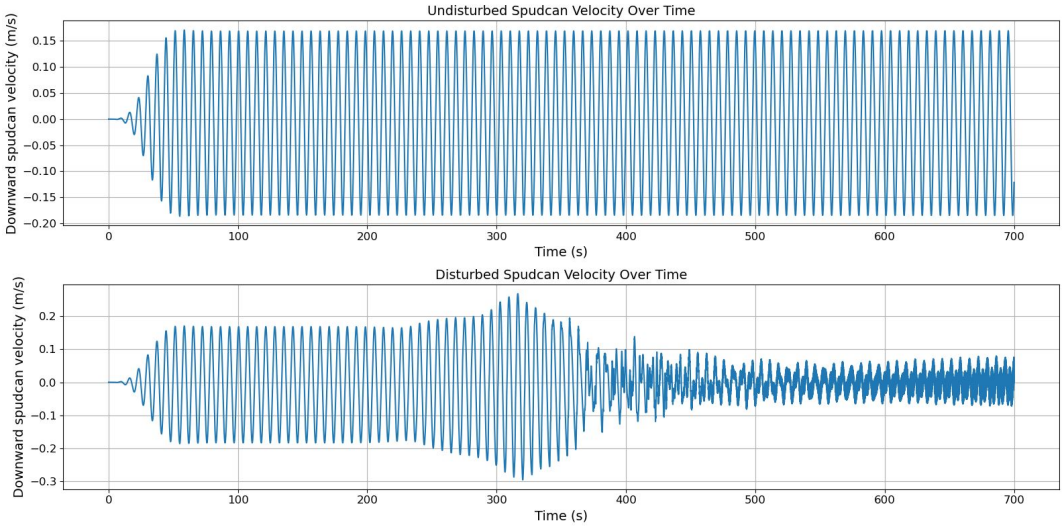

Figure 7.1: The upper graph illustrates the downward spudcan velocity for the undisturbed vessel, while the lower one depicts the same parameter over time for the disturbed vessel.

irregular sea states. The substantial statistical element inherent in irregular wave analyses should be properly considered if a similar correlation is to be established in irregular sea states.

When varying the parameters of irregular waves, the investigation focuses on the magnitude and occurrence of the maximum impact, as well as the duration of the going-on-location process. It was found that the wave height has a direct influence on the magnitude of the highest impact and also increases the variability of its occurrence. As for all 6 load cases for irregular sea states, the maximum impact force is considered to take place at the end of the impact, just prior to the pinned stage. The (maximum) impact phase appears to be more closely related to the pinned system than the free-floating system.
Additionally, when increasing the wave height and setting the wave period close to the natural roll period of the jack-up vessel, the maximum impact appears to have greater variability compared to smaller wave heights. For lower wave heights, the impacts gradually increase to their maximum just before the pinned situation is established. The occurrence of the maximum impact for higher wave heights seems to be a statistical variable, as the high impacts occur when all the significant parameters, such as wave height, position relative to the seabed, etc., align for a specific moment during the going-on-location process.

The wave direction remains constant throughout all analyses, for both regular and irregular waves. The jack-up modal analysis revealed a strong coupling between pitch and heave motions. No distinct rigid body modes were found for these two degrees of freedom, which suggests that the total energy approach should be applied which introduces considerable complexity. When considering beam waves, the aft-starboard spudcan is consistently identified as the limiting spudcan, experiencing the maximum impact.

The primary aim of this research is to enhance the workability of jack-up vessels. However, drawing a clear conclusion on this objective is challenging. This is due to the need for comparison between existing operational data for proceeding the going-on-location process and vessel motions connected to limiting impact forces retrieved from this study. Since this research does not address any limiting factors, it is difficult to provide a concrete conclusion on the improvement of workability for jack-up vessels during the going-on-location process. Identifying the limiting factors (such as certain magnitude as impact force) for the going-on-location process is recommended for future studies, as further detailed in Chapter 8.

7.2 Conclusion

To summarize, the following section addresses the three sub-questions, followed by an overarching conclusion on the key findings of this study.

1. A comprehensive framework for modeling the going-on-location phase has been developed, significantly contributing to the understanding of jack-up vessels during this operation. In jack-up models adhering to the framework, the jack-up vessel is represented as a multi-body structure, in contrast to the conventional rigid-body representation often employed. By combining hydrodynamic, structural, and soil-spudcan interaction elements, the framework offers a more accurate and detailed representation of the going-on-location process, with a focus on the impact phase. With potentially enabling better decision-making and increased workability for jack-up vessels.

2. The dynamic soil-spudcan interaction has been improved by incorporating an elasto-plastic soil behavior model with memory, which includes aspects of kinematic hardening. This enhancement allows for more accurate and complex descriptions of the soil resistance to spudcan vertical penetration and lateral displacement, leading to a better understanding of the interaction between the spudcan and seabed during the going-on-location process.

3. For regular waves, a correlation was established between the downward spudcan velocitey (DSV) and the impact forces on the spudcan. This finding strongly indicates that the vessel dynamics relate to the magnitude of impact forces. Hence, the downward velocity of the spudcan emerges as a potential parameter that could be correlated with the maximum impact forces exerted on the spudcans. In the case of irregular waves, parameters such as wave height and wave period have been identified as influencing factors on the variability of the maximum impact between the spudcan and the seabed. Furthermore, an increase in these parameters also determines an increase in the duration of the going-on-location process.

Overall the current state-of-the-art going-on-location modeling from the literature review has been identified to rely on simplified assumptions, resulting in conservatism in the analysis of the impact phase during the

going-on-location process. This thesis has successfully pinpointed and addressed this conservatism, enhancing the going-on-location analysis, particularly in the area of soil-spudcan interaction. By incorporating an elasto-plastic soil behavior model with a memory factor, the soil-spudcan interaction element has been significantly improved. Two simulation models have been developed around this enhancement, integrating hydromechanical and structural submodel elements, one in Python and the second within the OrcaFlex environment.
The performance of the simulation model in OrcaFlex, adhering to the comprehensive framework, is found to be accurate for analyzing and simulating the going-on-location. Three distinct simulation scenarios are examined: an undisturbed vessel, a disturbed vessel, and a pinned system. The model adhering to the framework demonstrates coherence in undisturbed vessel scenarios with free-floating simulations and in pinned vessel scenarios, i.e. the boundary stages. The impact phase is situated between these two stages, and therefore the comprehensive framework should effectively represent simulation for the impact phase. The framework offers a flexible and case-specific configuration, which allows for plug-and-play. The framework is therefore suited to perform workability studies for specific jack-up vessels under variable environmental conditions.
In addition, the findings from the regular wave simulations suggest that the dynamics of the vessel significantly influence the magnitude of impact forces. This causal relationship implies that vessels' dynamics directly affect the magnitude of the impact forces. On the other hand, in the case of irregular waves, a clear correlation similar to the one found in regular waves is yet to be identified. Future work should aim to validate these findings across a wider range of sea states and vessel parameters to further refine the developed model and thereby enhance decision-making in real-world scenarios.

Chapter 8

Recommendations

While the proposed comprehensive framework is expected to provide valuable and accurate insights into the going-on-location proces of jack-up vessels, several recommendations for further research can be identified. By addressing these recommendations for further research, a more thorough understanding of the impact phase during going on location of jack-up vessels can be achieved, ultimately leading to improved decision-making processes and increase workability. The future research suggestion can be divided into two categories; improvements to the soil-spudcan model and general recommendations and future studies based on the research.

8.1 Soil-spudcan model related recommendations

Combining the x and y components in the horizontal plane

As an enhancement to the soil-spudcan interaction model, it is recommended to combine the x and y components in the horizontal plane. Currently, two components are evaluated separately, joining the x and y components in the horizontal plane will lead to a more realistic horizontal soil behavior. The displacement of the spudcan in the horizontal plane is always a vector comprised of the x and y-components, instead of being perfectly along the x and y directions.

Incorperation of more advanced constitutive soil models

The current research incorporates elasto-plastic soil behavior, which can be seen as state-of-the-art soil behavior during the impact phase of the going-on-location. Future studies could explore more advanced constitutive soil models. Continuum soil modeling can provide a more accurate prediction of the behavior of the soil under instantaneous loads. An investigation into the most suitable constitutive soil models for simulating impact loads should be conducted. The findings should be tested to be incorporated into the model framework or adapted to meet the framework's requirements.

Real seabed characteristics

The soil-spudcan model assumes a homogeneous, sandy, and perfectly horizontal seabed. However, in reality, seabeds often exhibit variations composition, layering, and slope or even have old footprint history. These factors can significantly impact the interaction between the spudcan and the seabed. To enhance the model's applicability, it is recommended to incorporate these real-world seabed characteristics.

Employement of kinematic hardening laws

The soil response exhibits characteristics of kinematic hardening. In such analyses, the material's yield stress surface is updated throughout the simulation. However, it is recommended to pay closer attention to the kinematic hardening aspects and the governing rules for the establishment and translation function of the yield surface. This would enhance the accuracy and comprehensiveness of the soil-spudcan interaction model.

Suction resistance during unloading

It is recommended to integrate suction resistance during the unloading phase into the soil-spudcan interaction model. In a study conducted by Randolph and Quiggin (2009), a framework for a nonlinear hysteretic seabed

model for catenary pipeline contact was established, which incorporated suction resistance during uplift from the seabed. Implementing similar considerations in the soil-spudcan interaction model would lead to a more accurate representation of the forces experienced by the spudcan during it unloading mode.

8.2 General recommendations and future studies

After completing the current research, general recommendations can be considered for future work. First, exploring diverse soil types and conditions. The present study primarily focuses on various types of sandy soils, which are assumed to exhibit high stiffness and result in increased impact forces. However, other soil types, such as rocky seabeds and consolidated clays, may also generate significant impact forces. Incorporating a wider range of soil types would necessitate a new approach to soil-structure interaction. For a more comprehensive understanding of the system behavior during the going-on-location, future research should delve deeper into the effects of different soil types on the soil-structure interaction and the overall performance of jack-up vessels.

In line with the general recommendations for future work, it is essential to incorporate the elements discussed in Section 8.1. The literature review and the outcomes from the simulation model underscore the significance and the novelty of soil-spudcan interaction modeling. As this thesis potentially establishes a new state-of-the-art framework for analyzing impact forces between the spudcan and seabed, continuous improvement and adaptation to the soil-spudcan model will contribute to a more profound understanding and enhanced workability of jack-up vessels.

In this thesis, no in-depth investigation has been conducted on structural limitations. The developed framework mainly emphasizes determining impact loads but does not evaluate the limiting loads on the jacking system, spudcan, or legs of the jack-up vessel. Additionally, other structural factors, such as fatigue and fracture, especially in the spudcan where welds are prevalent, could considerably influence the structure's lifespan. Incorporating these structural limitations would contribute to a broader applicability of the framework. Additionally, by establishing limitations in the form of bending moments or impact forces, a more precise adaptation and conclusion on the workability of jack-up vessels could be achieved.

To gain a more comprehensive understanding of the underlying physics and correlations between various parameters, it is recommended to carry out an extensive simulation program and sensitivity analysis. The wide range of input parameters requires a thorough sensitivity study, which would encompass simulations for numerous seeds beyond the 50 seeds considered in the current research for irregular sea states. Conducting this large-scale sensitivity analysis suggest a statistical approach to data analysis, providing valuable insights into the relationships between different parameters and their impact on the overall system behavior.

The comprehensive framework presented in this thesis is primarily based on the understanding of jack-up vessel physics and an extensive review of the existing literature and expertise. Consequently, the conclusions drawn from the simulation model and its results are based on theoretical models and approaches. To enhance understanding and validation, it is advisable to monitor and investigate real jack-up vessel behavior during the going-on-location process. Experimental validation could be essential. Collaborating with industry-leading companies in the offshore market for experimental validation or research with hands-on jack-up engineers could significantly strengthen the findings of this study. Moreover, such collaborations may reveal alternative modeling approaches that could be incorporated, further enhancing the practical applicability of this research.

To conclude, the primary objective of this thesis is to enhance the workability of jack-up vessels, which may face limitations during the going-on-location process. A potential direction for future research could involve developing practical guidelines and recommendations for on-board decision-making. A promising correlation was observed in regular waves between maximum downward spudcan velocity (DSV) and impact forces, suggesting a potential rule of thumb that could be broadly applicable to various going-on-location circumstances. The exploration of this correlation should extend to diverse types of jack-up vessels and a wider array of sea state parameters, which should include the movements of free-floating vessels as well. By building on the insights gained from this thesis, further investigation could explore how the developed tool can effectively contribute to real-time, on-board decision-making in practical scenarios.

Appendix A

Stiffness matrix derivation

The stiffness matrix is obtained using the displacement method, where all the 9 degrees of freedom (DOFs) are positively displaced, and the resulting forces and moments are analyzed. The displacement method involves systematically displacing each DOF and evaluating the corresponding change in forces and moments. By examining these changes, the relationship between the vessel's and spudcans' motion and the internal forces and moments can be established. This information is then used to construct the stiffness matrix, which represents the linear relationship between the forces and moments acting on the vessel and the vessel's displacement in each DOF. This appendix provides a detailed description and visualization of the displacement process for each DOF in the system. It also presents the resulting forces and moments that arise from these displacements.

Due to symmetry considerations, the forces and moments derived for the left spudcan are the same as those for the right spudcan. To apply the displacement method, it is crucial to maintain a consistent sign convention for both force and moment balance. This consistency ensures the accuracy and coherence of the results obtained through the displacement method. Additionally, the standard deflection formulas found in Section 4.2.3 play an essential role in the analysis.

Horizontal displacement of the hull (x_1)

A positive horizontal displacement of the hull generates shear forces and bending moments in the hull-leg connection, leading to a transfer of these forces to the leg-spudcan connection. It is important to note that upon displacement of the hull, all other masses within the system maintain their original position, see Figure A.1. Standard deflection formulas in equation 4.4 should be used to find the internal moments and forces. The

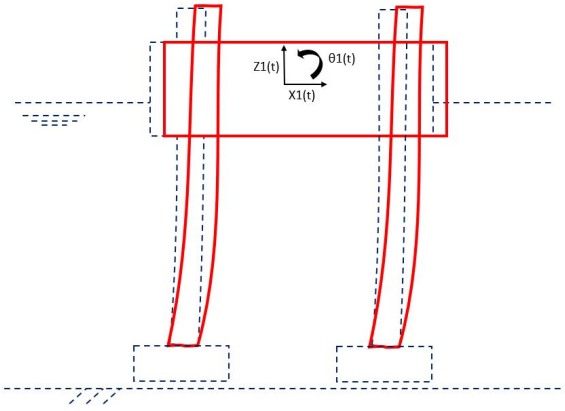

Figure A.1: A positive horizontal displacement of the hull, where x_1 represents the displacement in the horizontal direction.

moments and shear forces can have different signs however, the magnitude of the moment and forces couples are the same and shown in equation 4.6 and in the summation below.

- Negative shear force, V_1, from the leg on the hull.
- Positive shear force, V_2, from the hull on the leg.

- Positive bending moment, M_1, from the leg on the hull.
- Negative bending moment, M_2, from the hull on the leg.

The same horizontal positive displacement of the hull create force and moment couples at the leg-spudcan connection.

- Positive shear force, V_1, from the leg on the spudcan.
- Negative shear force, V_2, from the spudcan on the leg.
- Negative bending moment, M_1, from the leg on the spudcan.
- Positive bending moment, M_2, from the spudcan on the leg.

A check whether the force balance is in equilibrium, it should satisfy the following equation $\frac{M_1 * M_2}{l}$. Furthermore, displacement of the hull along the x-axis does not generate forces along the z-axis.

Vertical displacement of the hull (z_1)

A positive vertical displacement of the hull generates axial forces in the legs, see Figure A.2. The axial force couple is in the opposite direction and has the same magnitude given with equation 4.4. At the hull-leg connection, there is a negative force from the leg on the hull and a positive axial force from the hull on the leg. At the leg-spudcan connection, there is a positive force from the leg on the spudcan and a negative axial force from the spudcan on the leg. No shear forces or bending moments are generated for a hull displacement along the z-axis.

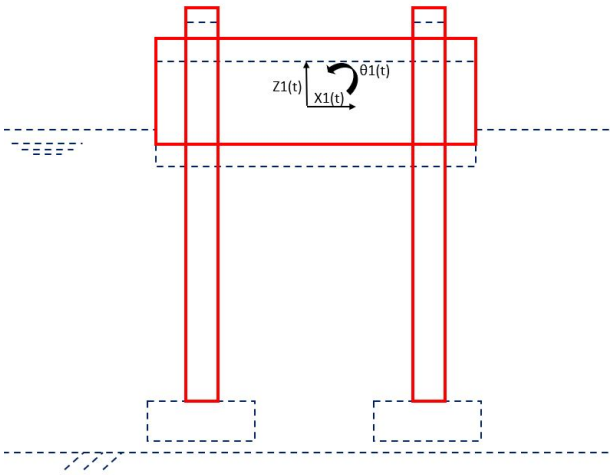

Figure A.2: A positive vertical displacement of the hull, where z_1 represents the displacement in the vertical direction.

Rotation of the hull (θ_1)

A positive rotation of the hull generates shear forces and bending moments in the hull-leg connection, see Figure A.3. Standard deflection formulas in equation 4.5 should be used to find the internal moments and forces. Rewriting the bending moments and shear forces in terms of θ the equations become as A.2.

$$T = \frac{4EI}{\ell}\theta \quad ; M_1 = \frac{4EI}{\ell}\theta; \quad V_1 = V_2 = \frac{6EI}{\ell^2}\theta \tag{A.1}$$

At the hull-leg interface the bending moments and forces are:

- Negative shear force, V_1, from the leg on the hull.
- Positive shear force, V_2, from the hull on the leg.
- Negative bending moment, M_1, from the leg on the hull.

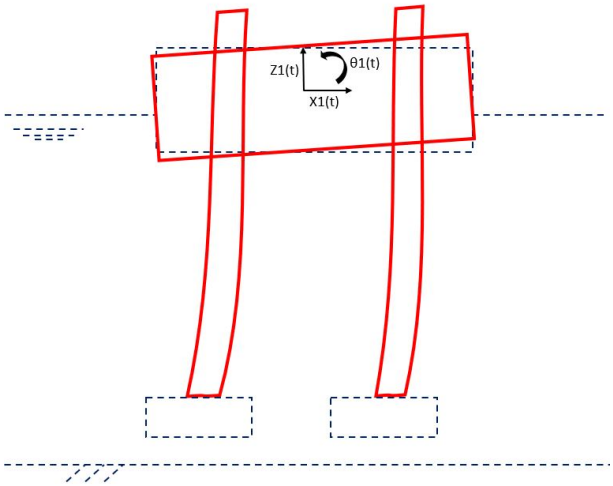

Figure A.3: A positive rotation of the hull, where θ_1 represents the rotation in positive direction.

- Positive bending moment, T, from the hull on the leg.
- Positive moment from the axial force on the hull $a\frac{AE}{\ell}$. Where a is the horizontal offset from the hulls' COG to the hull-leg connection. For the right spudcan, a positive moment is indicated, while for the left spudcan, a negative sign will be indicated.

At the leg-spudcan interface the bending moments and shear forces are:

- Positive shear force, V_1, from the leg on the spudcan.
- Negative shear force, V_2, from the spudcan on the leg.
- Negative bending moment, M_1, from the leg on the spudcan.
- Positive bending moment, M_1, from the spudcan on the leg.
- Negative moment from the axial force on the hull $a\frac{AE}{\ell}$. Where a is the horizontal offset from the hulls' COG to the hull-leg connection. For the right spudcan, a negative moment is indicated, while for the left spudcan, a positive sign will be indicated.

Horizontal spudcan displacement (x_3)

A positive horizontal displacement of the spudcan generates shear forces and bending moments in the hull-leg connection and the leg-spudcan interface, see Figure A.4. The forces and moments on the hull due to the displacement of the spudcan can be derived from the fact that the stiffness matrix is symmetrical, no derivation from the beam theory is necessary. At the leg-spudcan interface, the bending moments and shear forces can be established using standard deflection formulas in equation 4.4.

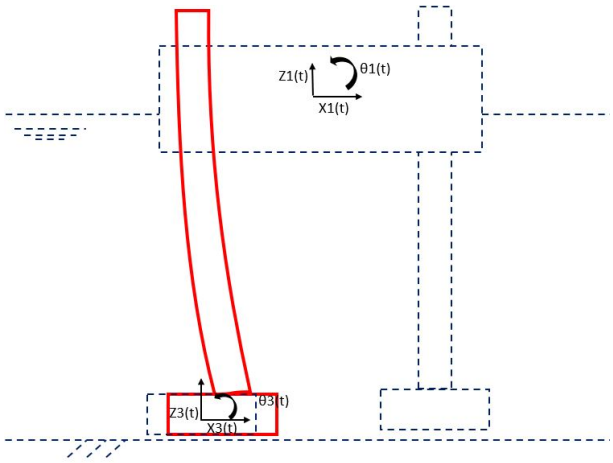

Figure A.4: A positive horizontal displacement of the spudcan, where x_3 represents the displacement in the horizontal direction.

- Negative shear force, V_1, from the leg on the spudcan.
- Positive bending moment, M_1, from the leg on the spudcan.

Vertical spudcan displacement (z_3)

A positive vertical displacement of the spudcan generates axial forces in the leg, see figure A.5. The forces and moments generated on the hull due to the displacement of the spudcan can be derived from the fact that the stiffness matrix is symmetrical, no derivation from the beam theory is necessary. The force as a result of a vertical displacement of one of the spudcans is the negative axial force from the leg on the spudcan, derived from equation 4.4. Since the two spudcan are not connected with a beam there are no direct force or moment transfers between the two bodies.

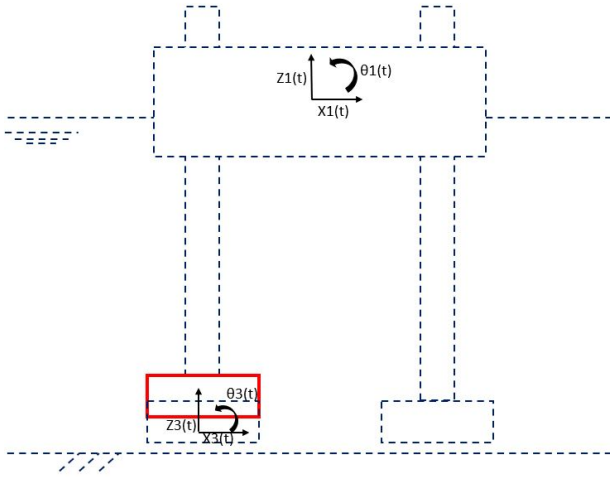

Figure A.5: A positive vertical displacement of the spudcan, where z_3 represents the displacement in the vertical direction.

Rotation of the spudcan (θ_3)

A positive rotation of the spucan results in shear forces and bending moments in leg-spudcan and hull-leg connection, see Figure A.6. Due to the symmetry of the stiffness matrix, only the shear force and bending moment on the leg-spudcan connection should be derived. Rewriting the bending moments and shear forces in terms of θ the equations become as A.2.

$$T = \frac{4EI}{\ell}\theta \quad ; M_1 = \frac{4EI}{\ell}\theta; \quad V_1 = V_2 = \frac{6EI}{\ell^2}\theta \tag{A.2}$$

At the leg-spudcan interface, the bending moments and shear forces are:

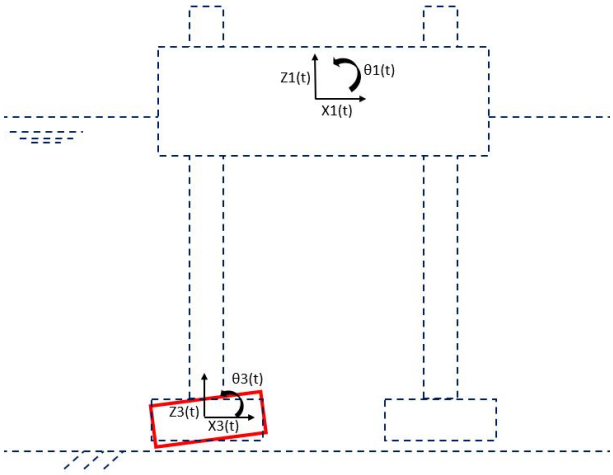

Figure A.6: A positive rotation of the hull, where θ_3 represents the rotation in positive direction.

- Positive shear force, V_1, from the leg on the spudcan.
- Negative bending moment, M_1, from the leg on the spudcan.

Appendix B

Modal analysis

A modal analysis provides insights into the natural periods and mode shapes of a dynamic system. The natural period of a structure refers to the time it takes for the structure to oscillate with minimal damping when subjected to an external force. Knowledge of these periods or frequencies is essential for predicting a structure's response to different types of loads and informing design decisions. Moreover, modal analysis reveals the mode shapes of a structure, which represent the vibrational patterns at each of its natural frequencies. These mode shapes illustrate the direction and relative amplitudes of each degree of freedom. They provide valuable information about the dynamic behavior of the structure, which can help identify stress points that may require attention. In a modal analysis, the eigenvalues and eigenvectors of the stiffness matrix and mass matrix are utilized to calculate the structure's natural frequencies (eigenvalues) and mode shapes (eigenvectors). The eigenvalues correspond to the system's stiffness in various directions, while the eigenvectors represent the associated displacement patterns. The stiffness matrix is a symmetric matrix, ensuring that its eigenvalues are always real. Furthermore, the eigenvalues are positive since the matrix is positive definite, meaning that the elements of the main diagonal are all greater than zero. Eigenvalues of the stiffness matrix are the values that satisfy the equation:

$$(K - \lambda M)x = 0 \tag{B.1}$$

K = stiffness matrix [NxN]
x = eigenvector [Nx1]
N = mass matrix [NxN]
λ = eigenvalue

Eigenvalues are paired with unique eigenvectors, where the magnitude of an eigenvalue signifies the system's stiffness in the direction defined by the corresponding eigenvector. A high eigenvalue suggests a high resistance to deformation in that direction, indicating that the system is relatively stiff in that particular direction. The natural period is associated with the eigenvalue and equals 2π multiplied by the square root of the inverse of the eigenvalue, i.e., $T_n = 2/\sqrt{(\lambda)}$. Eigenvectors depict the direction and magnitude of the displacement for each degree of freedom in the system, which results in deformation in the respective direction. Typically, eigenvectors are normalized so that their maximum entry is 1. This normalization ensures that eigenvectors have a magnitude of 1, making them easier to compare and interpret. As a result, the mode shapes of a structure are derived from the eigenvectors of the stiffness matrix. Mode shapes associated with zero eigenvalues represent the motion of the structure as a whole, without deformation or change in shape. These modes are known as rigid-body modes.

Within the context of a 2D, 9DOF jack-up representation, there will be nine natural periods and nine mode shapes, figure B.1. The first three mode shapes correspond to the rigid-body modes of a 2D vessel free-floating in water, which include surge, heave, and pitch. Rigid-body modes refer to the global movements of a structure without any internal deformation. In other words, the structure moves as a single, undistorted object. For a 2D vessel free-floating in water, there are three rigid-body modes: pitch, heave, and surge.

- Pitch: This mode signifies the rotational motion of the vessel about its center of mass in the xz-plane. In this mode, the structure rotates around an axis perpendicular to the plane without distorting its shape. The pitch mode corresponds to mode 1 in figure B.1.
- Surge: This mode represents the linear, horizontal motion of the vessel along the x-axis. The entire structure moves back and forth in the horizontal plane without any internal deformation. The surge mode corresponds to mode 2 in figure B.1.

- Heave: This mode corresponds to the linear, vertical motion of the vessel along the y-axis. In this case, the entire structure moves up and down in the vertical plane, without any internal deformation. The heave mode corresponds to mode 3 in figure B.1.

Coupled modes, on the other hand, involve simultaneous motion in multiple degrees of freedom. These modes result from the interaction of different components of the structure, and they exhibit both global and local deformation. Coupled modes are more complex than rigid-body modes, as they involve the interplay of multiple forces and displacements acting on the system. The natural periods of rigid-body modes are typically larger than those of the coupled mode shapes. In rigid-body modes, the structure moves as a single, undistorted object, and the energy is distributed across the entire structure without any internal deformation. This leads to a lower overall stiffness in these modes, which, in turn, results in larger natural periods.

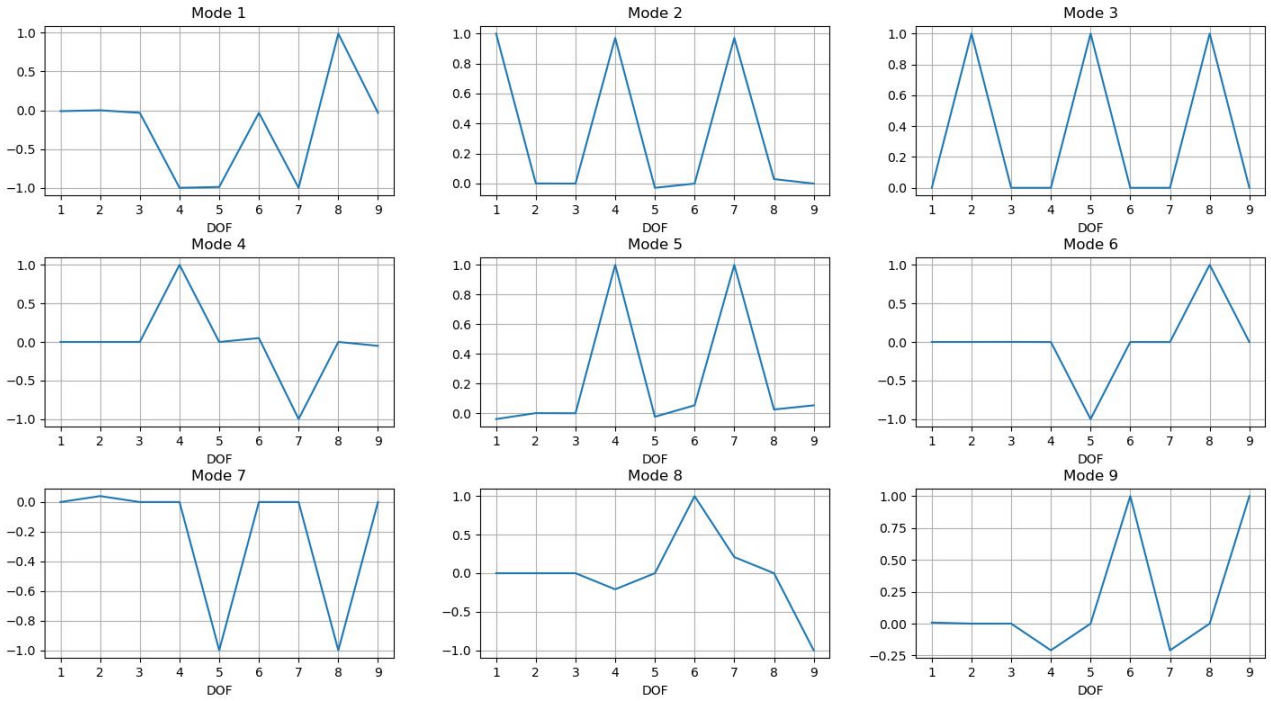

Figure B.1: The nine mode shapes of the system. DOF1 = ship's x-displacement, DOF2 = ship's z-displacement, DOF3 = ship's rotation, DOF4 = spudcan's x-displacement, DOF5 = spudcan's z-displacement, DOF6 = spudcan's rotation, DOF7 = spudcan's x-displacement, DOF8 = spudcan's z-displacement, and DOF9 = spudcan's rotation.

Appendix C

Personal Field Experience: Jack-Up Vessel going-off and going-on-location

This appendix provides a personal anecdote from my experience with the going-off and going-on location procedures of a jack-up vessel engaged in offshore wind installation and maintenance. Being part of real operations with a jack-up vessel provided an opportunity to enhance my understanding of my thesis subject. This experience, set in practical situations, amplified the theoretical knowledge acquired during my studies. During my time on board, we were in the harbor of Schiedam where the environmental conditions were mild. There was no necessity for a site-specific assessment (SSA) or a detailed weather report, as the weather was favorable and the sea was calm. This allowed us to operate with minimal restrictions, giving me an ideal environment to observe the practical aspects of the operation. In this unique setting, I witnessed theoretical concepts being translated into tangible actions. Each decision made by the on-deck crew was a careful exercise in blending procedural guidelines, reacting to real-time conditions, and acknowledging the capacities of the equipment. I was fortunate to closely observe an experienced jack-up engineer at work. His insightful decisions under safety constraints and adaptive responses to unforeseen situations were incredibly enlightening.

Figure C.1: A beautiful picture on the helideck

Figure C.2: A selfie on the JB117

References

Cassidy, M., & Houlsby, G. (1999). On the Modelling of Foundations for Jack-up Units on Sand.

Cassidy, M. J. (1999). *Non-Linear Analysis of Jack-Up Structures Subjected to Random Waves* (Tech. Rep.).

Cassidy, M. J. (2011, 4). Offshore foundation systems for resource recovery: Assessing the three-dimensional response of jack-up platforms. *KSCE Journal of Civil Engineering*, *15*(4), 623–634. doi: 10.1007/s12205-011-0003-9

Chakrabarti, P. (2012). *Going On Location Study For A Jack-up Rig* (Tech. Rep.). Retrieved from `http://www.asme.org/about-asme/terms-of-use`

Dier, A., Abolfathi, S., Carroll, B., & Great Britain. Health and Safety Executive. (2004). *Guidelines for jack-up rigs with particular reference to foundation integrity.* HSE Books.

DNV , P., CHPV Offshore Filming. (2021). *Fred. Olsen Windcarrier* (Tech. Rep.). Retrieved from `https://www.dnv.com/expert-story/maritime-impact`

DNV GL. (2015). *Recommended practice DNV GL AS Self-elevating units* (Tech. Rep.). Retrieved from `www.dnvgl.com.`

Ekici, D. (2018). *Site-specific assessment analysis; Differences between oil & gas and offshore wind farm jack-up applications* (Tech. Rep.). Retrieved from `http://onepetro.org/SNAMETOS`

Hoes, R. S. (2015). *Spudcan hydrodynamics: Analysis of hydrodynamic coefficients of spudcans in proximity to the seabed during jack-up installation* (Tech. Rep.).

Houlsby, & Puzrin. (2006). *Principles of Hyperplaticity.*

Hoyle, M. J. R., Denton, N., & Stiff, J. J. (2014). *OTC 23047 Background to the ISO 19905-Series and An Overview of the New ISO 19905-1 for the Site-Specific Assessment of Mobile Jack-Up Units* (Tech. Rep.). Retrieved from `http://info.ogp.org.uk/standards/downloads/StandardsIssued.pdf`

Hu, P., Haghighi, A., Coronado, J., Leo, C., Liyanapathirana, S., & Li, Z. (2021, 7). A comparison of jack-up spudcan penetration predictions and recorded field data. *Applied Ocean Research*, *112*. doi: 10.1016/j.apor.2021.102713

Izadi, E., & Vazquez, J. H. (2021). *WTIV Touch-Down Loads on Hard Seabeds* (Tech. Rep.).

Jia, J. (2018). *Soil Dynamics and Foundation Modeling Offshore and Earthquake Engineering.*

Journée, J. M. J., & Massie, W. W. (2001). *Offshore hydrodynamics, First Edition.*

Kaiser, M. J., & Snyder, B. F. (2013, 10). Empirical models of jackup rig lightship displacement. *Ships and Offshore Structures*, *8*(5), 468–476. doi: 10.1080/17445302.2012.736363

Le, C. h., Li, Y. e., Huang, L., Ren, J. y., Ding, H. y., & Zhang, P. y. (2021, 9). Collision Analysis Between Spudcan and Seabed During the Process of Jack-up Platform Lowering Jack-up Legs. *China Ocean Engineering*, *35*(5), 779–788. doi: 10.1007/s13344-021-0069-1

Matter, G. B., Rios da Silva Petrobras SA E, R. M., & Pao-Lin Tan, B. (2005). *Touchdown analysis of jack-up units for the definition of the installation and retrieval operational limits* (Tech. Rep.). Retrieved from `http://proceedings.asmedigitalcollection.asme.org`

Meyerhof. (1963). *Some recent research on the bearing capacity of foundations* (Tech. Rep.). Retrieved from `www.nrcresearchpress.com`

Olsson, F. (2014). *Impact loads on a self-elevating unit during jacking operation A methodology incorporating site-specific parameters for weather window assessment* (Tech. Rep.).

Orcina. (2021). Orcina help manual [Computer software manual]. Glasgow, UK.

Randolph, M., Cassidy, M., Gourvenec, S., & Erbrich, C. (2006). *Challenges of Offshore Geotechnical Engineering* (Tech. Rep.).

Randolph, M., & Quiggin, P. (2009). *Non-linear Hysteretic Seabed Model for Catenary Pipeline Contact* (Tech. Rep.). Retrieved from `http://www.asme.org/about-asme/terms-of-use`

Ringsberg, J. W., Daun, V., & Olsson, F. (2017, 6). Analysis of impact loads on a self-elevating unit during jacking operation. *Journal of Offshore Mechanics and Arctic Engineering*, *139*(3). doi: 10.1115/1.4035996

Selimovic, D., Lerga, J., Prpic-Oršic, J., & Kenji, S. (2020, 4). Improving the performance of dynamic ship positioning systems: A review of filtering and estimation techniques. *Journal of Marine Science and Engineering*, *8*(4). doi: 10.3390/JMSE8040234

Skinner, M., & Mote, T. (2015). *A risk based assessment of the punch-through potential of jack-up barges* (Tech. Rep.). Retrieved from `https://www.issmge.org/publications/online-library`

Smith, L., Lewis, T. C., Miller, B. L., Lai, P. S. K., & Frieze, P. A. (1995). *Limiting Motions for Jack-Ups Moving onto Location* (Tech. Rep.).

Smith, L., Maritime Ltd, G., Frieze, P., Frieze, P. A., Lai, P., Lewis, T., & Miller, B. (1994). *Evaluation of Leg Damage Risk fofr Jackups Going on Location* (Tech. Rep.).

SNAME. (2008). *The Society of Naval Architects and Marine Engineers* (Tech. Rep.).

Terzaghi, K. (1943). Theoretical soil mechanics.

Van Dalfsen, A. (2016). *Integral soil-jack-up modelling Modelling site-specific jack-up response and performing safety assessment* (Tech. Rep.).

Vazquez, J. H., & Grasso, B. D. (2016). *Jackup going on location-understanding energy principles on leg impact loads* (Tech. Rep.). Retrieved from `http://onepetro.org/SNAMETOS/`

Vazquez, J. H., Grasso, B. D., And, P. E., Gamino, M. A., Templeton, J. S., Eng, D., & Usa, P. E. S. (2017). *Using CEL to account for seabed deformation effects for jack-ups going on location* (Tech. Rep.). doi: 013S008R002

Xie, X., Yao, Y., Liu, J., Li, P., & Yang, G. (2016). Mechanical behavior of unsaturated soils subjected to impact loading. *Shock and Vibration*, *2016*. doi: 10.1155/2016/4703981

Yi, M. S., & Park, J. S. (2023, 2). Global Structural Behavior and Leg Strength for Jack-Up Rigs

with Varying Environmental Parameters. *Journal of Marine Science and Engineering*, *11*(2). doi: 10.3390/jmse11020405

Yung-Show, F., Liu, C., Sheng-Lin, C., & Ying-Chu, S. (2019). Penetration resistance of rack-up spudcan on dense sand overlying loose sand. *Journal of GeoEngineering*, *14*(3), 129–139. doi: 10.6310/jog.201909_14(3).2

Zheng, Y. k., Zhang, S. l., & Lai, L. (2015, 12). Load distribution on the hull-leg connection components of a jack-up. *Journal of Shanghai Jiaotong University (Science)*, *20*(6), 721–728. doi: 10.1007/s12204-015-1682-z